Investigation of Chemokine and Microbiome Profiles in Gingival Health and Disease in Humans

Shatha Bamashmous

A dissertation

submitted in partial fulfillment of the requirements

for the degree of

Doctor of Philosophy

University of Washington

2019

Reading Committee:

Richard P. Darveau, Chair

Jeffrey S. McLean

Frank A. Roberts

Program Authorized to Offer Degree:

Oral Biology

School of Dentistry

University of Washington

Abstract

Investigation of Chemokine and Microbiome profiles in Gingival Health and Disease in Humans

Shatha Bamashmous

Chair of the Supervisory Committee

Professor Richard P. Darveau

Department of Periodontics

Periodontal health is maintained by various host immune mechanisms. Neutrophils are a crucial component of health representing the first line of defense against microbial challenge. The migration and activation of these key effector cells in the gingiva are orchestrated by complex networks of host mediators called chemokines and cytokines. Recently, it has been shown that bacteria have an influential role in the immunomodulation of host mediators and hence host immune response. Indeed, dysregulation of the host immune response, as well as a dysbiosis of the oral microbial community, has been attributed to the pathogenesis of periodontal disease. However, the few investigations into the interaction between the subgingival microbial community and the host immune response have provided limited information to understand this relationship.

Therefore, a full assessment of the host-bacterial interaction in health and disease is necessary to further our understandings of the etiology of periodontal disease and identify novel biomarkers of this disease.

This thesis investigates the interaction of subgingival microbiome and the host immune response for both health and disease with disease defined as induced gingivitis. A comprehensive evaluation of forty major chemokines and inflammatory mediators in the gingival crevicular fluid (GCF) was achieved by multiplex immunoassay. In parallel, 16S rRNA next-generation sequencing was performed to characterize microbial community composition and structure. Lastly, neutrophil infiltration was assessed by myeloperoxidase (MPO) detection in the GCF to correlate neutrophil recruitment with chemokine expression patterns.

The cross-sectional study in healthy adolescents showed inter-individual variability in the chemokine expression patterns and the subgingival microbial profile. Two different chemokine expression patterns were observed among study participants; however, the different groups did not share common microbiome profiles. Additionally, there was no significant concordance between the combined chemokines and microbial profiles in gingival health. Altogether, this data provides a better understanding of the interaction between the immune response and microbiome in the state of clinical health.

Findings from the experimental gingivitis study demonstrated that during the initial transition from clinical health to gingivitis, there was a significant shift in the microbial composition that paralleled an alteration in host homeostasis. Despite variable immune responses to plaque accumulation, this alteration was characterized by a decrease in neutrophil chemotactic

factors within most patients. Furthermore, patients were able to be separated into three distinct categories with unique microbial and chemokine profiles based on their immune response. The result of this work highlights the influential effect of host response and microbiome in the susceptibility to periodontal disease.

In conclusion, this study contributes to our understanding of the host-bacterial interaction in health and the changes which occur during gingivitis induction. The significant alteration of multiple chemotactic factors within the GCF also provides the potential for a novel gingivitis diagnostic tool.

Acknowledgments

I want to extend my appreciation and gratitude to my supervisor, Professor Richard Darveau, for allowing me to join his lab and work on this project. His unwavering support, inspiration, and encouragement have been invaluable. This thesis would not have been possible without his help, and I hope that we continue working together.

I would like to express my deepest gratitude to my committee members, Dr. Jeffrey McLean, Dr. Frank Roberts, and Dr. Avina Paranjpe, for their guidance, insightful suggestions, and constant support.

I would also like to thank Dr. George Kotsakis for his help with the bioinformatics and statistical analysis, Dr. Amy Kim for her help in designing and conducting the clinical studies, Dr. Whasun Oh Chung for allowing me to access her lab equipment, and Dr. Lloyd Mancl for his statistical expertise.

I extend my appreciation to all the professors, graduate students, and department administrators in the Oral Health Science and Periodontics Departments at the University of Washington for their support and guidance throughout my residency and PhD training.

I am incredibly grateful for the past and present members of the Darveau lab for their encouragement and continuous support: Dr. Steve Coats, Dr. Sumita Jain, Dr. Ana Chang, Jirawan Wade, Dr. Nutthapong Kantrong, and Dr. Sunethra Rajapakse.

I am greatly thankful to Dr. Ana Chang and Dr. Abeer Almaimouni, who helped me get through the difficult moments, inspired me, and celebrated my accomplishment.

My deepest gratitude is owed to my parents (Othman and Khadijah), sisters (Nada and Hala), my brothers (Abdullah and Abdulaziz), my husband (Mohammad), and my boys (Yousef and Yamin) for their encouragement and unwavering support throughout my PhD journey.

I would like to acknowledge the financial and academic support provided by the Government of Saudi Arabia and King Abdulaziz University, Jeddah, Saudi Arabia, for my post-graduate studies.

Dedication

Dedicated to my parents, husband, children, brothers, and sisters for their unconditional love and support.

Table of Contents

LIST OF FIGURES

LIST OF TABLES

CHAPTER 1 . BACKGROUND AND LITERATURE REVIEW

The Relationship of Oral Microbiome to Periodontal Health and Disease

1.1.1 The oral microbiome

Oral bacteria are among the first micro-organisms to be discovered; they were described as animalcules over three centuries ago in Antony van Leeuwenhoek's observations into plaque biofilm obtained from human teeth in 1676 (Porter 1976). Due to its well-established role in the two most common oral diseases in man, dental caries and periodontal disease, in addition to the feasible acquisition of the microbial samples from the oral cavity, the oral microbiome is considered the most extensively studied and characterized microbial community in the human body. It is a heterogeneous population with over 1000 species identified using 16S ribosomal RNA (rRNA) gene sequencing (Wade 2013).

Recently, the interaction of residing microbes within the host has received significant attention. It is believed that the equilibrium between the host and residing microbes contributes to the state of health (symbiosis). Furthermore, commensal bacteria have shown to play a significant role in the proper development and function of host tissue (Xu and Gordon 2003). (Xu and Gordon 2003). Microbial community (dysbiosis) often times results in diseases such as caries and periodontitis (Kilian, Chapple et al. 2016).

Historically, the study of microbiology was entirely culture dependent, which resulted in the underestimation of the complexity of the human microbiome. However, over the years new

microbiology techniques have become available, the culture-independent techniques that are based on the analysis of nucleic acids such as DNA-DNA hybridization, PCR, and next-generation sequencing to more recent approaches such as metagenomics, metatranscriptomics, and proteomics (Dewhirst, Chen et al. 2010, Wade 2011) Many next-generation sequencing technologies are available and the most commonly used technologies are 454 pyrosequencing (Roche, Indianapolis, IN, USA), which cover longer sequences with high taxonomic resolution while sequencing on Illumina platforms (Illumina, San Diego, CA, USA) generates deep coverage at a low-cost (Kuczynski, Lauber et al. 2012). Increased progress in the methods of microbial identification and classification has fueled our appreciation of the complexity of the oral microbiome.

1.1.2 Role of the oral microbiome in periodontal tissue health

The contribution of commensal microbial colonization to the development and function of the periodontal tissue has been recently investigated. Although both germ-free (GF) and specific pathogen-free (SPF) mice were similar with respect to morphological features of a specialized tissue called the junctional epithelium (Heymann, Wroblewski et al. 2001), more neutrophils were reported in SPF mice in comparison to the GF mice (Listgarten and Heneghan 1971, Garant 1976, Yamasaki, Nikai et al. 1979). In fact, commensal bacterial colonization has been shown to influence the expression of innate defense mediators. For example, one study revealed that SPF mice express higher levels of IL-1β than GF mice. Moreover, it has been shown that oral bacteria significantly increase neutrophil recruitment to clinically healthy periodontal tissue by selective modulation of neutrophil chemoattractant GRO-β/CXCL2 but not GRO-α/CXCL1(Zenobia, Luo et al. 2013). However, the contribution of commensal oral bacterial to periodontal homeostasis in clinical healthy gingival tissue is not known.

1.1.3 Neutrophil biology and homeostasis

It is generally understood that periodontal diseases are initiated by a microbial infection in conjunction with a dysbiotic host immune response that significantly contributes to the progression of lesions and further tissue damage (Sahingur and Yeudall 2015). The junctional epithelium is located at the interface between the tooth surface, which is populated by the microbial biofilm, adjacent to the periodontal soft tissue. This specialized tissue has unique structural and functional characteristics that enable the host to control microbiological challenge. Maybe the most important host defense mechanism in the periodontal tissue is the constant migration of neutrophils through the junctional epithelium into the gingival crevice. The high permeability of the junctional epithelium is due to the low desmosomal interconnection of epithelial cells that allow the constant flow of neutrophils to the tooth surface (Bosshardt and Lang 2005). About 30,000 neutrophils have been identified to migrate through periodontal tissue every minute (Rindom Schiött and Löe 1970).

The healthy junctional epithelial tissue has been shown to expresses high levels of immune defense mediators such as IL-8/CXCL8, E-selectin, and ICAM-1 in the most coronal part that helps to direct neutrophils toward the area of the biofilm challenge (Tonetti, Imboden et al. 1998). Neutrophils are the most abundant immune cells, accounting for 50 to 70% of all circulating white blood cells, they are extensively formed in the bone marrow with a production rate of 1-2 x 10^{11} cells per day and then released to circulation (Borregaard 2010, Mayadas, Cullere et al. 2014). The process of neutrophil migration from blood vessels into tissue involves a cascade of interactions between the neutrophils and the endothelial cells (Nourshargh, Hordijk et al. 2010). Neutrophil migration in response to infection or inflammation can be induced by a plethora of chemoattractant including chemokines such as IL-8/CXCL8, complement fragments C3a and C5a, arachidonic acid

derivatives such as leukotriene B4 (LTB4), and platelet activating factor (PAF) (Sadik, Kim et al. 2011).

At peripheral tissues, neutrophils kill intruding pathogens through different mechanisms including the production of reactive oxygen species, the release of microbicidal molecules, and recently discovered release of neutrophil extracellular traps (NETs) (Nussbaum and Shapira 2011). In addition, neutrophils have an important role in the activation and recruitment of other inflammatory cells, influencing the inflammatory response by the release of many cytokines and chemokines (Mocsai 2013).

Products released from neutrophils have been measured GCF to evaluate periodontal One of the diagnostic biomarkers for neutrophil infiltration and activation is myeloperoxidase (MPO), an antimicrobial enzyme in the neutrophil azurophilic granules that are found to be elevated in areas of inflammation. In patients with periodontal disease. MPO has been shown to increase in comparison to healthy controls (Wolff, Smith et al. 1988). The high incidence of periodontal disease in individuals with deficiencies in neutrophil number or function shows the importance of neutrophils as a key component of periodontal tissue innate defense (Darveau 2010). There is a body of evidence in the literature that a decrease in the number of circulating neutrophils in situations such as congenital neutropenia (Carrassi, Abati et al. 1989, Hart, Shapira et al. 1994, Deas, Mackey et al. 2003) or chemically induced neutropenia (Attström and Schroeder 1979, Sallay, Listgarten et al. 1984, Yoshinari, Kameyama et al. 1994) is associated with severe periodontal destruction. Likewise, individuals or knockout mice that manifest a defect in neutrophil recruitment or function invariably develop periodontal disease (Meyle 1994, Niederman, Westernoff et al. 2001). On the other hand, increased neutrophil numbers and uncontrolled release of neutrophil potent enzymes into the surrounding tissue can cause considerable destruction to the host. Therefore neutrophil homeostatic regulation is very critical

during health and disease states.

1.1.4 Periodontal disease pathogenesis

Periodontal disease usually refers to either gingivitis or periodontitis. Gingivitis is the inflammation of gingival tissues without alveolar bone loss in response to the microbial biofilm and is modified by factors such as smoking, drugs, and hormonal changes associated with pregnancy and puberty. For unclear reason, a subset of the population develops periodontitis following gingivitis (Kinane 2001). Periodontitis is a chronic inflammatory disease that involves the destruction of the supporting structures of the teeth including the periodontal ligament, bone, and gingival tissues, affecting more than half the US adult population (Eke, Dye et al. 2015). Periodontitis has been shown to be associated with several systemic diseases such as cardiovascular diseases, adverse pregnancy outcomes, rheumatoid arthritis, diabetes, pulmonary diseases, and even cancer (Hajishengallis 2015).

Periodontitis has a complex etiology as bacterial plaque is generally believed to initiate the disease either by a direct pathogenic effect or by stimulating a damaging host inflammatory response (Griffen, Beall et al. 2012). At the biofilm interface, the host immune system can detect bacterial invasion through Toll-like receptors (TLR), which leads to downstream activation of many transcriptional factors, including nuclear factor-κB (NF-κB) and subsequent production of various mediators. The initial result of the interaction of microbial biofilm and host is the release of inflammatory mediators and the recruitment of immune cells. The ability to bring host immune cells to a site of infection within the body depends on the release of many microbial and host chemotactic factors such as macrophage migration inhibitory factor (MIF), chemokines such as IL-8, complement system components C5a and C3, and arachidonic acid products such as the leukotrienes (Sadik, Kim et al. 2011, Sahingur and Yeudall 2015). The goal of the initial inflammatory response to plaque biofilm is to both protect the host by eliminating infection and

aid in the development of the adaptive immune response. The extent of immune response determines whether the infection is cleared with the restoration of the tissue homeostasis, or progression to a state of chronic inflammation. In fact, studies have shown that the persistence of chronic inflammatory response state may result in local periodontal tissue damage and further systemic influences due to the continuous release of inflammatory mediators and microbial factors into the circulation (Graves and Cochran 2003, Hajishengallis 2015).

1.1.5 Microbiology of periodontal disease

Periodontitis has a polymicrobial etiology. With the recent development of advanced microbiologic techniques, a more in-depth analysis of the dental plaque from healthy or diseased periodontal tissue has become possible. The major bacterial species found during periodontal disease differ from those found in gingival health, although periodontitis associated pathogens can often be identified in low abundance in a healthy gingival sulcus. The transition from periodontal health to disease is associated with a subgingival microbial flora shift from aerobic gram-positive to anaerobic gram-negative species (Marsh 1994). Early studies that were culture-based did not give complete results since many of oral community members are considered uncultivable and were difficult to identify. More advanced approaches using whole genomic DNA probes and checkerboard DNA-DNA hybridization have led to the identification of additional major species associated with either periodontal health or disease. Socransky *et al.* (1998) described the well-known red-complex, which has a set of three species: *Porphyromonas gingivalis*, *Tannerella forsythia*, and *Treponema denticola* that showed a strong association with periodontitis (Socransky, Haffajee et al. 1998). Subsequently, more targeted characterization of plaque biofilm using 16S rRNA gene amplification has provided a comprehensive view of bacterial community complexity and identified numerous uncultivable potential periodontal pathogens. Bacterial

community diversity differences were evident between health and disease, with 123 species identified and associated with the disease while 53 bacterial species were associated with health (Griffen, Beall et al. 2012). Nevertheless, the reasons behind such observed bacterial shifts are not understood, it could be related to oral hygiene, host modulators, or emergence of strains or species of bacteria that act as triggers for this shift and therefore this area deserves further research. Understanding plaque microbial community composition and stability can be a useful tool for disease diagnosis and prognosis.

1.1.6 The experimental gingivitis model

The original experimental gingivitis protocol developed by Löe *et al.* in 1965 established a model that has served as a reference guideline in clinical and translational research for over 40 years. (Löe, Theilade et al. 1965, Theilade, Wright et al. 1966). Löe's work demonstrated the essential role of plaque in the initiation of gingivitis. After no-brushing period, the reinstitution of oral hygiene resulted in re-establishment of gingival health at both the clinical and microbiological levels, which proved the causal relationship between plaque and gingivitis. Early experimental gingivitis studies using microscopy revealed the microbial composition shift during the period of plaque accumulation. In health, the plaque microbial community is mainly dominated by gram-positive cocci and rods. During plaque development in the experimental phase, an increase in the number and distinct changes in the composition of bacteria takes place, which starts with the proliferation of gram-positive and appearance of gram-negative rods and cocci. This is followed by proliferation of fusobacteria, filaments and later the predominance of gram-negative rods and spirochetes. Culture-based technique in later experimental gingivitis work confirmed the microbial shift that occurs during plaque maturation (Loesche and Syed 1978, Moore, Holdeman et al. 1982). With the introduction of more advanced techniques, additional knowledge was gained regarding

the microbial composition shift during plaque accumulation since the majority of bacteria in the oral cavity are not cultivable.

One recent experimental gingivitis study using high-throughput 454-pyrosequencing of 16S rRNA genes displayed a similar significant increase in microbial community diversity as gingivitis developed (Kistler, Booth et al. 2013). However one of the limitations of this study is that gingivitis was induced for 14 days only, since an earlier report has shown that it might take 10-21 days for gingivitis to fully develop in different individuals (Löe, Theilade et al. 1965). This might result in the inclusion of healthy sites in the gingivitis data. Another study examined the plaque microbial community using pyrosequencing in 50 adults who went through transitions from naturally occurring gingivitis to gingival health (baseline) and then to experimental gingivitis (EG) (Huang, Li et al. 2014). The study revealed the microbial basis for disease heterogeneity and identified two types of hosts (type I and type II) with distinct sensitivity and susceptibility to gingivitis, where type II patients showed more acute changes in the microbial plaque structure and gingivitis development than type I patients. However, the study did not longitudinally follow the changes in the microbial community as gingivitis developed. A more recent study used Illumina MiSeq sequencing platform to compare the microbial composition changes over time during experimental gingivitis in subject-matched posterior teeth and implant sites. The results of the study revealed that teeth were associated with more changes in the microbial community during plaque accumulation whereas implants did not (Schincaglia, Hong et al. 2017). However, this study is missing a healthy control group and conclusions were based on data from only 15 subjects.

Earlier gingivitis studies have shown increased GCF levels of neutrophil chemokines including IL-1β and LTB4 in addition to other neutrophil enzymes such as matrix metalloproteinases (MMP8) (Heasman, Collins et al. 1993, Söder, Jin et al. 2002). Recent efforts in the field have examined classic gingivitis mechanism through various experimental models to

learn more about the effects of gingivitis at both the micro and macroscopic levels. Further, as increased inflammatory mediators are observed in chronic gingivitis, experimental models have adapted to include new candidate biomarkers (Offenbacher, Barros et al. 2010). Recently, the stent-induced biofilm overgrowth model (SIBO) has been utilized to study localized changes in biofilm and inflammatory responses (Burrell and Walters 2008). The application of the stent model allows comparison of local changes in biofilm and the inflammatory response of the experimental side with the contralateral control side over time within subjects.

Chemokines as Selective Recruiters of Inflammatory Cells

1.1.7 Diagnostic biomarkers for periodontal disease

Routinely used periodontal diagnostic parameters like pocket depth, bleeding on probingn and radiographic alveolar bone level can give insights about the history but not necessarily the current status of periodontal disease (Taba, Kinney et al. 2005). The use of biomarker-based diagnostics has been extensively evaluated to improve our understanding of the disease process and help identify possible diagnostic parameters for periodontal disease progression (Delima and Van Dyke 2003, Teles, Teles et al. 2013). A non-invasive methodology that has been used to study the host immune response in healthy and diseased gingival tissue is to examine the composition of the gingival crevicular fluid (GCF). GCF is a serum exudate that contains locally and systemically produced inflammatory factors such as cytokines, chemokines, antibodies, proteins, and host and bacteria-derived enzymes (Taba, Kinney et al. 2005). During periodontal disease, several inflammatory biomarkers have shown to be upregulated. Several techniques have been applied to measure specific biomarkers in GCF including ELISA, immunoblotting, bead-based multiplexing, and more recently mass spectrometry technology (Carneiro, Nouh et al. 2014). The volume of GCF also increases during periodontal disease. The Periotron is an electric device that measures

the volume of GCF to help assess the severity of gingival inflammation (Garnick, Pearson et al. 1979). There is an increased interest in expanding beyond the identification of factors associated with periodontal disease and the development of methods to predict disease progression to allow enhanced monitoring and control of periodontal disease activity (Kinney, Morelli et al. 2014).

1.1.8 Chemokines

Chemokines or chemotactic cytokines are small secreted polypeptides (from 5 to 20 kDa) that are involved in immune cells chemotaxis. They are classified into four subfamilies according to the position of conserved cysteine residues in the polypeptide: CXC, CX3C, CC and C, and they specifically bind to two major chemokine receptors families CCR and CXCR. Over 40 different chemokines have been identified in humans, and in addition to their known functions as inflammatory mediators, chemokines are involved in angiogenesis, cell proliferation, apoptosis, tumor metastasis, and host defense (Zlotnik and Yoshie 2000). Binding of chemokine receptors with their ligands generate intracellular signaling pathways, which result in the rearrangement of the cytoskeleton and cell adhesion receptors, causing the cells to migrate toward the chemoattractant gradient to the inflammatory sites (Terricabras, Benjamim et al. 2004). The CXC chemokine ligands are mainly chemotactic to neutrophils. On the other hand, CC chemokines are chemotactic to macrophages and lymphocytes, that play a role in the transition from acute to chronic inflammation and in the development of adaptive immunity (Sahingur and Yeudall 2015). The chemokines' role in the amplification of immune response can be linked to the pathogenesis of various inflammatory diseases including periodontal disease (Emingil, Atilla et al. 2004). Neutrophils express both CXCR1 and CXCR2 receptors, which bind to various CXCL chemokines including GRO-α/CXCL1, GCP-2/CXCL6, and IL-8/CXCL8 (Zlotnik and Yoshie 2000). Intriguingly, once thought to be redundant, neutrophil chemokines efficiently function to direct

neutrophils to the site of infection through distinct patterns of temporal and spatial expression (Sadik, Kim et al. 2011). For example, the CXCR2 ligands, CXCL1/KC, CXCL2/MIP-2, and CXCL5/Lix (mouse model) have shown different affinities for the CXCR2 receptors resulting in a hierarchy of neutrophil activation and chemotaxis (Lee, Cacalano et al. 1995, Wuyts, Haelens et al. 1996). Furthermore, the differences in the induction and tissue distribution profiles of these three chemokines LIX, KC, and MIP-2 in an endotoxemia model suggest different functional roles for these chemokines (Rovai, Herschman et al. 1998). These studies provide evidence that chemokines show different distinct functions when expressed in the different tissues.

1.1.9 Chemokines in periodontal disease from host protection to tissue destruction

The host immune response to the microbial challenge is highly regulated by cytokine signals, that control inflammation initiation and progression. In particular, the role of various chemokines in each stage of periodontal pathogenesis has as received a lot of attention. While not much is known about the role of chemokines in periodontal health. Several factors can trigger chemokine expression including periodontal microbial-associated molecular patterns (MAMPs) such as lipopolysaccharide (LPS) and nucleic acids, damage/danger associated molecular patterns (DAMPs), inflammatory mediators, and other host factors. In the oral cavity, many cell types including fibroblasts, osteoblasts, endothelial cells, epithelial cells, mast cells, and leukocytes can produce chemokines (Silva, Garlet et al. 2007). Neutrophil homing to the periodontium is required to maintain periodontal tissue health, however, most studies focus on neutrophil homing during inflammatory disease (Tonetti, Imboden et al. 1994, Tonetti 1997). Several studies have shown selective expression of neutrophil chemokines in the periodontal tissue. Probably the most abundant chemokine expressed is IL-8 (CXCL8), and it can be detected in both periodontally healthy and diseased sites (Gamonal, Acevedo et al. 2000, Ertugrul, Sahin et al. 2013). The level

of major neutrophil chemokines such as IL-8/CXCL8 and GCP-2/CXCL6 is significantly higher in the GCF of diseased compared to healthy individuals, suggesting a potential diagnostic for periodontal disease progression (Tsai, Ho et al. 1995, Kebschull, Demmer et al. 2009).

The use of knockout animal models where the expression of chemokines or chemokine receptors is altered has helped in understanding the role of these mediators in health and disease conditions (Silva, Garlet et al. 2007). Evidence in the mouse model has confirmed the role of CXCR2 receptor ligands for neutrophils homing to the periodontium. One study showed that neutrophils in CXCR2 $^{-/-}$ mice demonstrated normal killing activity but impaired migration. These CXCR2 KO mice were susceptible to significant periodontal bone loss even in the absence of exogenously added oral pathogens, which suggests that CXCR2 ligands contribute to normal bone homeostasis (Yu, Ruddy et al. 2007). Another study has provided the evidence that neutrophil homing into the periodontal tissue in mice is entirely dependent on CXCR2 expression and that commensal bacterial colonization is not required for neutrophil migration across the junctional epithelium. In addition, mice express the CXCR2 chemokine ligands CXCL1 and CXCL2, the analog of human IL-8, differently in response to bacterial colonization (Zenobia, Luo et al. 2013). Moreover, a recently published work has shown that CXCL1 is associated with neutrophil migration around the entire tooth circumference wherase CXCL2 is associated with neutrophil migration in the interproximal region (Greer, Irie et al. 2016). These studies demonstrate that neutrophil homing to clinically healthy tissue, similar to the inflammatory response, is a highly selective process where the expression of different neutrophil chemoattractant is regulated both spatially and temporally in response to oral commensal bacteria colonization. Similarly, humans are highly selective in the expression of neutrophil chemokines in the periodontal health and disease states (Garlet, Martins et al. 2003, Davanian, Stranneheim et al. 2012).

Little is known regarding the contribution of the microbial community to different chemokine expression in gingival tissue during health and disease. Few studies have investigated the correlation between the subgingival microbiome and host inflammatory mediators by analyzing subgingival microbial samples and GCF biomarkers collected from the same site. Most of these studies looked into a small number of bacterial species in association with a limited number of biomarkers (Teles, Sakellari et al. 2010). One study showed an association between higher levels of periodontal pathogens and the GCF total amounts of vascular endothelial growth factor (VEGF), monocyte chemoattractant protein-1 (MCP-1), and interleukin 8 (IL-8) (Lee, Yang et al. 2003). Another study demonstrated periodontitis subjects had significantly higher levels of IL-1β, MMP-8, and IL-8 in GCF samples than the periodontally healthy subjects and there were significant associations between the microbial composition and expression of the three biomarkers (Teles, Sakellari et al. 2010). Nevertheless, a complete understanding of the contributions of the various microbial communities associated to the innate host immune response during health or disease remains unclear.

CHAPTER 2 . CHEMOKINE AND MICROBIOME PROFILES IN GINGIVAL HEALTH

Introduction

Maintenance of healthy periodontal tissue is an active and dynamic process. One key component of periodontal host defense is the transit of neutrophils from the vasculature into gingival tissue. It has been shown that in the healthy mouse model, periodontal tissues benefit from oral commensal bacteria (Tsukamoto, Usui et al. 2012). The commensal bacterial colonization role in the selective regulation of neutrophil chemokine expression significantly contributes to the neutrophils homing to specific areas in clinically healthy periodontal tissue (Zenobia, Luo et al. 2013). Thus the crucial role of neutrophils in periodontal homeostasis is of great interest. Currently, there is little, or possibly no, research with a focus on thoroughly examining neutrophil chemokine expression in clinically healthy human gingiva. Therefore, our understanding regarding the mechanisms involved in controlling neutrophil migration into human periodontal tissue during health is not as clear.

In this chapter, a cross-sectional clinical study was conducted to investigate the chemokine and microbiome profiles in gingival health. The objectives of this study, first, is to evaluate the levels of major neutrophil and immune cell chemokines in the gingival crevicular fluid (GCF) collected from healthy adolescents. The second objective is to assess neutrophil migration by measuring myeloperoxidase (MPO) in the GCF. The third objective of this study is to characterize subgingival plaque microbiome composition and structure.

Understanding how the host regulates neutrophil transit through non-diseased gingiva is important in that it will begin to define key mechanisms for the maintenance of gingival health. In addition, the study findings will enhance our understanding of the relationship between the

microbiome and the chemokines pattern in gingival health. Ultimately, understanding specific details on chemokine behavior in gingival states of health and disease will allow for assessment and evaluation of gingival crevicular fluid as a potential diagnostic marker for gingival health.

Clinical Study Design and Methods

2.1.1 Study Procedures and Biospecimens Collection

2.1.1.1 Sample size determination

As this is a pilot exploratory study being performed for feasibility, no power analysis was performed to show the rationale for the number of subjects to be enrolled. The selection of 20 participants is a convenience sample.

2.1.1.2 Study population and informed consent

This pilot study enrolled twenty generally healthy adolescents aged 12-17 years that are self-referred or referred to the UW School of Dentistry. The study design and informed consent were approved by the UW Human Subjects Review Committee. Upon undergoing parental consent and individual assent, participants were screened and enrolled in the study if eligible.

Inclusion Criteria:

For eligibility, the following inclusion criteria were met 1) generally healthy patients, ASA I; 2) gingival health: gingival Index (GI) = 0, probing depth (PD) ≤ 3.0 mm, bleeding on probing (BOP)(-), and attachment aoss (AL) = 0 mm; 3) patients aged 12 - 17 years; 4) patients of record at the Center for Pediatric Dentistry, presenting for non-restorative visits; 5) patients and parent/guardian able to execute assent and consent and are English speaking

Exclusion Criteria.

Participants were excluded if 1) patients on antibiotic therapy or anti-inflammatory drugs within 90 days of enrollment; 2) patients had a history of periodontal disease.

2.1.1.3 Study procedure and clinical exam

After completing their regular dental appointment at the Center for Pediatric Dentistry research participants underwent an abbreviated periodontal health assessment and biospecimen

sampling of plaque and gingival crevicular fluid (GCF). Gingival crevicular fluid and plaque samples were collected from the Ramjford teeth (Ramfjord 1959). Ramjford teeth include specific sites that are consistently used for periodontal clinical research studies including upper right 1st molar, upper left central incisor, upper left 1st premolar, lower left 2nd molar, lower right central incisor, and lower right 1st premolar (Teeth #'s 3, 9, 12, 19, 25, and 28). Clinical data documented based on probing depth (PD), attachment level (AL), visible plaque index (VPI) (Ainamo and Bay 1975), gingival index (GI) (Löe and Silness 1963) and bleeding on probing (BOP). All clinical measurements were conducted using a UNC-15 periodontal probe (Hu-Friedy, Chicago, IL, USA). All measurements were assessed at six surfaces per tooth: mesiobuccal, direct buccal, distobuccal, distolingual, direct lingual, and mesiolingual. The BOP was recorded within 20 seconds of probing.

2.1.1.4 GCF Sampling

The sites to be sampled were isolated with cotton rolls and gently air-dried. GCF samples were collected with sterile paper strips (Periopaper; Oraflow Inc., Smithtown, NY, USA) that were inserted into the gingival crevice until mild resistance was felt and left in place for 30 seconds. The volume of GCF collected in the strips was measured with a previously calibrated measuring device (Periotron 6000; Oraflow Inc., Smithtown, NY, USA) and converted into fluid volume (µl) using the provided software (Periotron Professional software V3.0; Oraflow Inc., Smithtown, NY, USA) (Chapple, Landini et al. 1999). The GCF samples were collected from the mesiobuccal surfaces of all six Ramjford teeth, and samples were pooled into one 1.5 ml microcentrifuge tube. Paper strips visibly contaminated with saliva or blood were excluded from the study. After collection, GCF samples were stored immediately on ice and transported to the lab for processing.

2.1.1.5 Plaque Sampling

After GCF samples collection, the subgingival plaque samples were collected using sterile paper points (STER-I-CELL Paper Points, Size M; Coltene, Whaledent, Cuyahoga Falls, OH, USA) inserted in the gingival sulcus for 30 seconds. Plaque samples were collected from the mesiobuccal surfaces of Ramjford teeth and were pooled into one 1.5 ml sterile microcentrifuge tube. Plaque samples were transported to lab on ice and stored immediately at -80 ^{o}C until processing.

2.1.2 Laboratory Assessments

2.1.2.1 GCF Elution from Periopapers

GCF samples were eluted in 200 µl sample diluent (Bio-Plex Pro™ Human 40-plex Chemokine Panel, Bio-Rad Laboratories, Hercules, CA, USA) with 0.5% bovine serum albumin (Blocker™ BSA (10X) in PBS; Waltham, MA, Thermo Scientific, USA) and then continuously mixed on a tube rotator for 60 minutes at 4°C. The strips were then removed and placed into a 0.5 ml PCR tube with a hole punctured at the base, and this tube was returned in the 1.5 mL tube and centrifuged at 13,000 rpm for 1 min at 4°C to extract the remaining fluid from the paper strips into the tube. Paper strips were then removed and eluted samples were stored at -80°C until further analysis. Samples were immediately thawed prior to performing immunoassays.

2.1.2.2 MPO Quantification in GCF

The concentration of myeloperoxidase (MPO) in GCF samples was assayed using a commercially available ELISA kit (Human Myeloperoxidase ELISA Kit; Abcam, Cambridge, MA, USA) according to the manufacturer's instructions. The assay has a detection range between 15.6 pg/ml and 2000 pg/ml. The GCF samples were added in duplicate to the wells of a precoated

96-well plate at a 1:2000 dilution. Subsequently, the antibody cocktail (capture and detector antibody) was added and the plate was incubated at room temperature for 1 hour on a plate shaker. After washing to remove unbound analyte, a substrate solution (TMB) was added to each well and incubated for 10 minutes at room temperature in the dark on a plate shaker. The reaction was stopped with the addition of stop solution (Sulphuric acid) and absorbance was measured on a microplate reader at 450 nm (VMax microplate reader; Molecular Devices Sunnyvale, CA, USA). Concentrations for MPO in the samples were calculated from the standard curve with a five-parameter fit curve (Softmax Pro Software; Molecular Devices Sunnyvale, CA, USA).

2.1.2.3 Chemokine Quantification in GCF

Bead based multiplex analysis was performed on GCF samples (Bio-Plex Pro™ Human 40-plex Chemokine Panel; Bio-Rad Laboratories, Hercules, CA, USA) allowing for simultaneous quantification of multiple chemokines. The following list of chemokines were analyzed with the assay working range level in pg/ml shown in paraentheis ( ): 6Ckine/CCL21 (21.9-3,923), BCA-1/CXCL13 (0.7-1,200), CTACK/CCL27 (1.2-5,000), ENA-78/CXCL5 (7.3-120,000), Eotaxin/CCL11 (1.5-3,859), Eotaxin-2/CCL24 (6.2-4,073), Eotaxin-3/CCL26 (0.9-12,109), Fractalkine/CX3CL1 (4-11,463), GCP-2/CXCL6 (0.8-11,135), GM-CSF (5.3-35,000), Gro-α/CXCL1 (3.1-7,024), Gro-β/CXCL2 (4.6-13,257), I-309/CCL1 (1.8-1,015), IFN-γ (2.3-20,236), IL-1β (0.4-7,000), IL-2 (0.8-13,000), IL-4 (1.2-4,804), IL-6 (0.7-12,000), IL-8/CXCL8 (0.5-7,640), IL-10 (1.3-18,708), IL-16 (2.1-34,000), IP-10/CXCL10 (1.6-7,714), I-TAC/CXCL11 (0.1-2,298), MCP-1/CCL2 (0.3-4,812), MCP-2/CCL8 (0.3-4,056), MCP-3/CCL7 (1.9-20,133), MCP-4/CCL13 (0.2-3,368), MDC/CCL22 (0.9-14,649), MIF (23.1-377,724), MIG/CXCL9 (1.8-19,600), MIP-1α/CCL3 (0.4-1,543), MIP-1δ/CCL15 (1.7-9,100), MIP-3α/CCL20 (0.3-4,675), MIP-3β/CCL19 (3.0-48,494), MPIF-1/CCL23 (1.0-14,450), SCYB16/CXCL16 (0.5-2,867), SDF-

1α+β/CXCL12 (8.3-115,730), TARC/CCL17 (1.7-430), TECK/CCL25 (20.6-114,493), and TNF-α (0.9-13,879). Samples were not diluted for the assay. Briefly, different fluorescently dyed magnetic microspheres populations were covalently conjugated with capture antibodies specific for the different chemokines. In the multiplex immunoassay, the coupled beads were incubated with 50 µl of GCF samples or standards in a 96-well plate in duplicate at room temperature for one hour. After washing (Bio-Plex Pro Wash Station; Bio-Rad, Hercules, CA, USA), 25 µl of biotinylated detection antibodies was added and incubated for 30 minutes at room temperature. After incubation, wells were washed and 50 µl streptavidin-phycoerythrin as a reporter was added to each well and incubated for 10 min. After the wash cycle was completed, 125 µl of assay buffer was added to each well. The data was obtained using a flow cytometry laser detection system (Bio-Plex 200 reader; Bio-Rad Laboratories, Hercules, CA, USA) by acquiring the signal from the fluorescent dye within each bead for assay identification along with the fluorescent signal from the reporter for quantification. The concentrations of different chemokines were calculated based on the respective standard curve for each chemokine with a five-parameter logistic (5PL) equation (Bio-Plex Manager Software V6; Bio-Rad Laboratories, Hercules, CA, USA). Mediator data are reported in total amounts per sample collected in 30 seconds (pg per 30-s sample).

2.1.2.4 DNA extraction from subgingival samples

DNA was extracted using a commercially available kit (QIAamp DNA Microbiome Kit; Qiagen, Germany) following the manufacturer's protocol, that uses both mechanical and chemical cell lysis. To confirm the absence of other DNA contamination in the sequencing results, negative controls were implemented by performing the DNA extraction protocol without plaque samples with either kit reagents only or kit reagents with the sterile paper points. Also, to validate the efficiency of the technique, positive controls using known bacterial cultures were included. Sample

purification was performed using a purification kit (the DNA Clean & Concentrator -5 kit; Zymo Research, Orange, CA, USA) to further purify and increase the DNA yield. After DNA extraction and purification, DNA concentrations in the samples were determined fluorometrically (Quant-iT dsDNA HS Assay Kit; Invitrogen, Carlsbad, CA, USA) with Fluorometer (Qubit 2.0; Life Technologies, Carlsbad, CA, USA). Samples were then stored at -20^{o}C until ready for sequencing.

2.1.2.5 Library preparation of Next Generation Sequencing.

Comprehensive microbial profiling of subgingival plaque samples was performed via high-throughput sequencing of 16S rRNA gene following the standard Illumina Miseq System protocol. Briefly, amplification of DNA was performed using primers with overhang Illumina flow cell adapter sequences targeting hypervariable (V3 and V4) regions of the bacterial 16s rRNA gene. The primers used were 16S amplicon PCR forward primer (5'-TCGTCGGCAGCGTCAGATGTGTATAAGAGACAGCCTACGGGNGGCWGCAG-3') and 16S amplicon PCR reverse primer (5'-GTCTCGTGGGCTCGGAGATGTGTATAAGAGACAGGACTACHVGGGTATCTAATCC-3'). Samples were amplified in singletons in a 96 well plate format. Each reaction was performed using a PCR kit (KAPA HiFi HotStart PCR kit; Kapa Biosystems, Boston, MA, USA) in a 25 µl reaction volume containing 3 µl of the extracted DNA template, 5 µl 5X HiFi Reaction Buffer, 0.75 µl of 10 µM KAPA dNTP mix, 0.5 µl KAPA HiFi HotStart DNA Polymerase, 5.75 µl PCR grade nuclease-free H_2O, and 5 µl forward/reverse primer mix (1 µM each primer). Amplicon PCR was performed on a thermocycler (GeneAmp PCR System 9700; Applied Biosystems, Foster City, CA, USA) utilizing the following program: a denaturation stage at 95°C for 3 minutes, followed by 40 cycles of denaturation at 95°C for 30 seconds, annealing at 55°C for 30 seconds, and extension at 72°C for 30 seconds, and then a final extension stage at 72°C for 5 minutes. The generated amplicons from the first PCR were approximately 460 bp in size that was verified visually by running each reaction on 1% agarose

gel electrophoresis at 100V for 30 minutes. Amplicons were subsequently purified using magnetic beads (Agencourt AMPure XP beads; Agencourt Bioscience Corporation, Beckman Coulter Inc., Beverly, MA, USA) and indexed (Illumina Nextera Index Kit; Illumina, San Diego, CA, USA). The indexing PCR conditions included a denaturation stage at 95°C for 3 min, followed by 8 cycles of denaturation at 95°C for 30 s, annealing at 55°C for 30 s and extension at 72 °C for 30 s, and then a final extension stage at 72°C for 5 min. The indexed PCR amplicons were further purified with magnetic beads (Agencourt AMPure XP beads; Agencourt Bioscience Corporation, Beckman Coulter Inc., Beverly, MA, USA), and the quality and size of the library were assessed with a bioanalyzer (Agilent High Sensitivity DNA Kit & the Agilent 2100 bioanalyzer; Agilent Technologies, Santa Clara, CA, USA). Subsequently, library normalization was performed (Quant-iT Picogreen dsDNA Assay Kit; Invitrogen, Carlsbad, CA, USA), the normalized library was pooled and denatured with sodium hydroxide (NaOH) (Fisher Scientific, Pittsburgh, PA, USA). The denatured library was diluted to a 18 pM loading concentration and spiked with at least 20% control DNA (PhiX Control v3 library, Illumina, San Diego, CA, USA) prior to loading to the sequencer. Paired-end sequencing was carried out on a sequencing platform (MiSeq System, Illumina, San Diego, CA, USA) using a 2 x 300 cycle sequencing kit (MiSeq Reagent Kits v3, Illumina, San Diego, CA, USA).

2.1.2.6 Analysis of Sequences

Analysis of sequencing data was performed using the Quantitative Insights into Microbial Ecology QIIME2 (Bolyen, Rideout et al. 2018) following the Divisive Amplicon Denoising Algorithm 2 (DADA2) pipeline workflow (Callahan, McMurdie et al. 2016, Callahan, Sankaran et al. 2016). Following demultiplexing with Casava V1.8, forward reads were truncated at position 290 and reverse reads at position 200, subsequently reads acquired at least 35 bp overlap when

merged. After quality filtering and denoising of sequences, chimeras and singletons were removed. Taxonomic assignment to classify to the amplicon sequence variants (ASVs) was performed using the current Human Oral Microbiome Database (HOMD 16S rRNA RefSeq V15.1) (Chen, Yu et al. 2010, Dewhirst, Chen et al. 2010). A phylogenetic tree was constructed using FastTree (Price, Dehal et al. 2010). Unrarefied data was used for the downstream analysis. The sequencing data were integrated into a single object using the "*phyloseq*" R package (McMurdie and Holmes 2013) and all subsequent data analysis and plots were produced in R Studio.

Alpha diversity, within sample diversity, was calculated using both richness and evenness metrics by functions estimate_richness() and pd() in the "*phyloseq*" and "*picante*" R packages (Kembel, Cowan et al. 2010). The plots for richness estimates were generated using "*ggplot2*" packages in R. The community richness was measured by observed species; total count of unique OTUs in the sample and by the nonparametric richness estimator (Chao1); account for the number of singletons and doubletons (Chao 1984). The total community diversity (richness and evenness) was measured by Simpson's inverse diversity index (Simpson 1949), Shannon index and the phylogenetic diversity (Faith's PD); that uses phylogenetic distance to calculate diversity (Faith 1992) (Lozupone and Knight 2008).

Beta diversity, between samples diversity, was determined using phylogenetic-based Unifrac distances; that measure phylogenetic distances between samples both unweighted (presence\absence) and weighted (relative abundance) (C. Lozupone & Knight, 2005), and OTU based Bray-Curtis dissimilarity matrix (Bray and Curtis 1957, Lozupone and Knight 2005); account for both the presence/absence and abundance of OTUs. Beta diversity metrics were calculated with the ordinate() function in "*phyloseq*" and were visualized by non-metric multidimensional scaling (NMDS) plots using the plot_oridination() function in "*phyloseq*". The

core microbiome was calculated and visualized using the plot_core() function in "*microbiome"* package (Lahti 2019).

2.1.2.7 Microbial Load Quantification

Quantitative real-time PCR was performed to determine the total bacterial load in each sequenced sample. Samples were analyzed in singletons in a 96-well plate using a thermocycler (CFX96 Real-time system C1000 Thermocycler; BioRad Laboratories, Hercules, CA, USA). A qPCR standard curve was generated from serially diluted *Fusobacterium nucleatum* ATCC 10953 genomic DNA in a range of 10^8 to 10^1 16s copy number. Each reaction was performed in a total volume of 20 µl consisted of 2 µl of DNA or standards added to 10 µl of the master mix (TaqMan™ Fast Advanced Master Mix; Applied Biosystems, Foster City, CA, USA). Primers set that specifically target the 16S rRNA gene were added with 900 nM final concentrations for both forward primer, 5′-TCCTACGGGAGGCAGCAGT-3′, and reverse primer, 5′-GGACTACCAGGGTATCTAATCCTGTT -3′; and 200 nM of TaqMan probe, (6-FAM)-5′-CGTATTACCGCGGCTGCTGGCAC- 3′-(TAMRA), (Sigma Aldrich, St Louis, MO, USA) (Nadkarni, Martin et al. 2002). Nuclease-free water was added to bring the total volume of the reaction to 20 µl. The negative control sample was included in the run using nulcease-free water to ensure no contamination occurred. The qPCR run consisted of the following amplification conditions: 50°C for 2 minutes (UNG incubation); 95°C for 20 seconds (Polymerase activation); 40 cycles of 95°C for 3 seconds (denature) and 60°C for 30 seconds (anneal/extend). The subgingival bacterial load was calculated (BioRad CFX software V3.1; BioRad Laboratories, Hercules, CA, USA) using regression mode (Cq determination mode). A logarithmic transformation of the bacterial load data was performed.

2.1.3 Statistical Analyses

2.1.3.1 Clinical and chemokine data

All statistical analysis was performed using R software, version 3.5.1(Team 2018). Clinical data including VPI, PD, and GCF volume were summarized into a single average score for each participant and were recorded in mean and standard deviation. Mean and standard deviations of chemokine total amounts (pg per 30-s sample) are reported in Table 1. Samples with non-detectable chemokines were considered zero for the calculations. The correlation of neutrophil chemokines levels and neutrophil numbers (MPO) was assessed using the Spearman rank order tests. Multiple comparisons were adjusted with false discovery rate (FDR) method (Benjamini and Hochberg 1995). Principal component analysis (PCA) analysis was carried on to examine variation in the chemokine data and whether any clustering was present. Hierarchical clustering of chemokine profiles was performed with the hclust() in R using Euclidean distances with Ward's linkage. Heatmaps were created via the "*clustvis*" package in R (Metsalu (2019)). The optimal number of clusters was determined using the Silhouette method (Rousseeuw 1987).

2.1.3.1 Microbial diversity and composition

Hierarchical clustering of microbial communities based on species relative abundances was performed with the hclust() in R using correlation distances with Ward's linkage. Heatmaps were created via the "*clustvis*" package in R (Metsalu (2019)). The optimal number of clusters was determined using the Silhouette method (Rousseeuw 1987). The correlation between microbes and chemokine were computed by the Mantel test. Correlations between relative abundances of individual species and chemokine expression levels were performed via Spearman rank order tests. The significance threshold for all statistical tests was adjusted using the False Discovery Rate (FDR) method (Benjamini and Hochberg 1995). Differences in relative abundances of species

were determined with LEfSe (Segata, Izard et al. 2011), using an alpha value of 0.01 for the Kruskal−Wallis test and a threshold of 3.5 for logarithmic linear discriminant analysis scores.

Results

2.1.4 Study implementation

A total of twenty-two subjects was screened for study enrollment. Twenty participants, twelve females (60%) and eight males (40%), met the study inclusion criteria and were enrolled. The age range of study participants was between 12 – 17 years with a mean age of 14.55 ± 1.67 years.

2.1.5 Clinical results

All subjects had generalized gingival health with no attachment loss, absence of bleeding on probing, probing depth ≤ 3.0 mm and gingival index score equal to zero at the time of the study. In summary the subjects had a mean visible plaque index (VPI) score of 7.78 ± 15.44%, a mean probing depth (PD) of 1.85 ± 0.20 mm, and gingival crevicular fluid (GCF) mean volume of 0.41±0.14 µl.

2.1.6 Chemokines results

2.1.6.1 Chemokines profiles in the gingival crevicular fluid

Results of the multiplex immunoassay of the forty cytokines and chemokines are shown in Table 1. Of the examined 40 chemokines, only one chemokine, EOTAXIN-2/CCL24, was not detectable in any of the samples and was excluded from the analysis. The following chemokines I-309/CCL1, MCP-3/CCL7, IL-4, TARC/CCL17, IL-4, EOTAXIN-3/CCL26, and GM-CSF had were detected at a frequency between 55% and 80%, all other chemokines were detectable in more than 90% of the samples. The data showed great variability in the levels of cytokines and chemokines expressions among individuals, Figure 2.1. The levels of mediators can be categorized

into three concentration ranges; high (>100 pg per 30-s sample), intermediate (100-10 pg per 30-s sample) and low (< 10 pg per 30-s sample) levels of expression. We found that macrophage inhibitory factor (MIF), a neutrophil chemokine, was the most abundant chemokine by far in all the samples examined, with a mean value 2683.5 ± 985.82 pg per 30-s sample, Figure 2.1.

The next most abundant chemokines were IL-8/CXCL8, Gro-α/CXCL1, ENA-78/CXCL5, also major neutrophil chemokine, with mean values 170.98, 160.42 and 137.76 pg per 30-s sample, respectively. Intermediate level of expression mediators included IL-16, MIG/CXCL9, 6CKINE/CCL21, IL-1β, TECK/CCL25, IP-10/CXCL10, and Gro-β/CXCL2.

The neutrophil chemokine GCP-2/CXCL6 were among the low expressed mediators. Inflammatory cytokines including IL-6, TNF-α, and IFN-γ had low expression levels with mean values of 3.37, 1.76 and 0.92 pg per 30s sample, correspondingly. Myeloperoxidase (MPO) which is a marker for neutrophil was also quantified in the GCF by ELISA (Cao and Smith 1989). Significant variability was observed in the number of neutrophils among the healthy subjects, Figure 2.3. The mean MPO value was 163.16 ± 92.21 ng per 30-s sample ranging from 46.25 to 419.39 ng per 30-s sample.

The association between different neutrophil chemokines (GRO-α/CXCL1, GRO-β/CXCL2, ENA-78/CXCL5, GCP-2/CXCL6, IL-8/CXCL8, and MIF) and the neutrophil marker MPO was performed using Spearman's rank-order correlation tests, Figure 2.2. Only MIF, GCP-2/CXCL6, IL-8/CXCL8 showed a significant correlation with MPO. The highest correlation was between MPO and IL-8/CXCL8 ($r = 0.54$, $P = 0.0.14$). A strong correlation was observed between IL-8/CXCL8 and ENA-78/CXCL5 ($r = 0.94$, $P < 0.001$).

Table 1: Gingival crevicular fluid mediators (mean ± SD).

	Mean	SD	Min.	Max.
MPO	163155.32	92211.90	46252.40	419392.40
MIF	2683.54	985.82	1202.22	5028.19
IL-8/CXCL8	170.98	176.96	12.22	832.26
Gro-α/CXCL1	160.42	94.21	9.67	289.83
ENA-78/CXCL5	137.76	76.02	0.00	287.12
IL-16	100.09	66.73	8.89	236.24
MIG/CXCL9	81.25	159.10	2.33	679.05
6CKINE/CCL21	55.30	59.94	10.56	251.11
IL-1β	51.39	37.23	7.02	135.58
TECK/CCL25	43.07	16.71	16.87	80.61
IP-10/CXCL10	18.69	36.09	0.18	127.78
Gro-β/CXCL2	11.64	9.15	0.00	34.13
GCP-2/CXCL6	9.86	9.50	1.07	38.14
SDF-1α+β/CXCL12	4.42	2.02	1.54	8.70
MIP-3β /CCL19	4.38	3.27	0.31	12.41
FRACTALKINE/CX3CL1	3.87	3.02	1.30	12.66
MIP-1δ/CCL15	3.42	4.57	0.43	21.29
IL-6	3.37	8.47	0.16	38.92
MIP-1α/CCL3	2.92	3.49	0.17	15.21
MCP-3/CCL7	2.76	2.90	0.00	11.01
MCP-4/CCL13	2.23	1.34	0.19	4.20
I-309/CCL1	2.13	1.85	0.00	6.54
TNF-α	1.76	1.79	0.46	8.69
SCYB16/CXCL16	1.32	1.76	0.11	7.55
EOTAXIN-3/CCL26	1.12	1.19	0.00	4.63
MIP-3α/CCL20	0.96	1.78	0.09	7.86
IFN-γ	0.92	0.54	0.30	2.65
EOTAXIN/CCL11	0.88	0.38	0.34	1.89
BCA-1/CXCL13	0.86	1.03	0.09	3.64
MCP-1/CCL2	0.82	1.11	0.10	5.05
MDC/CCL22	0.81	0.58	0.16	2.71
TARC/CCL17	0.74	0.68	0.00	2.33
IL-10	0.69	0.32	0.13	1.31

GM-CSF	0.67	0.76	0.00	2.17
MPIF-1/CCL23	0.49	0.30	0.07	1.23
I-TAC/CXCL11	0.46	0.59	0.04	1.95
CTACK/CCL27	0.45	0.28	0.13	1.20
IL-4	0.25	0.21	0.00	0.75
MCP-2/CCL8	0.18	0.32	0.02	1.45
IL-2	0.17	0.10	0.03	0.44

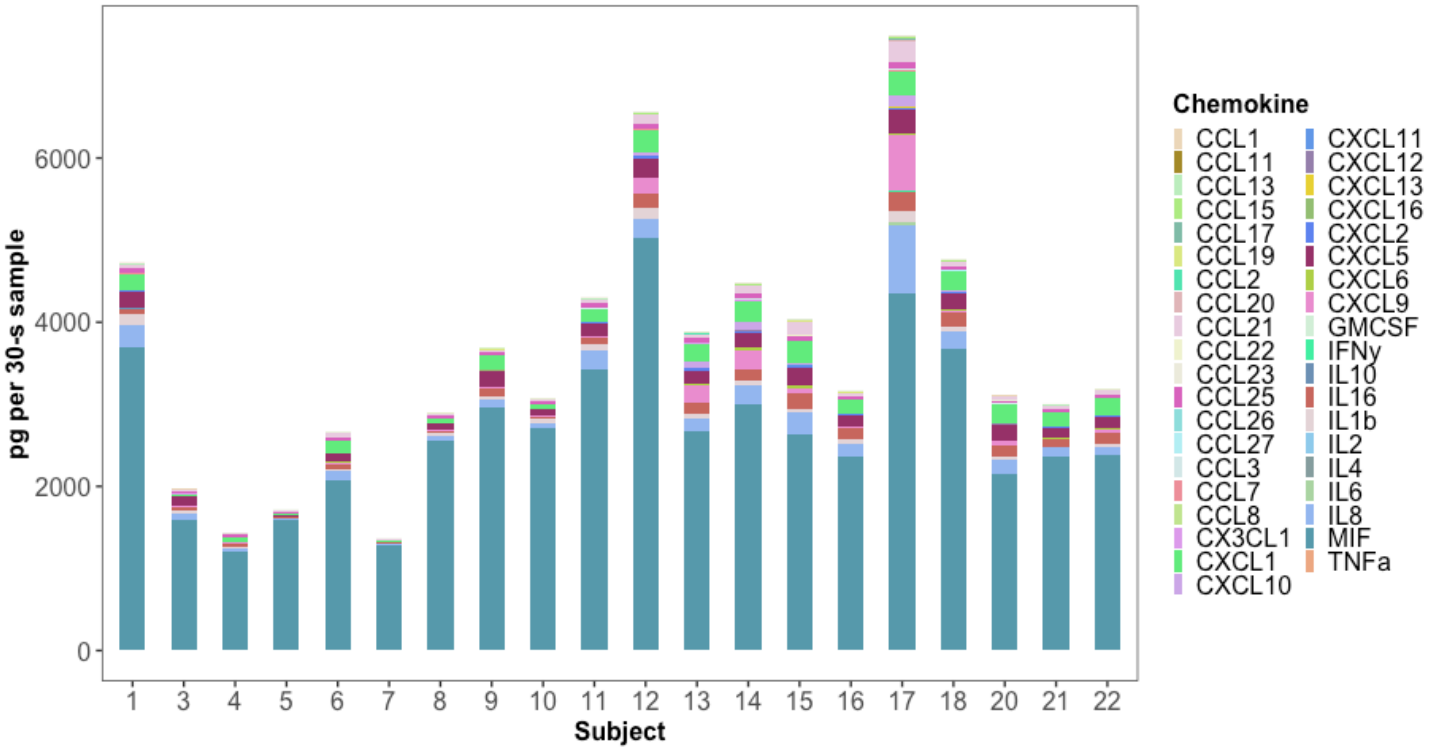

Figure 2.1: Variability in the chemokine profiles among study subjects.
Bar plot of the GCF chemokines total amount (pg per 30-s sample) among study participants. MIF is the most abundant chemokine in healthy GCF.

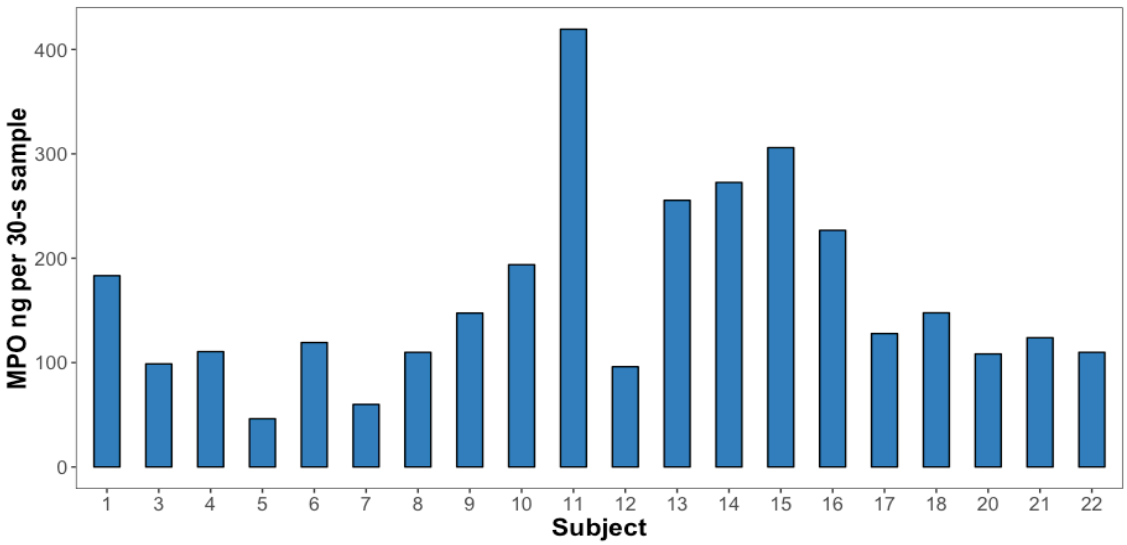

Figure 2.3: Variability in MPO total amount (ng per 30-s sample) among study subjects.
The total number of neutrophils is variable in the GCF of healthy subjects.

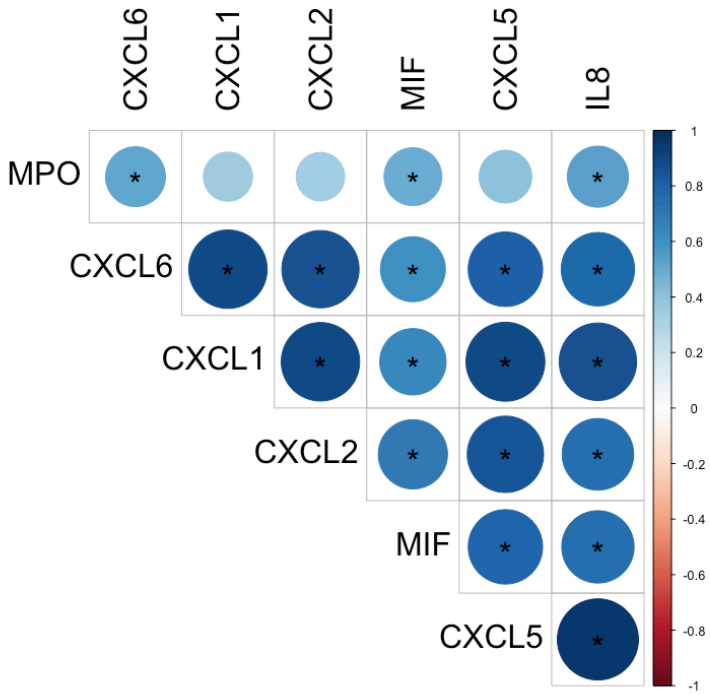

Figure 2.2: Spearman Correlation correlogram based on hierarchical clustering between MPO and different neutrophil chemokines.
Strong correlations between different neutrophil chemokines and neutrophil marker (MPO) in gingival health. Correlation coefficients are expressed by color scale from red to blue. Blue designate a positive correlation while red color designate a negative correlation. Significant correlations $*p< 0.05$

2.1.6.2 Inter-individual variability in the chemokines profiles

To explore variability in chemokine profiles between individuals, hierarchical clustering analysis based on chemokine profiles was performed. Clustering analysis generated two groups with different intensities of chemokine patterns, the high and low expression groups, Figure 2.4. High expression group, which included 9 participants, was associated with overall higher chemokine expression levels. In comparison, the low group represented by 11 participants showed overall lower chemokine profiles. Neutrophil chemokines including MIF, IL-8/CXCL8, Gro-α/CXCL1, and ENA-78/CXCL5, and other cytokines such as IL-1β, TNF-α, and IFN-γ were among the differentially expressed mediators between the two groups. Principal component analysis (PCA) was used to visualize the chemokines data, each point in Figure 2.6 represents the chemokine profile of each participant. The first principal component (PC1) explained 89.77% of the variation of the data and the second principal component (PC2) explained 10.32%. Individuals with similar chemokine profile formed two distinct groups, corresponding to the hierarchical groups identified based on chemokine expression intensities.

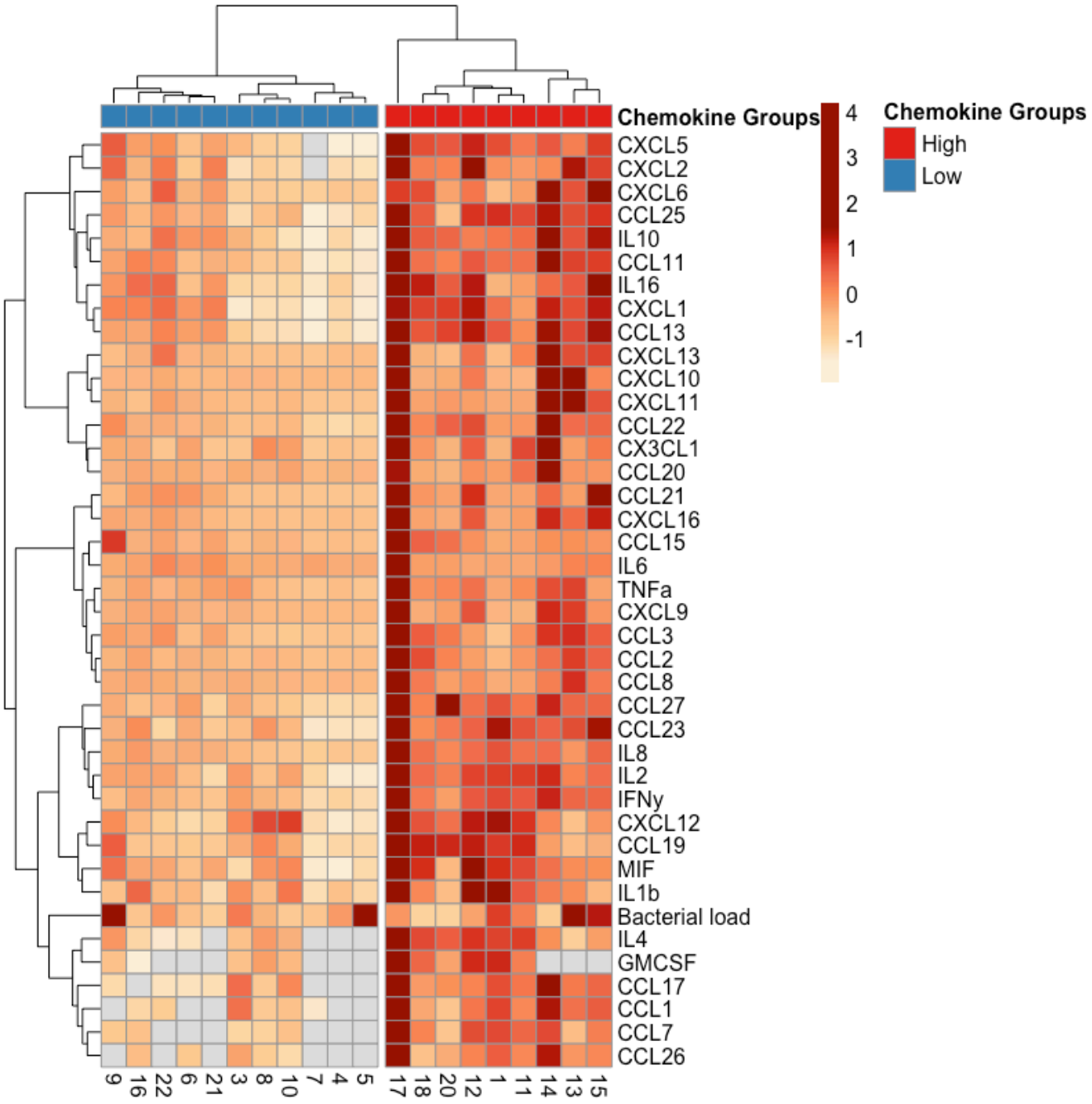

Figure 2.4: Z-score heatmap of GCF chemokine expression.
Clustering analysis based on the chemokine expression patterns generated two groups high (red) and low (blue).
Columns are subjects and rows are chemokines. Color scale for heatmap appears in the top right high expression in red and the low expression in orange. Color bars in the right depict annotation according to chemokine profile (columns)

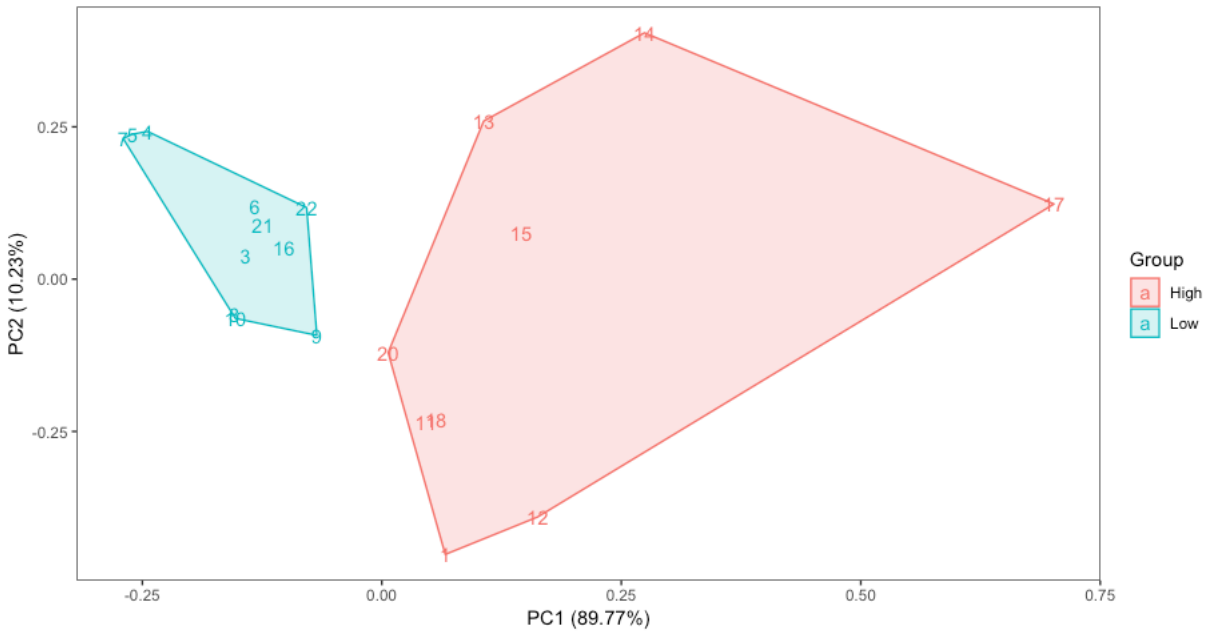

Figure 2.6: Principal component analysis (PCA) of the chemokines for all study subjects.
Complete separation of the groups was evident based on the chemokines profiles. Each points on the graph represents one Subject. Each color represents one group; high in red and low in blue.

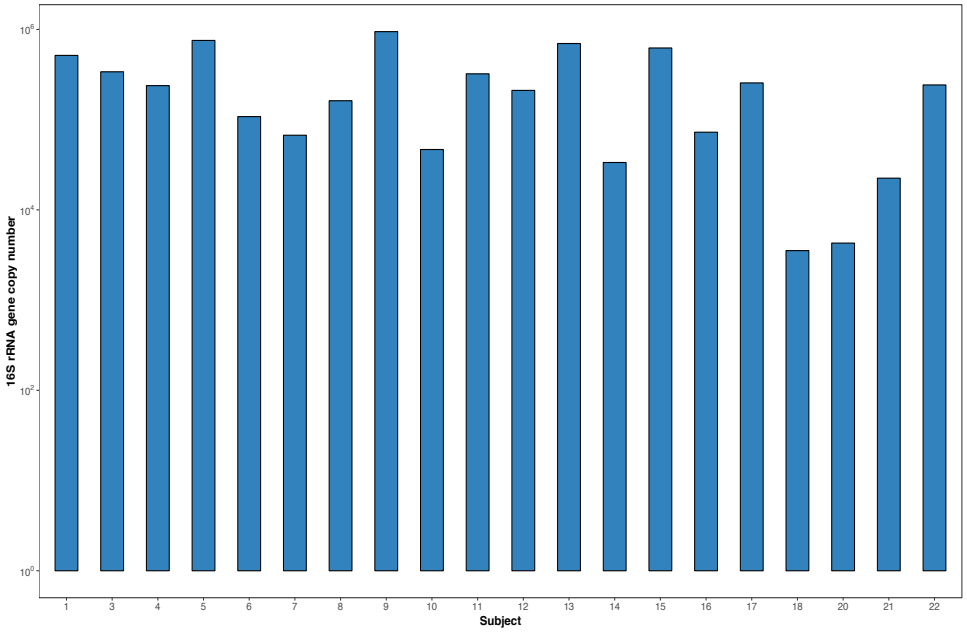

Figure 2.5: Variability in the bacterial load of subgingival plaque among study participants.
The copy number of 16S rRNA genes represent the total bacterial load for each participant.

2.1.7 Microbial results

2.1.7.1 Bacterial load of the subgingival plaque

Total bacterial load was quantified with real-time PCR for 16S rRNA. The subgingival bacterial load for study participants is shown in Figure 2.5. The average microbial load was approximately 10^5 mean copy numbers. The lowest and highest mean bacterial load were $10^{3.5}$ and 10^6, respectively.

2.1.7.2 Sequencing summary

The bacterial 16S rRNA gene V3-V4 region sequencing resulted in a total of 6736 identified amplicon sequence variants (ASVs) in 20 samples. A total of 863,833 reads were obtained from sequencing with 43191.65 average and 3,3851 median numbers of reads per sample. The maximum and minimum reads per sample were 142,220 and 1,414, respectively. Approximately, 0.77 % of the OTUs are singletons. In the subgingival plaque samples, a total of 10 phyla, 23 classes, 37 orders, 121 genera, and 427 species were identified.

2.1.7.3 Alpha diversity of the subgingival bacterial communities

The alpha diversity, within sample, was calculated using four different metrics at the species level. Alpha diversity indices were highly variable between samples, Figure 2.7. The species richness as measured by the observed number of species was ranging from 43 to 271 species with a mean value of 152.95 observed species per sample. The subgingival community diversity was estimated by the Shannon and Inverse Simpson index where the mean scores of 3.5 and 17.2, respectively. Faith's phylogenetic diversity index mean value was 13.88 with 6.25 minimum and 22.22 maximum scores.

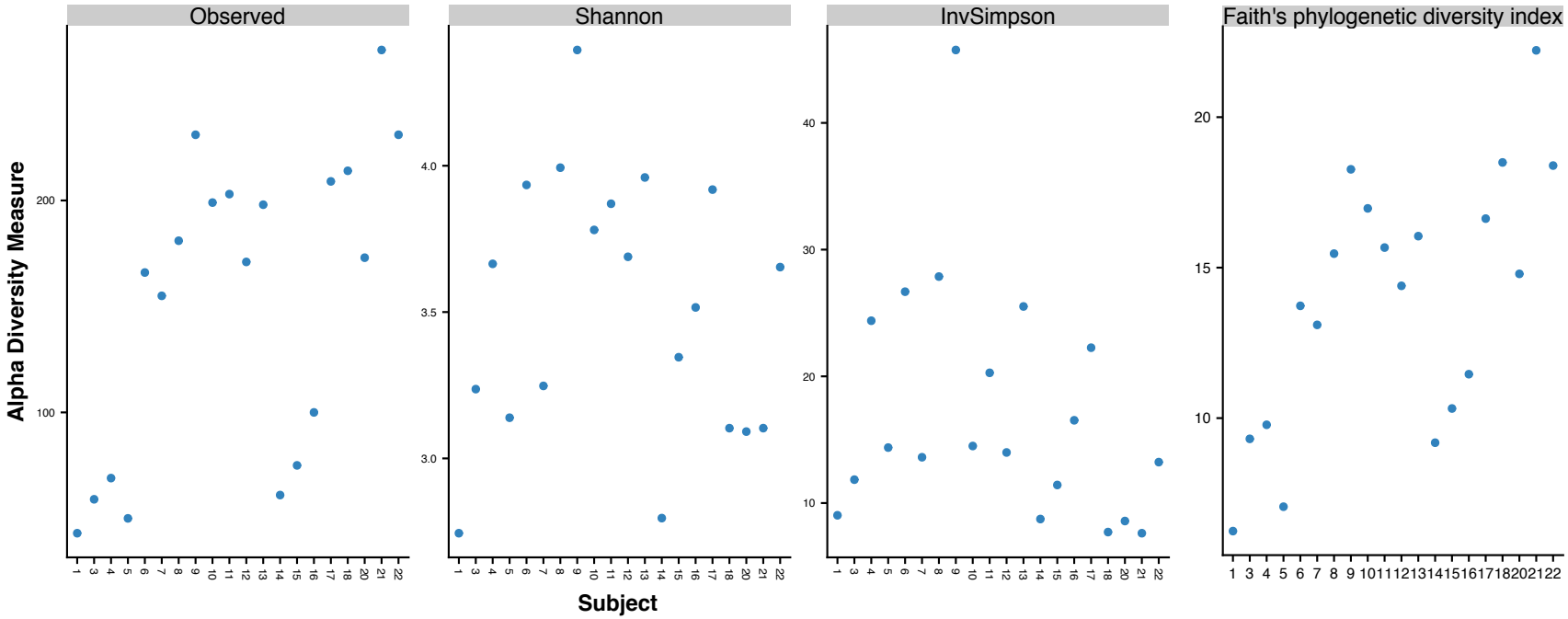

Figure 2.7: Variability in the different alpha diversity indexes among study subjects.
Diversity was measured using observed species, Shannon index, Inverse Simpson index and Faith's phylogenetic diversity index.

2.1.7.4 Microbial composition of the subgingival plaque

Great inter-individual variation in the diversity and abundance of the compositional profile was seen. Five phyla were predominant in all subjects; Firmicutes (37.9%), Proteobacteria (19.6%), Bacteroidetes (16.3%), Fusobacteria (12.3%), and Actinobacteria (11.3%). Conversely, Saccharibacteria_(TM7), Spirochaetes, Gracilibacteria_(GN02), Absconditabacteria_(SR1) and Synergistetes were found in low relative abundances in the study samples, Figure 2.8. Top fifteen genera identified in all samples were *Streptococcus, Haemophilus, Fusobacterium, Prevotella, Veillonella, Actinomyces, Porphyromonas, Neisseria, Leptotrichia, Corynebacterium, Rothia, Capnocytophaga, Gemella, Alloprevotella, and Saccharibacteria_(TM7)_[G-1]* representing 75% of the plaque microbiome, Figure 2.9. The most abundant species were *Streptococcus tigurinus* (13.3%), *Streptococcus parasanguinis* (6.3%), *Haemophilus parainfluenzae* (5.3%), *Veillonella dispar* (3.2%), *Haemophilus influenzae (2.9%), Fusobacterium nucleatum subsp. animalis (2.7%), Corynebacterium matruchotii (2.7%), Fusobacterium nucleatum_subsp._polymorphum* (2.3%), Prevotella pleuritidis (1.8%), and *Gemella haemolysans* (1.7 %), Figure 2.10.

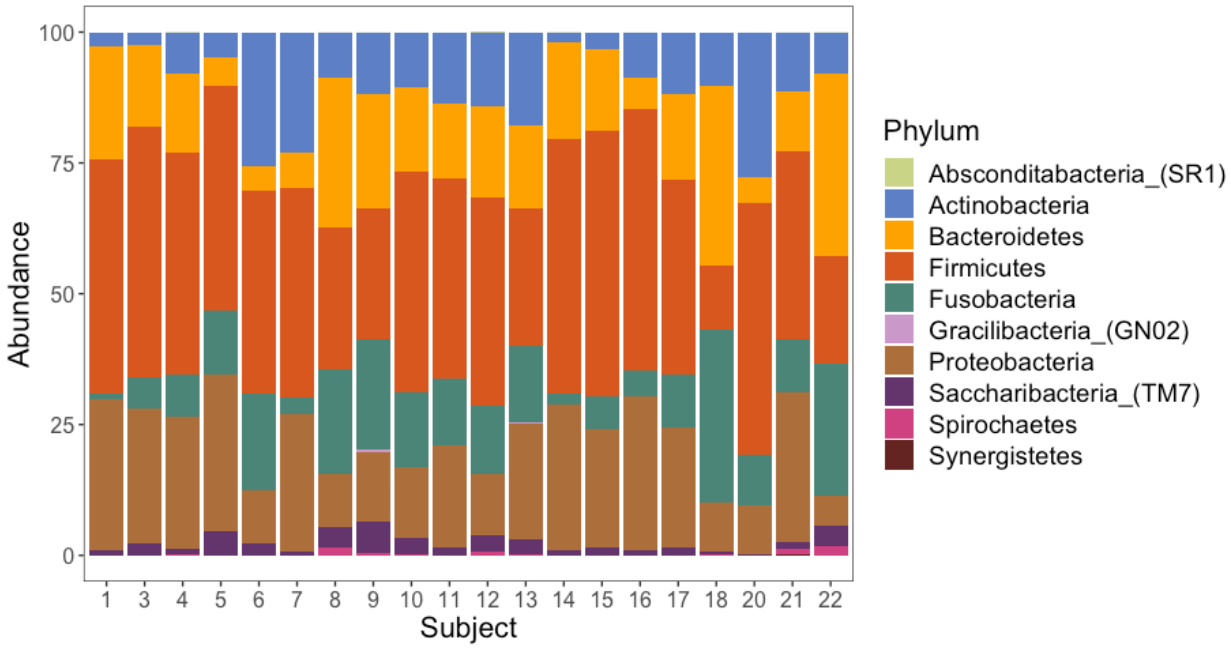

Figure 2.8: Taxonomic profiles at the phylum level.
Bar plot displaying relative abundances of the different phyla among study subjects. Five phyla were predominant in all subjects; Firmicutes, Proteobacteria, Bacteroidetes, Fusobacteria, and Actinobacteria.

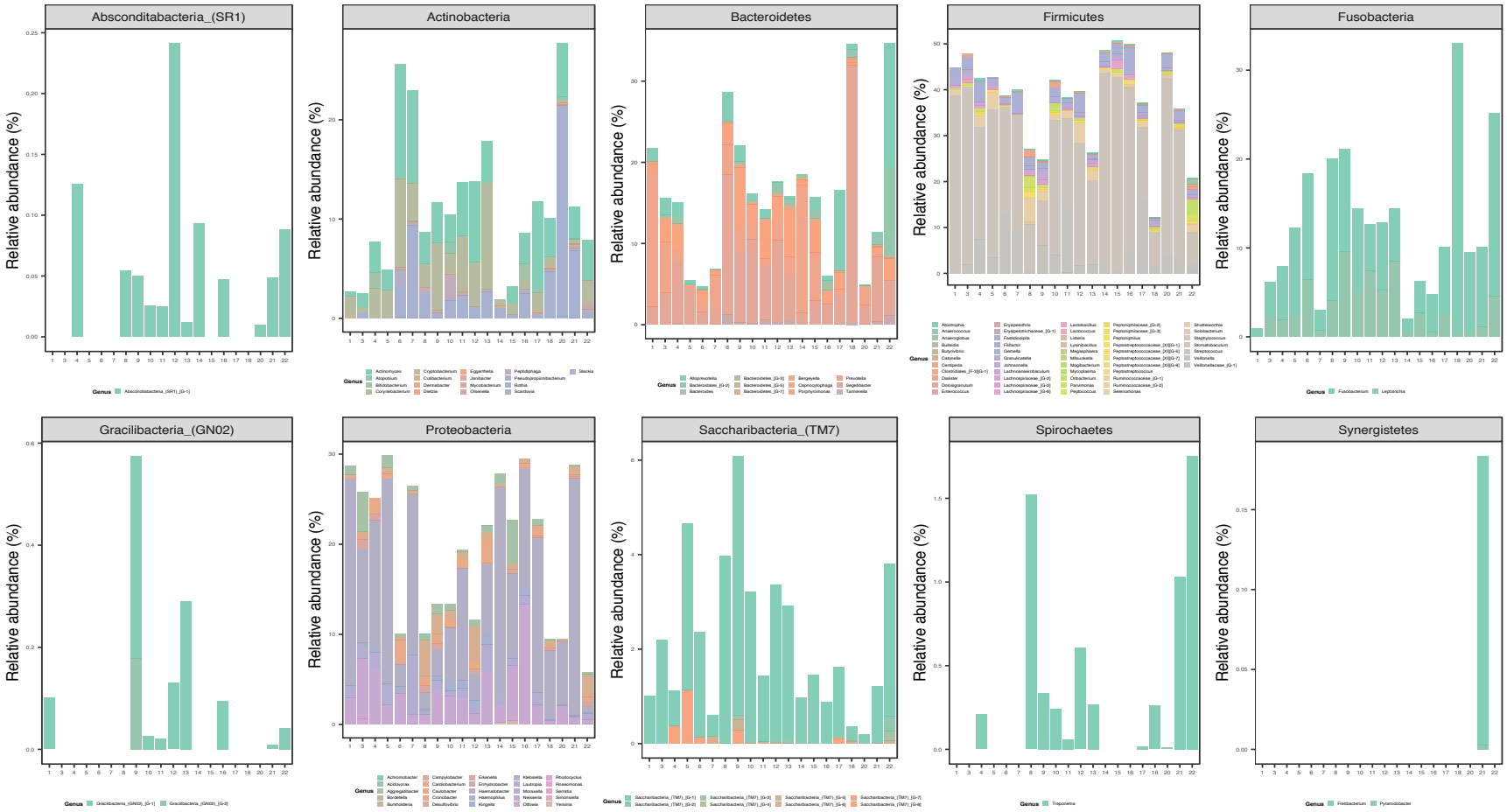

Figure 2.9: Relative abundances of the microbial community at the genus level in the different phyla.
Bar plots displaying relative abundance within each study subject. Great variability was observed in the compositional profile among study subjects.

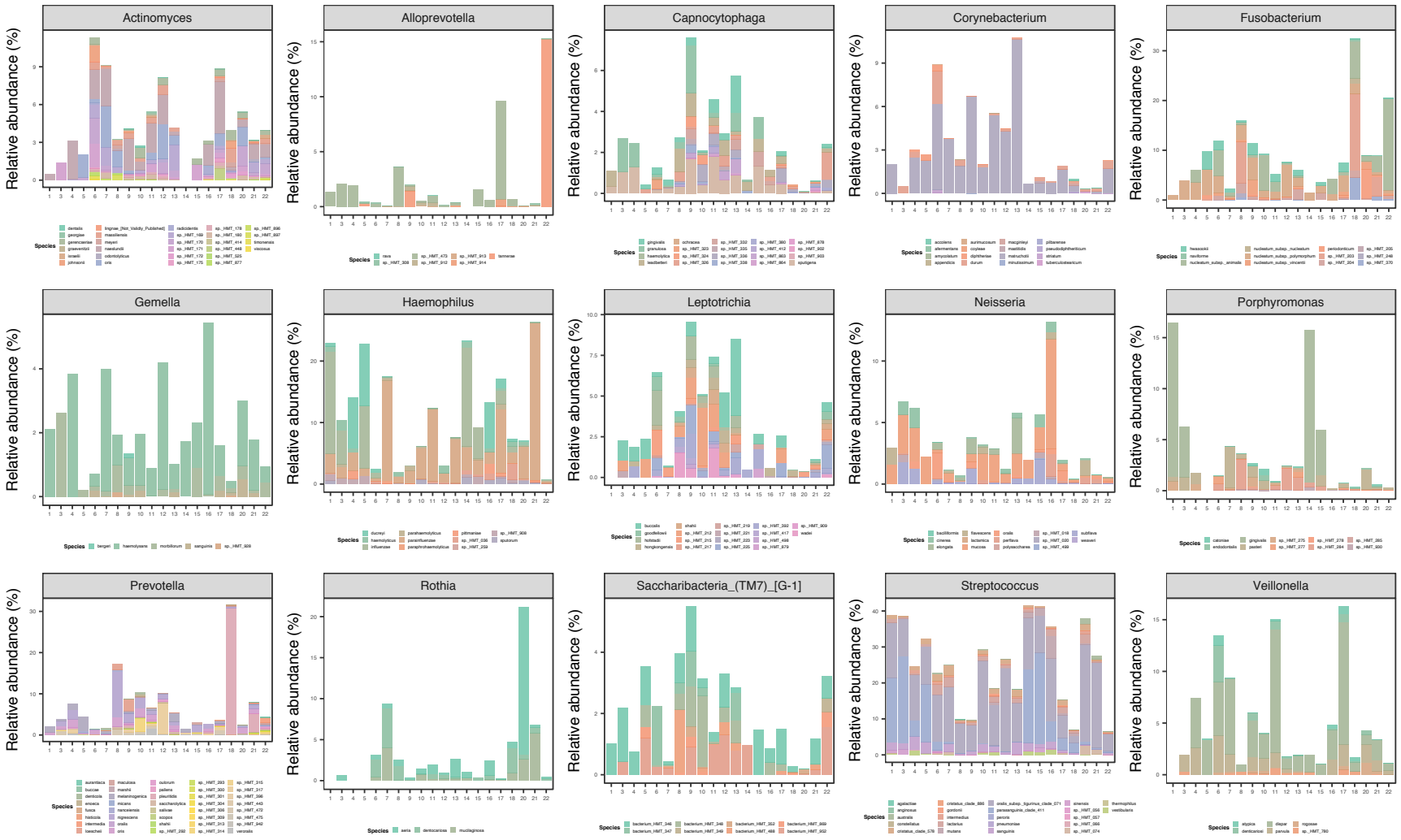

Figure 2.10: Relative abundances of at the species level for the top fifteen abundant Genera.
Bar plots displaying relative abundance within each study subject. Great variability was observed in the compositional profile among study subjects.

The phylum Firmicutes was dominated by the genus *Streptococcus* (25.4%), *Veillonella* (5%), *Gemella* (2.1%), *Selenomonas* (1.5%), and Granulicatella (0.7%) among study participants. The genus *Streptococcus* was dominated by *Streptococcus tigurinus* (13.3%) and *Streptococcus parasanguinis* (6.3%), *Streptococcus sanguinis* (1.5%), *Streptococcus lactarius* (1.1%), *Streptococcus crista* (1%), and *Streptococcus mutans* (0.6%).

The genus *Veillonella* was mainly represented by *Veillonella dispar* (3.2%) and *Veillonella parvula* (1%). The representative for the genus *Gemella* was *Gemella haemolysans (1.7%),* for *Selenomonas was Selenomonas noxia* (0.3%), and for *Granulicatella* were *Granulicatella elegans* and *Granulicatella adiacens*.

The second highest abundant phylum was Proteobacteria, which was dominated by the genus *Haemophilus* (11.4%), *Neisseria* (3.3%), *Lautropia* (1.3%), *Campylobacter* (1.0%), and *Aggregatibacter* (1.0%). The genus *Haemophilus* was represented mainly by *Haemophilus parainfluenzae* (5.3%) and *Haemophilus influenzae* (2.9%). The genus *Neisseria* was dominated by *Neisseria mucosa* (1.6%), and the genus *Lautropia* was represented by *Lautropia mirabilis* (1.3%). *Campylobacter gracilis* (0.5%), *Campylobacter showae* (0.4%), and *Campylobacter concisus* (0.1%) dominated the genus *Campylobacter*. *Aggregatibacter* was represented mainly by unclassified Aggregatibacter and *Aggregatibacter aphrophilus.*

The third dominant phylum was Bacteroidetes: *Prevotella* (6.8%), *Porphyromonas* (3.5%), *Capnocytophaga* (2.3%), and *Alloprevotella* (2.1%). *Prevotella pleuritidis* (1.8%), *Prevotella nigrescens* (1.3%), *Prevotella oris* (0.8%), and *Prevotella melaninogenica* (0.6%) represented the Genus *Prevotella.* The genus *Porphyromonas* was dominated by *Porphyromonas gingivalis* 2.0 % and *Porphyromonas pasteri* (0.7%). The gram negative *Capnocytophaga* was dominated by

Capnocytophaga sputigena, Capnocytophaga, Capnocytophaga leadbetteri, and *Capnocytophaga gingivalis.*

The phylum Fusobacteria was represented by the genus *Fusobacterium* (8.9%) and *Leptotrichia* (3.3%). *Fusobacterium nucleatum_subsp._animalis* (2.7%) and *Fusobacterium nucleatum_subsp._polymorphum* (2.3%) formed the majority of the genus *Fusobacterium.* *Leptotrichia buccalis* and unclassified *Leptotrichia* dominated the genus *Leptotrichia.*

The phylum Actinobacteria was dominated by *Actinomyces* (4.3%), *Corynebacterium* (3.1%) and *Rothia* (3.0%). The genus *Actinomyces* was dominated by *Actinomyces* naeslundii (1.3%), *Actinomyces oris* (0.3%), *and unclassified Actinomyces.* The Genus *Rothia* was represented by three species *Rothia aeria* (1.4%), *Rothia mucilaginosa* (0.8%), and *Rothia dentocariosa* (0.8%). *Corynebacterium* genus was dominated by *Corynebacterium matruchotii* (2.7%) *and Corynebacterium durum* (0.3%).

The phylum Spirochaetes was represented by the genus *Treponema* which was dominated by *Treponema socranskii* while two genera represented the phylum Synergistetes: *Fretibacterium* and *Pyramidobacter* which was only present in one subject (#021).

The low abundant phylum Saccharibacteria_(TM7) was represented by the genus Saccharibacteria_(TM7)_[G-1] (2%), while Gracilibacteria_(GN02) and Absconditabacteria_(SR1) were dominated by unclassified species.

2.1.7.5 The core microbiome of the subgingival plaque

Although the microbiome composition was highly variable between subjects, some OTUs were present in most individuals, representing the core subgingival microbiome in the healthy plaque samples. The highly prevalent species associated with health that were present in all samples at the minimum detection threshold of 0.1% relative abundance included five

Streptococcus spp.: *Streptococcus sanguinis, Streptococcus parasanguinis, Streptococcus tigurinus, Streptococcus crista,* and *Streptococcus lactarius* in addition to *Neisseria mucosa,* Figure 2.11. Furthermore, by reducing the stringency in the prevalence threshold to 50%, a total of 26 out of the 427 identified species were shared by ≥ 50% of subjects at abundances of at least 0.1% and accounted for 41.79%, range from 13.37 to 63.24%, of the total plaque microbiome in each subject. These health-associated species belonged to 13 genera including: *Streptococcus, Fusobacterium, Haemophilus, Veillonella, Rothia, Granulicatella, Gemella, Prevotella, Cardiobacterium, Capnocytophaga, Neisseria, Actinomyces,* and *Lautropia.* The core species comprised six *Streptococcus spp*., four *Fusobacterium spp*., two *Haemophilus spp.*, two *Veillonella spp*., *two Granulicatella spp.,* and two *Rothia spp.*, in accordance to previous reports (Griffen, Beall et al. 2012, Abusleme, Dupuy et al. 2013). In addition, eight individual species belonging to different genera were part of the core microbiome; *Actinomyces naeslundii, Capnocytophaga sputigena, Cardiobacterium hominis, Gemella haemolysans, Lautropia mirabilis, Neisseria mucosa, Prevotella nigrescens, and Saccharibacteria_(TM7)_[G-1] bacterium_HMT_346.*

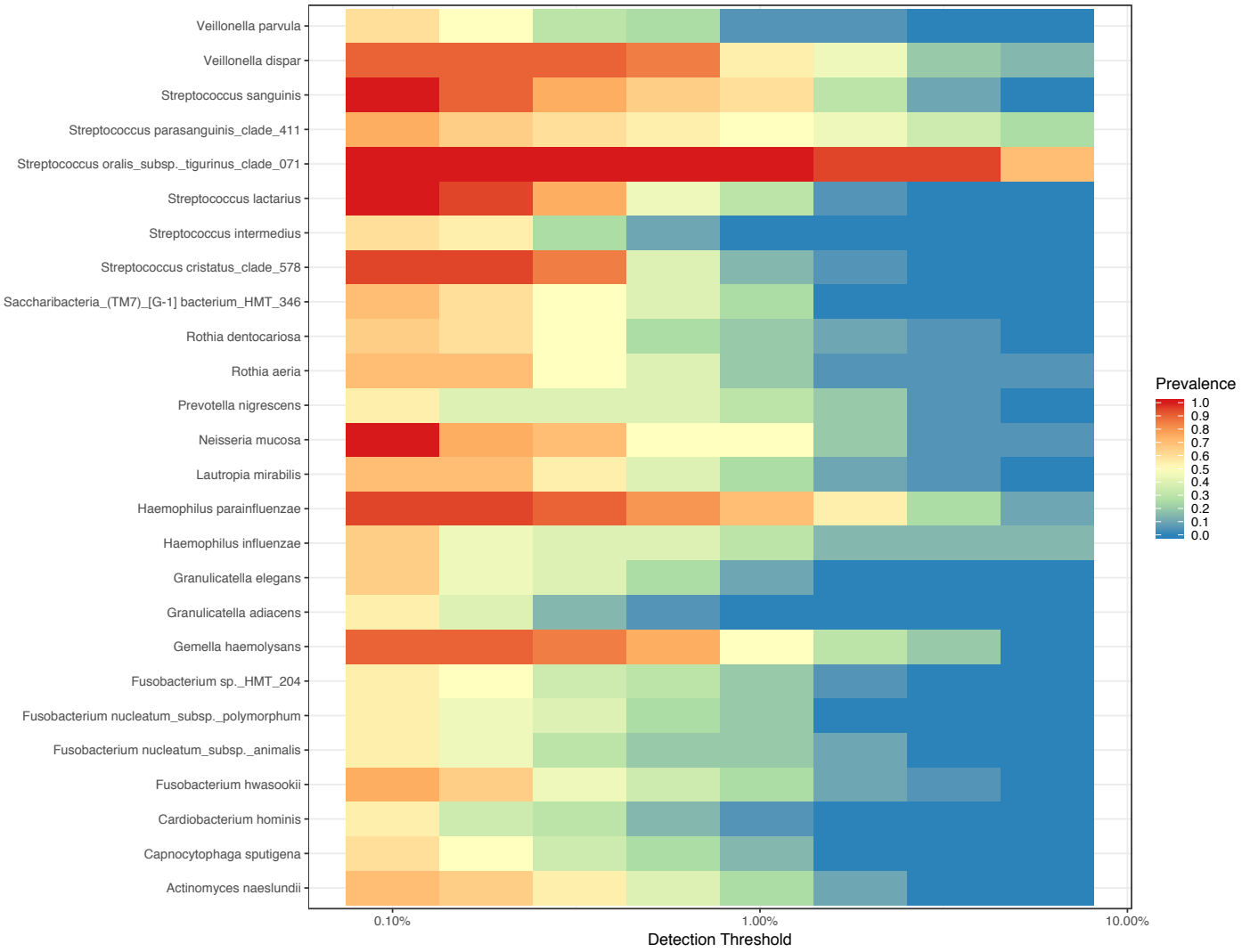

Figure 2.11: Core microbiome in the subgingival plaque.
The core species identified in the healthy subgingival microbiome shared by 50% of subjects and at 0.1% abundance.

2.1.7.6 Inter-individual variability of the subgingival bacterial communities

The difference in the microbial communities between study subjects was investigated by clustering technique. Hierarchical clustering of study subjects based on species abundance resulted in subjects separation into two clusters. The heatmap in Figure 2.12 shows the relationship of subjects microbial profiles in the different clusters (cluster A and cluster B). The microbiome of cluster A was mainly dominated by Firmicutes and Proteobacteria, meanwhile, the cluster B was dominated by Fusobacteria, Bacteroidetes, and Actinobacteria.

The microbial community membership and structure were further investigated by performing beta diversity analysis using Bray-Curtis and UniFrac distance matrices. Non-metric multidimensional scaling (NMDS) plots of the beta diversity analysis showed, similar to hierarchical clustering, separation of the study participants' bacterial community into two distinct clusters, Figure 2.13 A and B. Partitioning of the microbial community confirmed that the microbial composition is different between the individuals belonging to the different clusters.

Differential abundance analysis was performed to identify species that were responsible for overall community differences between the clusters. LEfSe analysis identified the most differentially abundant taxa at the species level between the two clusters, Figure 2.14. Cluster B was statistically significantly associated with health-associated and core species in accordance with previous reports (Griffen, Beall et al. 2012, Abusleme, Dupuy et al. 2013). The signature species for cluster A was a mixture of health-associated, core and periodontitis-associated species, *Porphyromonas gingivalis* were among abundant species for cluster A, which have a well-known association with periodontitis.

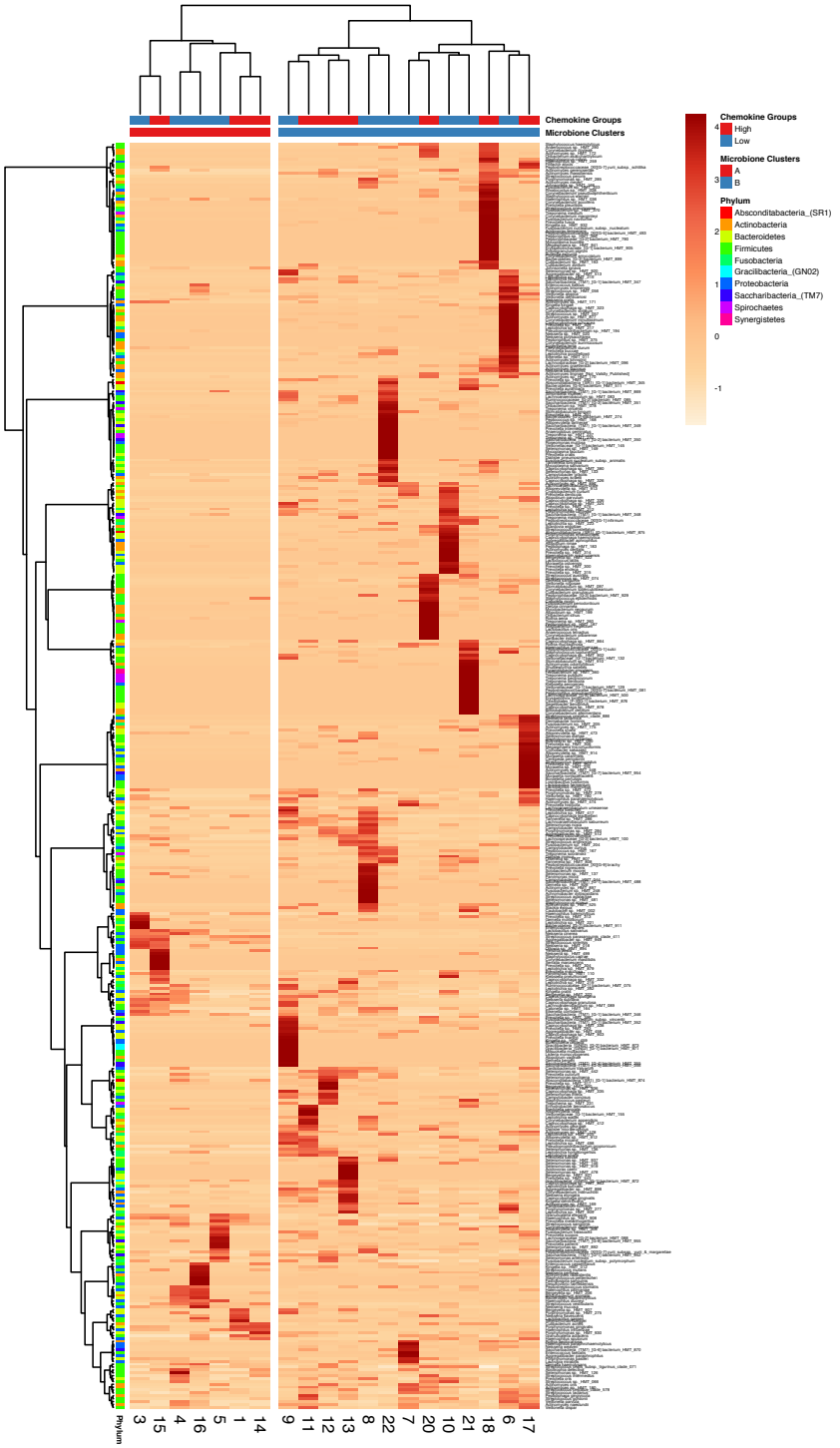

Figure 2.12: Z-score heatmap of relative abundance for the species found in the subgingival microbial communities.
Clustering analysis based on the microbial profile generated two clusters; A (red) and B (blue). Each row corresponds to species and each column represent study subject. Color scale for heatmap appears in the top right with the most abundant species in red and the least abundant in orange. Color bars in the right depict annotation according to chemokine profile groups and microbiome profile clusters (columns) and phylum (rows).

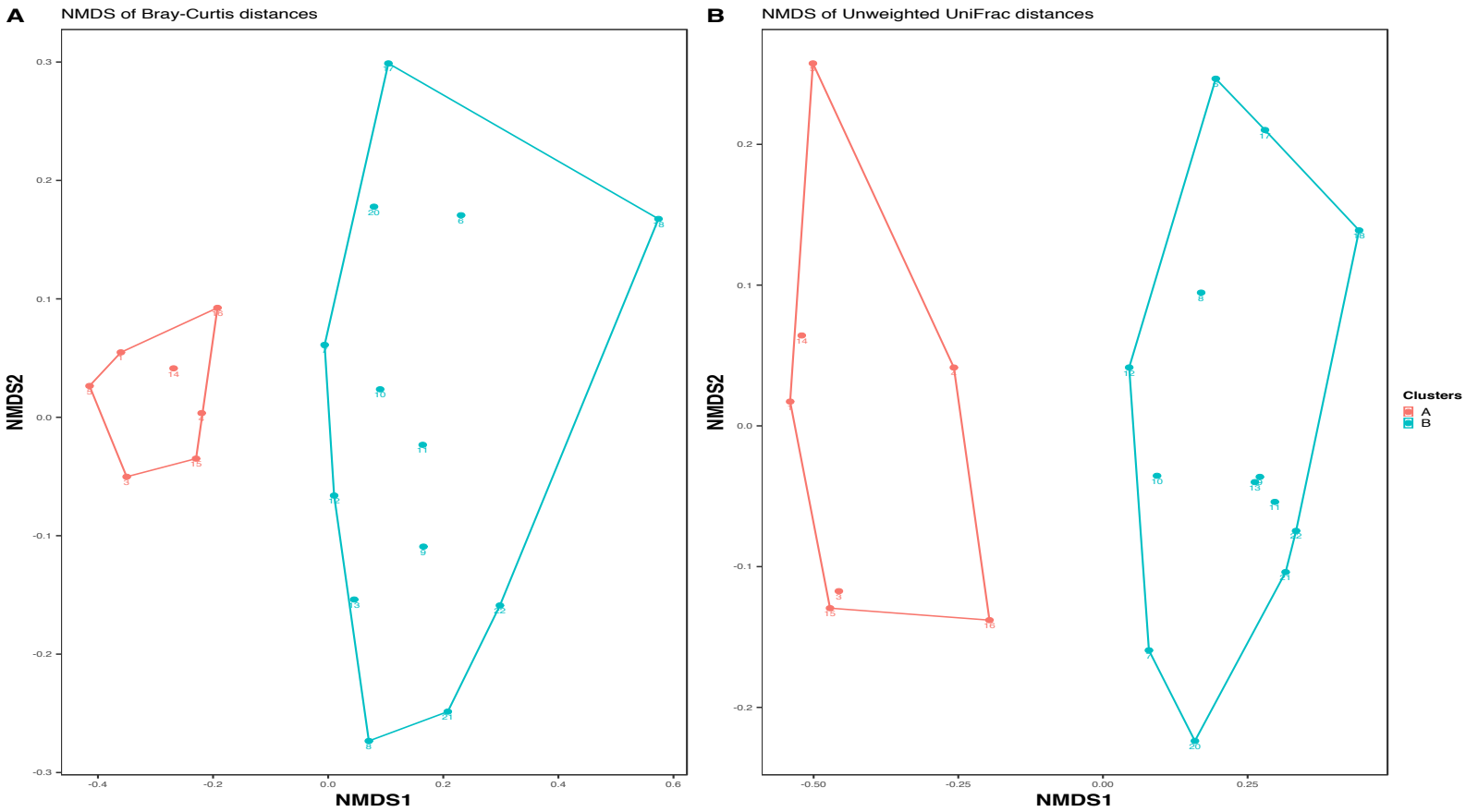

Figure 2.13: Non-metric multidimensional scaling (NMDS) plots of subgingival samples according to bacterial composition.

NMDS were performed with (A)Bray-Curtis dissimilarity, (B)Unweighted Unifrac distance matrix. Complete separation of the clusters was evident based on the microbial profile. Each points on the graph represents one Subject. Each color represents one cluster; A in red and B in blue.

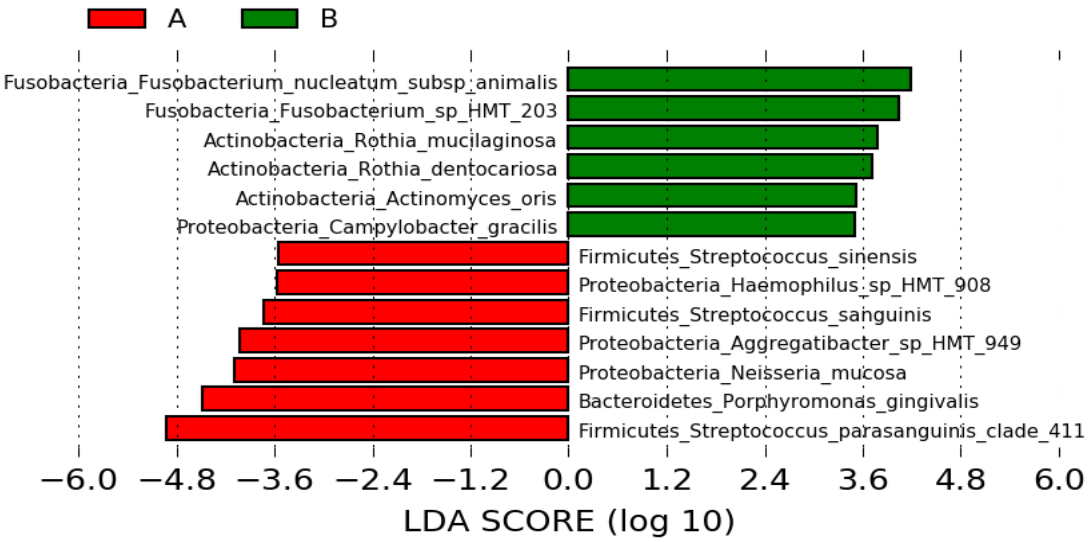

Figure 2.14: Differential abundant taxa based on LEfSe analysis in the different microbiome clusters.
Bars represent linear discriminant analysis scores (LDA) and can be interpreted as the degree of difference in relative abundance. Cluster A in red and cluster B in green.

2.1.7.7 Correlations between chemokines and the subgingival bacterial communities

Correlations between chemokines and the microbial relative abundances at the genus and at species levels were investigated. The Mantel test revealed non-significant concordance between combined chemokines and microbiome at the genus level in the healthy group (Mantel statistic r = 0.03, P =0.3). Spearman's Rank-Order correlations test revelated positive correlations between core species and MIF, Gro-β/CXCL2, and MIP-1δ/CCL15, Figure 2.15 On the other hand, core microbiome was negatively correlated with I-309/CCL1, TARC/CCL17, and EOTAXIN-3/CCL26. *Haemophilus influenzae* and *Streptococcus parasanguinis* exhibited a positive correlation with most of the assayed chemokines however showed a negative correlation with all other core specie.

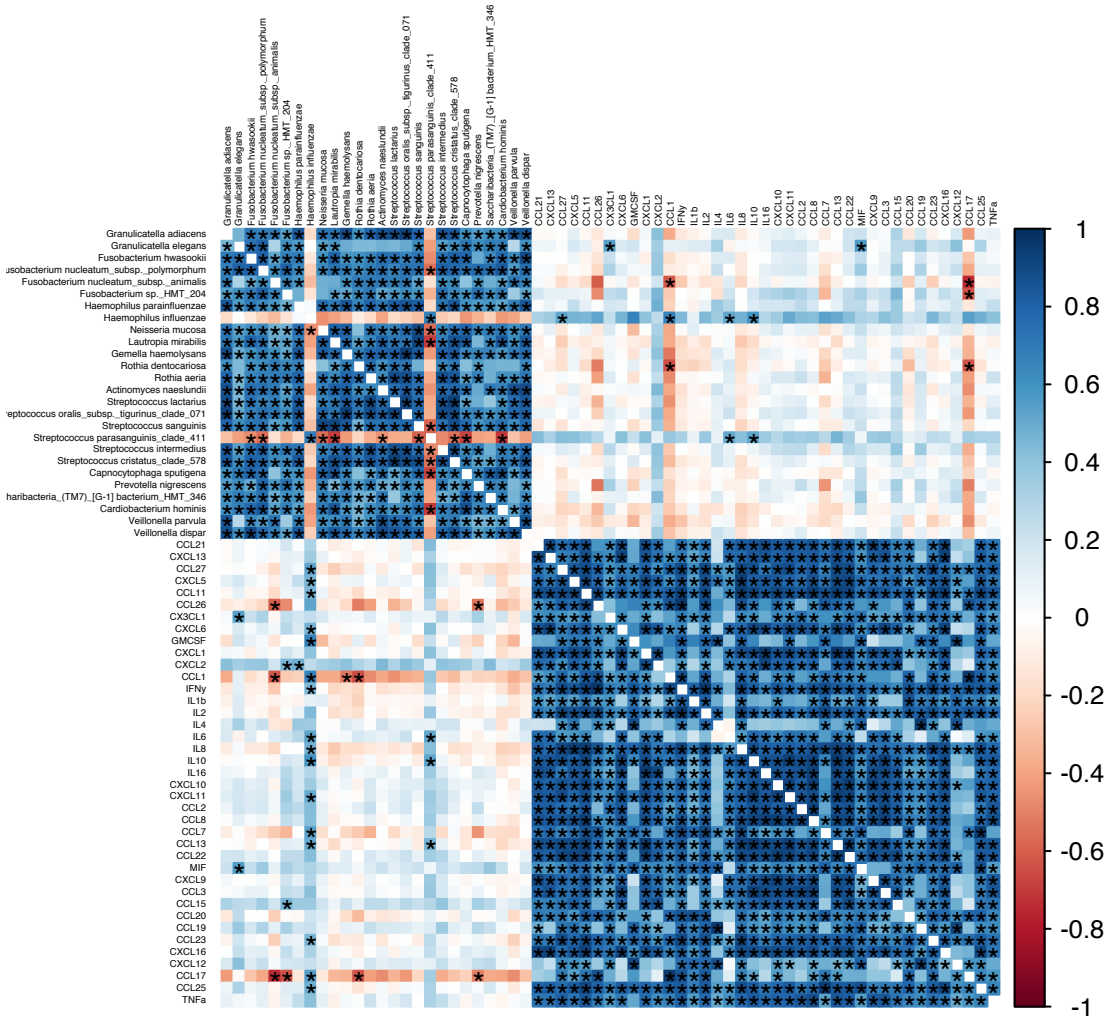

Figure 2.15: Spearman Correlation heatmap between core species relative abundances and chemokines.

Correlations between major neutrophil chemokines and core species was evident.

Correlation coefficients are expressed by color scale from red to blue. Blue designate a positive correlation while red color designate a negative correlation. Significant correlations $*p< 0.05$

Discussion

This cross-sectional study aimed to investigate the combined profile of the subgingival microbiome and the major chemokines in health. The results showed significant inter-individual variability in chemokine expression patterns and subgingival microbial composition in health. Two different chemokine expression patterns were identified among study participants; however, the different groups did not share common microbiome profiles. Moreover, the Mantel test revealed no significant correlation between the microbiome composition and the chemokine profiles. The lack of concordance may be a reflection of the unique microbial composition of each individual coupled with variations in host response in health.

Chemokines are produced by a variety of cells in the periodontium, and play a significant role in inflammation by the selective recruitment and activation of immune cells. Imbalance in the cytokine and chemokine network has been connected to periodontal disease pathogenesis (Graves 2008). Previous investigations into the chemokine expression during the various stages of periodontal disease have been attempted with a subset of select chemokines and fail to provide a full description of the complex inflammatory networks. Therefore, these inflammatory networks and their involvement in the periodontal homeostasis needs further clarification (Preshaw and Taylor 2011).

In contrast to previous studies, this study utilizes bead-based multiplex immunoassays to simultaneously catalog the levels of forty chemokines in a single sample. To our knowledge, this is the first study that comprehensively examines these GCF mediators in the healthy gingival sulcus. Results reveal high degrees of variability among healthy individuals in regard to the total amount of measured chemokines, Figure 2.1. It has been shown that variations in chemokine production can be attributed to the microbiome composition, host factors and genetic variation

(Bakker, Aguirre-Gamboa et al. 2018). This inter-individual variation in chemokine profiles may influence immune responses to the plaque biofilm and hence periodontal disease susceptibility.

Several cytokines and chemokines that are known to be involved in periodontitis etiology were also detected in the clinically healthy GCF. One major finding of this study is that macrophage migration inhibitory factor (MIF), an important cytokine of the innate immune system, was the most abundant in all samples examined. MIF levels in GCF showed a significant positive correlation with neutrophil numbers as measured by MPO. MIF expression across the entire human gingival epithelium has been reported in contrast to human skin where MIF expression is localized only to the basal layer (Morimoto, Nishihira et al. 2003). High MIF expression levels in GCF may be explained by the continuous exposure of the gingiva to external stimuli which induce the constitutive expression of MIF by the epithelial cells. Therefore, MIF may have an important role in gingival health and disease but the exact function is not yet clear. Future studies are needed to further elucidate the participation of MIF in gingival homeostasis.

Neutrophil migration into the periodontal tissue is essential for maintaining homeostasis. Three major neutrophil chemokines IL-8/CXCL8, Gro-α/CXCL1, and ENA-78/CXCL5, which share the same chemokine receptors CXCR2, were among the most abundant chemokines detected in the GCF samples. IL-8/CXCL8 is secreted by different gingival cells but the highest expression is preferentially located to the junctional epithelium, which helps in regulating neutrophil influx to periodontal tissues (Tonetti, Imboden et al. 1998). Similarly, ENA-78/CXCL5, Gro-α/CXCL1, and GCP-2/CXCL6 are involved in neutrophil chemotaxis and activation (Kebschull, Demmer et al. 2009). Correlation analyses showed that IL-8 was highly associated with neutrophil migration as measured with MPO, and both ENA-78/CXCL5 and Gro-α/CXCL1. However, interestingly, there was no correlation between ENA-78/CXCL5 and neutrophil numbers. Similarly, no correlation was observed between Gro-α/CXCL1 and MPO. The lack of parallel relationships

between all three chemokines (IL-8/CXCL8, ENA-78/CXCL5, Gro-α/CXCL1) with neutrophil numbers indicates a complex chemokine network orchestrating neutrophil migration and activation in the periodontal tissue during health. Consistent with variability in chemokine expressions, there was significant variability in MPO in health. The strong correlations between the number of neutrophils (MPO) and neutrophil chemokines IL-8/CXCL8, MIF, and GCP-2/CXCL6, suggest that these could be the major neutrophil chemokines in health. These findings emphasize the important role of neutrophils in maintaining periodontal health, where they represent the first line of defense against microbial challenge.

In the periodontium, cytokines and chemokines interact and function in networks modulating the innate and adaptive immune responses (Preshaw and Taylor 2011). Host chemokines which facilitate chemotaxis of other immune cells including lymphocytes, natural killer cells, and dendritic cells were also detected in the healthy GCF. For example, IL-16, chemotactic for T cells, monocytes, and eosinophils; and TECK/CCL25, chemotactic for thymocytes, dendritic cells, and activated macrophages were among the most abundant chemokines in the GCF. Increased levels of TECK/CCL25 has been associated with deep pocket in periodontitis patients (Panezai, Ghaffar et al. 2017), while IL-16 low levels have been reported in diseased compared to healthy sites (Tsai, Tsai et al. 2005).

Assessing the expression patterns of a broad range of cytokines and chemokines in health will facilitate our understanding of their role in periodontal pathogenesis. Pro-inflammatory cytokines including IL-1β, IL-6 and TNF-α and IFN-γ which have a major role in the pathogenesis of periodontal disease were detected in the healthy GCF samples. The healthy gingival tissue is infiltrated by inflammatory cells which could be the source of inflammatory cytokines such as IL-1β in GCF (Rawlinson, Dalati et al. 2000). IL-1β is an inflammatory cytokine, which mediates the gingival inflammatory response, was detected in the healthy GCF similar to previous reports

(Preiss and Meyle 1994, Rawlinson, Dalati et al. 2000), and in contrast to Ishihara *et al.* which did not detect IL-1β in health (Ishihara, Nishihara et al. 1997). The correlation between the severity of gingival inflammation and the level of IL-1β in the GCF has been proposed as elevated IL-1β concentrations were found in diseased sites in comparison to healthy sites (Preiss and Meyle 1994). Anti-inflammatory cytokines IL-4 and IL-10 were also detected in the GCF, emphasizing the importance of the balance between pro-inflammatory and anti-inflammatory cytokines in the healthy periodontium.

Two distinct clusters were identified based on chemokine profiles in the healthy GCF. One group was associated with an overall higher chemokine expression in comparison to the low expression group, Figure 2.4 and Figure 2.6. In addition, the high chemokine expression group showed higher MPO levels. Genetic variability, host factors, and microbiome can influence the levels of inflammatory mediators which may contribute to the observed inter-individual variation in the host response to bacterial plaque (Shapira, Wilensky et al. 2005, Bakker, Aguirre-Gamboa et al. 2018).

Comprehensive analysis of the subgingival microbial composition is essential to understand the interactions between the microbiome and the host. The introduction of high-throughput sequencing technology allowed for a more thorough understanding of the diversity and structure of the subgingival microbiome. The microbial profiles of the healthy subgingival plaque were investigated using high-resolution Illumina MiSeq sequencing technology. A total of 10 phyla, 121 genera, and 427 species were identified in the subgingival microbiome. These results are consistent with the previously reported number of species in the subgingival plaque; 750 species by Abusleme et al., 596 species by Griffen et al., 347 species Paster et al. (Paster, Boches et al. 2001, Griffen, Beall et al. 2012, Abusleme, Dupuy et al. 2013). In contrast, another study identified 1,016 species in the subgingival plaque samples (Park, Yi et al. 2015). Differences in

the number of identified species may be due to the use of different sequencing and analytical methods. The average number of species in subgingival samples in this study ranged from 43 to 271 species in accordance with 30–194 species reported by Abusleme *et al*. (Abusleme, Dupuy et al. 2013).

In a similar manner to chemokine profiles, there was high variability in the subgingival microbiome profiles between healthy subjects. The uniqueness of the microbial community associated with health has been described where taxa dominating each subject community are highly personalized (Human Microbiome Project 2012). The subgingival microbial community was dominated by five phyla; Firmicutes, Proteobacteria, Bacteroidetes, Fusobacteria, and Actinobacteria. Firmicutes (37.9%) was the most predominant phylum in the healthy subgingival plaque in accordance with previous reports (Kumar, Griffen et al. 2005, Human Microbiome Project 2012).

Within the phylum Firmicutes, *Streptococcus tigurinus* (13.3%) and *Streptococcus parasanguinis* (6.3%) were the most abundant taxa among the healthy subgingival plaque as was described previously (Abusleme, Dupuy et al. 2013). Proteobacteria was the second among the most predominant phyla in the healthy subgingival plaque, in contrast with Griffen *et al*. and Park *et al*. where Proteobacteria was found to be the most prevalent phylum (Griffen, Beall et al. 2012, Park, Yi et al. 2015). These discrepancies between studies could be the result of differences in the target population in addition to differences in the microbial collection and analysis methods.

This study showed a broad range of taxa among healthy individuals. However, some species were shared by a majority of participants, representing the core subgingival microbiome Figure 2.11. It has been suggested that the core species play a key role in maintaining homeostasis. The subgingival core species in the subgingival samples included *Rothia dentocariosa, Rothia aeria, Streptococcus sanguinis, Streptococcus intermedius, Streptococcus cristatus, Actinomyces*

naeslundii, Veillonella parvula, Prevotella nigrescens, Lautropia mirabilis, Haemophilus parainfluenzae, Granulicatella adjacens, Gemella haemolysans, Fusobacterium nucleatum ss animalis, Fusobacterium nucleatum ss polymorphum, and *Capnocytophaga sputigena*. Similar results have been described by other reports (Griffen, Beall et al. 2012, Abusleme, Dupuy et al. 2013).

Known disease-associated species including *Treponema denticola, Tannerella forsythia and Porphyromonas gingivalis* were detected in the plaque samples from healthy individuals but in a low abundance and at a lower frequency (Socransky, Haffajee et al. 1998, Griffen, Beall et al. 2012, Abusleme, Dupuy et al. 2013). Periodontitis is associated with the shift in the species predominance of subgingival microbial community rather than the result of new species colonization. Community dysbiosis and associated imbalance in the host inflammatory mediators may lead to destructive immune response and periodontal tissue destruction (Darveau 2010).

Inter-subject variation in the subgingival microbial community was evaluated in the adolescent's healthy population. The study identified two types of microbial communities based on hierarchical clustering techniques, cluster (A) and cluster (B), Figure 2.12. The microbial compositions of the two clusters were different; which was evident by the complete separation of the different clusters microbiome based on beta diversity analysis, Figure 2.13. Cluster (B) was dominated by health-associated species whereas cluster (A) was inhabited by health-associated and periodontitis-associated species such as *Porphyromonas gingivalis*. Interestingly, the alpha diversity (within sample diversity) indexes were also variable between the individuals in the different clusters, alpha diversity scores associated with individuals in cluster (A) were noticeably lower, however, higher subgingival bacterial loads were observed, Figure 2.5 and Figure 2.7. In agreement, two subgingival community clusters in health were identified in a previous report; one

cluster was characterized by higher abundance of the periodontitis-associated genera *Porphyromonas* and *Treponema* (Zhou, Mihindukulasuriya et al. 2014).

Additionally, the two groups identified based on the chemokine expression patterns did not share common microbiome profiles, Figure 2.12. This could be attributed to the cross-sectional nature of the study and the dynamic nature of the host response and microbiome. Thus, assessment of the microbial community composition and host response variation between individuals is crucial in understanding the microbiome and host factors involvement with disease risks.

Few studies have investigated the influence of the microbial community composition on host response in the healthy periodontal tissue. The Mantel test revealed no significant correlation between combined chemokines and microbiome profiles in the study. However, significant correlations were found between core species and neutrophil chemokines. MIF and Gro-β/CXCL2 showed a positive association with core species, both involved in neutrophils influx into the periodontal tissue. TARC/CCL17 was negatively associated with core microbiome, increased TARC/CCL17 levels are connected to chronic periodontitis (Hosokawa, Hosokawa et al. 2008). The observed association between major neutrophil chemokines and core species highlight the role of the microbiome in gingival health maintenance.

This study has several potential limitations. The sample size was small and the cross-sectional nature of the study. In addition, pooling of subgingival microbial samples may result in lost site-specific data (Socransky and Haffajee 2005). Therefore, the study results should be interpreted carefully. Evaluating the changes in the chemokine profile and the microbiome composition in a larger size longitudinal trial during the transitional stages from the state of health to disease will provide valuable data for future diagnosis and treatment of periodontal disease.

In summary, the findings of the study provide new insights in regard to the interaction between microbiome and host response in gingival health. The observed inter-individual variation in the microbial composition and chemokine expression patterns in health may warrant further examination.

CHAPTER 3 . CHEMOKINE AND MICROBIOME PROFILES DURING INDUCED GINGIVITIS

Introduction

The original experimental gingivitis study developed by Löe *et al.* in 1965 established an induced gingivitis model that has served as a reference guideline in clinical and translational research for over 40 years (Löe, Theilade et al. 1965). There is an increased interest in expanding beyond the identification of factors associated with chronic periodontal disease and the development of methods to predict periodontal disease progression (Kinney, Morelli et al. 2014). Further, as increased inflammatory mediators are observed in chronic gingivitis, experimental models have been adapted to identify new candidate biomarkers through the utilization of localized stent-induced biofilm overgrowth models (SIBO) during the inflammatory response (Offenbacher, Barros et al. 2010). Much of the current literature on induced gingivitis models include an experimental phase as a period of 21 days where subjects refrain from all oral hygiene practices. All induced gingivitis models in related studies indicate a successful reversal of gingival inflammation in a resolution phase lasting approximately two weeks (Tatakis and Trombelli 2004, Trombelli, Tatakis et al. 2004, Offenbacher, Barros et al. 2010).

In this chapter, changes in the clinical parameters, chemokine profiles as well as microbial profiles were evaluated during 21 days of induced gingivitis. The objectives of this study, first, is to perform a comprehensive immunoassay analysis of known neutrophil chemokines and other inflammatory chemokines to evaluate their expression in clinically healthy and diseased GCF. The second objective is to assess neutrophil migration by measuring myeloperoxidase (MPO) in the

GCF during gingivitis induction. The third objective of this study is to characterize the shift in subgingival plaque microbiome during the transition from health to disease.

The split-mouth design allowed the investigation of localized changes in the gingiva due to plaque accumulation, and the comparison of these changes to a contralateral control side within the same individual. These findings will allow identifications of individuals who are susceptible or resistant to development gingivitis and characterization of possible underlying of host immune response associated with varied susceptibility.

Understanding specific details on chemokine behavior in gingival states of health and disease will ideally allow for assessment and evaluation of GCF as a potential diagnostic marker for gingival health.

Clinical Study Design and Methods:

3.1.1 Study Procedures and Biospecimens Collection

3.1.1.1 Study Population and informed consent

This study enrolled twenty-one generally healthy adults aged 18-35 years that are self-referred or referred to the UW School of Dentistry. The study design and informed consent were approved by the UW Human Subjects Review Committee (HSD# 50151). All study participants underwent informed consent process with a thorough discussion of study participation details, prior to enrollment in the study. The inclusion and exclusion criteria were confirmed. All female participants were provided with a pregnancy test prior to enrollment.

Inclusion Criteria:

To be enrolled the participant met the following inclusion criteria: 1) aged 18-35 years; 2) in good general health, ASA I; 3) no clinical signs of gingival inflammation at > 90% of sites observed at time of screening; 4) probing depth (PD) ≤ 3.0 mm; 5) attachment loss (AL) = 0 mm; 6) gingival health at baseline visit in the sites of interest (Day 0): gingival Index (GI) = 0 and bleeding on probing (BOP)(-); 7) fluent in English.

Exclusion Criteria.

Exclusion criteria included: 1) medical condition which requires premedication prior to dental treatments/visits; 2) subjects unable or unwilling to sign the informed consent form; 3) history of periodontal disease; 4) history of systemic inflammatory or immune conditions; 5) use of antibiotic or anti-inflammatory drugs within 30 days of enrollment; 6) pregnant or breastfeeding at the time of screening; 7) concurrent orthodontic treatment; 8) untreated carious lesions and/or inadequate restorations, implants, crowns on maxillary posterior teeth; 9) participation in any other clinical study or test panel within 1 week prior to enrollment into this study;10) use of tobacco products; 11) subjects who must receive dental treatment during the study dates; 12) orthodontic

bands, appliances, or crowns and bridges, or removable partial dentures affecting the maxillary posterior teeth; 13) history of allergy to common dentifrice ingredients; 14) immune-compromised individuals (HIV, AIDS, and immune-suppressive drug therapy)

3.1.1.2 Quadrant assignment, and teeth and site selection

Using online randomization tool (2017 GraphPad Software), in each participant, one maxillary quadrant was assigned randomly as test quadrant (experimental gingivitis) and contralateral quadrant as control. In each test and control quadrant, the following three maxillary teeth were used: first premolar, second premolar, and first molar. If a premolar was missing, the second molar replaced it. Clinical examination and sample collection were performed on the mesiobuccal and mesiopalatal surfaces of each study tooth.

3.1.1.3 Study procedure

The study included the following phases 1) Hygiene phase for one to two weeks prior to baseline 2) Gingivitis induction phase with the stent lasting for three weeks, and 3) Resolution phase for two weeks (**Figure** 3.1) (Trombelli, Tatakis et al. 2004). At Day -14, after obtaining informed consents and verification of inclusion/exclusion criteria, full clinical assessment and biospecimens collection were performed. After obtaining a maxillary impression for stent fabrication, full mouth prophylaxis was administered and thorough oral hygiene instructions were given. Participants returned 7 to 14 days after this initial visit and their baseline (Day 0) measurements and biospecimens collection were acquired. The acrylic stent was given to the participant with detailed instructions for use during regular brushing with the purpose of preventing accidental brushing of the experimental sites. Participants were instructed not to brush teeth on the test side (under the provided stent) and not to use any other measure of oral hygiene

such as flossing or interdental aids. For the control side and rest of the mouth, participants were instructed to use the provided toothbrush (Colgate® Gum Comfort Toothbrush), toothpaste (Colgate® Cavity Protection Great Regular Flavor Fluoride Toothpaste), and dental floss (Oral B Glide), and to refrain from using mouth rinses and chewing gums during entire study period. Participants returned on Day 4 and on weekly basis afterward, clinical assessments were performed and samples collected each time using the same criteria as at the baseline visit. The course of the "no brushing" part of the experiment lasted 21 days to allow all the participants to develop gingivitis. After acquiring samples and clinical assessment on day 21, additional thorough prophylaxis was administered. Participants were given again detailed instructions in oral hygiene methods using the provided electric toothbrush (Philips Sonicare Electric Toothbrush), toothpaste (Colgate® Cavity Protection Great Regular Flavor Fluoride Toothpaste), and dental floss (Oral B Glide) beginning the same day and continued twice daily during the resolution phase. Assessment of gingival condition and biospecimens collection continued weekly during the reversal phase. Medical history and exclusion criteria were reviewed at each study visit.

3.1.1.4 GCF Sampling

For each study visit, GCF samples were collected first followed by acquiring plaque samples. Subsequent to biospecimens collection, clinical indices were recorded. GCF samples were collected from the mesiobuccal and mesiopalatal surfaces of teeth (#'s 3, 4, 5, 12, 13 and 14). The sites to be sampled were isolated with cotton rolls to avoid contamination from saliva and gently air-dried in an apico-coronal direction without disrupting supragingival plaque. Followed by gentle insertion of sterile paper strips (Periopaper; Oraflow Inc., Smithtown, NY, USA) into the gingival crevice until mild resistance is felt and left in place for 30 seconds. The volume of GCF samples collected was immediately quantified with a previously calibrated measuring device

(Periotron 8010; OraFlow Inc, Smithtown, NY, USA). Paper strips visibly contaminated with saliva and blood were excluded from the study. At each study visit, a total of six peripapers were collected per study side and then pooled into a single microcentrifuge tube. Samples were placed immediately on ice and transported to the lab for processing.

3.1.1.5 Periotron Calibration

Periotron (OraFlow Inc, Smithtown, NY, USA) is an instrument that measures the electrical capacitance of a wet strip placed between the jaws of the device. Periotron 8010 was calibrated with known volumes of distilled water in triplicate and a standard calibration curve was generated. Gingival crevicular fluid volumes were calculated from the Periotron scores using the Periotron Professional Software V3.0 (OraFlow Inc, Smithtown, NY, USA) utilizing a 4th order polynomial regression (Ciantar and Caruana 1998, Chapple, Landini et al. 1999)

3.1.1.6 Plaque Sampling

Subgingival plaque samples were collected at each study visit from both control and test sides. Sterile paper points (STER-I-CELL Paper Points, Size M; Coltene, Whaledent, Cuyahoga Falls, OH, USA) were inserted into the gingival sulcus of mesiobuccal and mesiopalatal surfaces of the six maxillary teeth for 30 seconds. At each study visit, a total of six samples per study side were collected and pooled into a single sterile microcentrifuge tube. Samples were transported to the lab on ice and then frozen at -80^{o}C until further analysis.

3.1.1.7 Clinical exam

Following biospecimens collection, clinical data were documented based on probing depth (PD), attachment level (AL), plaque index (PI) (Silness and Löe 1964), gingival index (GI) (Löe and Silness 1963), and bleeding on probing (BOP). All clinical measurements were conducted

using a manual UNC-15 periodontal probe (Hu-Friedy, Chicago, IL, USA). BOP was recorded within 20 seconds of probing.

3.1.1.8 Stent fabrication

The stent was fabricated to include only the occlusal surface of the study teeth and eliminate contact with the cervical margin of each tooth, thereby reducing the risk of plaque being disturbed during insertion or removal of the stent. The stent was constructed from 3-mm-thick plastic mouthguard material. Elimination of cervical contact was accomplished by blocking out around the gingival margin and proximal surfaces using a spacer made from 1-mm-thick mouthguard material. The stent was trimmed vertically on the buccal side to a length just short of the vestibule and extending 4-5 mm on the palatal side. Also, it was trimmed mesially to the middle of the canine, and distally to the middle of the second molar.

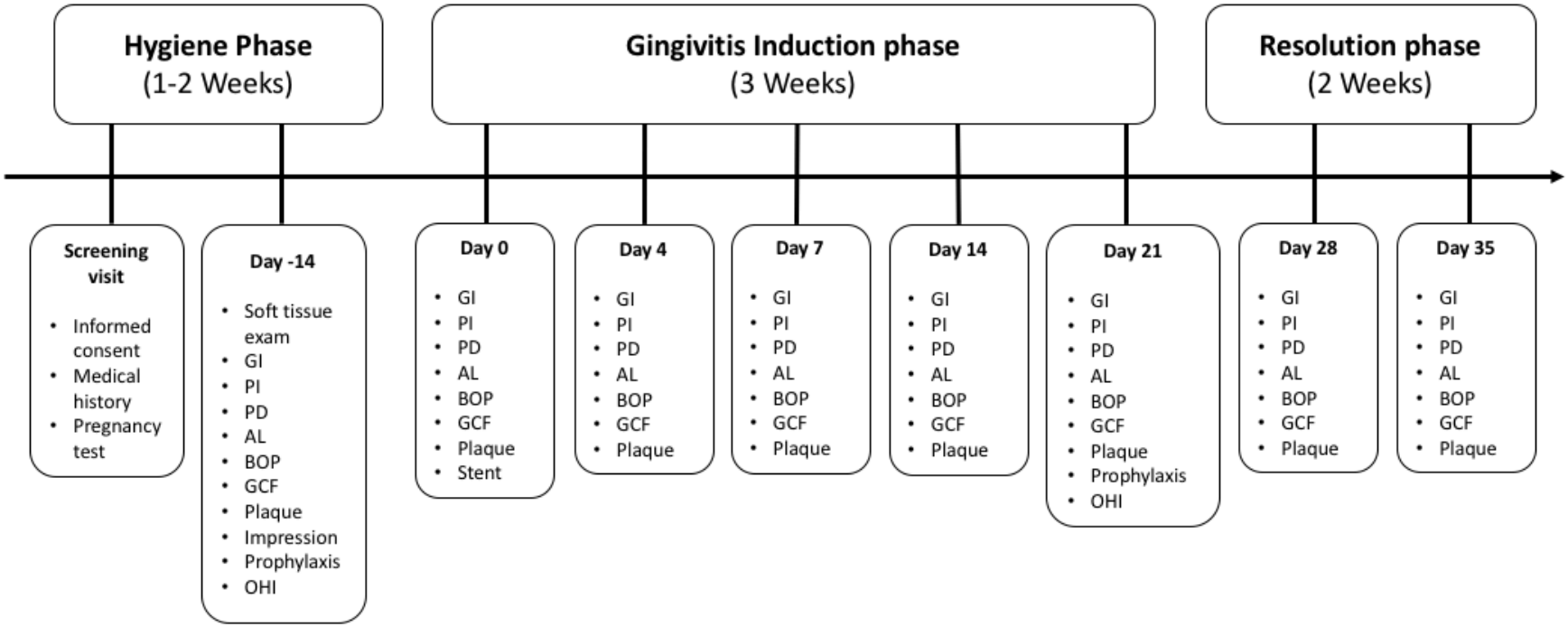

Figure 3.1: Induced gingivitis study design.
Probing depth (PD), attachment level (AL), plaque index (PI), gingival index (GI) and bleeding on probing (BOP), gingival crevicular fluid (GCF), oral hygiene instructions (OHI)

3.1.2 Laboratory Assessments

3.1.2.1 GCF Elution from Periopapers

GCF samples were eluted in 200 µl sample diluent (Bio-Plex Pro™ Human 40-plex Chemokine Panel, Bio-Rad Laboratories, Hercules, CA, USA) with 0.5% bovine serum albumin (Blocker™ BSA (10X) in PBS; Waltham, MA, Thermo Scientific, USA) and then continuously mixed on a tube rotator for 60 minutes at 4°C. The strips were then removed and placed into a 0.5 ml PCR tube with a hole punctured at the base, and this tube was returned in the 1.5 mL tube and centrifuged at 13,000 rpm for 1 min at 4°C to extract the remaining fluid from the paper strips into the tube. Paper strips were then removed and eluted samples were stored at -80°C until further analysis. Samples were immediately thawed prior to performing immunoassays.

3.1.2.2 MPO Quantification in GCF

Myeloperoxidase (MPO) is considered a good marker of neutrophils infiltration (Cao and Smith 1989). The concentrations of myeloperoxidase (MPO) in GCF samples were assayed using commercially available ELISA kit, (Instant ELISA®, Affymetrix eBioscience, San Diego, CA, USA) according to manufacturer's instruction. The assay has detection range between 156 pg/ml and 10,000 pg/ml. GCF samples were added in duplicate to the wells of precoated 96-well plates with anti-human MPO antibodies at a 1:200 dilution. Samples were incubated at room temperature for 3 hours; the biotinylated detection antibodies bind to MPO captured by detection antibody followed by Streptavidin-HRP binding to the biotinylated antihuman MPO. After the washing step, a substrate solution (TMB) was added to visualize the enzymatic reaction. The reaction was stopped with the addition of stop solution (Sulphuric acid) and absorbance was measured on a microplate reader at 450 nm (VMax microplate reader; Molecular Devices Sunnyvale, CA, USA).

Concentrations for MPO in the samples were calculated from the standard curve with a five-parameter fit curve (Softmax Pro Software; Molecular Devices Sunnyvale, CA, USA).

Both assay concentrations and total amounts of chemokines and MPO were determined, concentrations were calculated from the standard curves whereas total amounts (total amount per 30-s samples) were determined after dilution correction. Mean values and standard deviations of the total amount per 30-s sample for the chemokines and MPO were computed at each study visit for both the control and test sides.

3.1.2.3 Chemokine Quantification in GCF

Bead based multiplex analysis was performed on GCF samples (Bio-Plex Pro™ Human 40-plex Chemokine Panel; Bio-Rad Laboratories, Hercules, CA, USA) allowing for simultaneous quantification of multiple chemokines. The following list of chemokines were analyzed with the assay working range level in pg/ml shown in paraentheis ( ): 6Ckine/CCL21 (21.9-3,923), BCA-1/CXCL13 (0.7-1,200), CTACK/CCL27 (1.2-5,000), ENA-78/CXCL5 (7.3-120,000), Eotaxin/CCL11 (1.5-3,859), Eotaxin-2/CCL24 (6.2-4,073), Eotaxin-3/CCL26 (0.9-12,109), Fractalkine/CX3CL1 (4-11,463), GCP-2/CXCL6 (0.8-11,135), GM-CSF (5.3-35,000), Gro-α/CXCL1 (3.1-7,024), Gro-β/CXCL2 (4.6-13,257), I-309/CCL1 (1.8-1,015), IFN-γ (2.3-20,236), IL-1β (0.4-7,000), IL-2 (0.8-13,000), IL-4 (1.2-4,804), IL-6 (0.7-12,000), IL-8/CXCL8 (0.5-7,640), IL-10 (1.3-18,708), IL-16 (2.1-34,000), IP-10/CXCL10 (1.6-7,714), I-TAC/CXCL11 (0.1-2,298), MCP-1/CCL2 (0.3-4,812), MCP-2/CCL8 (0.3-4,056), MCP-3/CCL7 (1.9-20,133), MCP-4/CCL13 (0.2-3,368), MDC/CCL22 (0.9-14,649), MIF (23.1-377,724), MIG/CXCL9 (1.8-19,600), MIP-1α/CCL3 (0.4-1,543), MIP-1δ/CCL15 (1.7-9,100), MIP-3α/CCL20 (0.3-4,675), MIP-3β/CCL19 (3.0-48,494), MPIF-1/CCL23 (1.0-14,450), SCYB16/CXCL16 (0.5-2,867), SDF-1α+β/CXCL12 (8.3-115,730), TARC/CCL17 (1.7-430), TECK/CCL25 (20.6-114,493), and TNF-α (0.9-13,879). Samples were not diluted for the assay.

Briefly, different fluorescently dyed magnetic microspheres populations were covalently conjugated with capture antibodies specific for the different chemokines. In the multiplex immunoassay, the coupled beads were incubated with 50 µl of GCF samples or standards in a 96-well plate in duplicate at room temperature for one hour. After washing (Bio-Plex Pro Wash Station; Bio-Rad, Hercules, CA, USA), 25 µl of biotinylated detection antibodies was added and incubated for 30 minutes at room temperature. After incubation, wells were washed and 50 µl streptavidin-phycoerythrin as a reporter was added to each well and incubated for 10 min. After the wash cycle was completed, 125 µl of assay buffer was added to each well. The data was obtained using a flow cytometry laser detection system (Bio-Plex 200 reader; Bio-Rad Laboratories, Hercules, CA, USA) by acquiring the signal from the fluorescent dye within each bead for assay identification along with the fluorescent signal from the reporter for quantification. The concentrations of different chemokines were calculated based on the respective standard curve for each chemokine with a five-parameter logistic (5PL) equation (Bio-Plex Manager Software V6; Bio-Rad Laboratories, Hercules, CA, USA). Mediator data are reported in total amounts per sample collected in 30 seconds (pg per 30-s sample).

3.1.2.4 DNA extraction

DNA was extracted using a commercially available kit (QIAamp DNA Microbiome Kit; Qiagen, Germany) following the manufacturer's protocol, that uses both mechanical and chemical cell lysis. To confirm the absence of other DNA contamination in the sequencing results, negative controls were implemented by performing the DNA extraction protocol without plaque samples with either kit reagents only or kit reagents with the sterile paper points. Also, to validate the efficiency of the technique, positive controls using known bacterial cultures were included. Sample purification was performed using a purification kit (the DNA Clean & Concentrator -5 kit; Zymo

Research, Orange, CA, USA) to further purify and increase the DNA yield. After DNA extraction and purification, DNA concentrations in the samples were determined fluorometrically (Quant-iT dsDNA HS Assay Kit; Invitrogen, Carlsbad, CA, USA) with Fluorometer (Qubit 2.0; Life Technologies, Carlsbad, CA, USA). Samples were then stored at -20^{o}C until ready for sequencing.

3.1.2.5 Library preparation of Next Generation Sequencing.

Comprehensive microbial profiling of subgingival plaque samples was performed via high-throughput sequencing of 16S rRNA gene following the standard Illumina Miseq System protocol. Briefly, amplification of DNA was performed using primers with overhang Illumina flow cell adapter sequences targeting hypervariable (V3 and V4) regions of the bacterial 16s rRNA gene. The primers used were 16S amplicon PCR forward primer (5'-TCGTCGGCAGCGTCAGATGTGTATAAGAGACAGCCTACGGGNGGCWGCAG-3') and 16S Amplicon PCR Reverse Primer (5'-GTCTCGTGGGCTCGGAGATGTGTATAAGAGACAGGACTACHVGGGTATCTAATCC-3'). Samples were amplified in singletons in a 96 well plate format. Each reaction was performed using a PCR kit (KAPA HiFi HotStart ReadyMix; KAPA Biosystems, Boston, MA, USA) in a total volume of 25 µl which included the following reagents: 2.5 µl of extracted DNA, 5 µl of both forward and reverse primers (1 µM each primer) and 12. 5 µl of 2x KAPA HiFi HotStart ReadyMix. Amplicon PCR was performed on a thermocycler (C1000 Touch thermal cycler; BioRad, Hercules, CA, USA) utilizing the following program: a denaturation stage at 95°C for 3 minutes, followed by 35-40 cycles of denaturation at 95°C for 30 seconds, annealing at 55°C for 30 seconds and extension at 72°C for 30 seconds, and then a final extension stage at 72°C for 5 minutes. The generated amplicons from the first PCR were approximately 460 bp in size which was verified visually by running each reaction on 1% agarose gel electrophoresis at 100V for 30 minutes. Amplicons were subsequently purified using magnetic beads (Agencourt AMPure XP beads; Agencourt Bioscience Corporation, Beckman

Coulter Inc., Beverly, MA, USA) and indexed (Nextera XT v2 Index Kits, Set A, B, and D; Illumina, San Diego, CA, USA). The indexing PCR conditions included a denaturation stage at 95 °C for 3 min, followed by 8 cycles of denaturation at 95 °C for 30 s, annealing at 55 °C for 30s, and extension at 72 °C for 30s, and then a final extension stage at 72 °C for 5 min. The indexed PCR amplicons were further purified with magnetic beads (Agencourt AMPure XP beads; Agencourt Bioscience Corporation, Beckman Coulter Inc., Beverly, MA, USA), and the quality and size of the library were checked (High Sensitivity D1000 Reagents and Agilent 4200 TapeStation system; Agilent Technologies, Santa Clara, CA, USA). Subsequently, library normalization was achieved using a normalization kit (SequalPrep Normalization Plate Kit; ThermoFisher Scientific, Waltham, MA, USA). The normalized library was pooled and denaturated with sodium hydroxide (NaOH) (Fisher Scientific, Pittsburgh, PA, USA). The denatured library (20 pM) was spiked with at least 20% control DNA (PhiX Control v3 library, Illumina, San Diego, CA, USA) prior to loading to the sequencer. Paired-end sequencing was carried out on a sequencing platform (MiSeq System, Illumina, San Diego, CA, USA) using a 2 x 300 cycle sequencing kit (MiSeq Reagent Kits v3, Illumina, San Diego, CA, USA).

Analysis of 16s rRNA sequence data

Analysis of sequencing data was performed using the Quantitative Insights into Microbial Ecology QIIME2 (Bolyen, Rideout et al. 2018) following the Divisive Amplicon Denoising Algorithm 2 (DADA2) pipeline workflow (Callahan, McMurdie et al. 2016, Callahan, Sankaran et al. 2016). Following demultiplexing with Casava V1.8, forward reads were truncated at position 290 and reverse reads at position 200, subsequently reads acquired at least 35 bp overlap when merged. After quality filtering and denoising of sequences, chimeras and singletons were removed. Taxonomic assignment to classify to the amplicon sequence variants (ASVs) was performed using the current Human Oral Microbiome Database (HOMD 16S rRNA RefSeq V15.1) (Chen, Yu et

al. 2010, Dewhirst, Chen et al. 2010). A phylogenetic tree was constructed using FastTree (Price, Dehal et al. 2010). Unrarefied data was used for the downstream analysis. The sequencing data were integrated into a single object using the "*phyloseq*" R package (McMurdie and Holmes 2013) and all subsequent data analysis and plots were produced in R Studio.

Alpha diversity, within sample diversity, were calculated using both richness and evenness metrics by functions estimate_richness() and pd() in the "*phyloseq*" and "*picante*" R packages (Kembel, Cowan et al. 2010). The plots for richness estimates were generated using "*ggplot2*" packages in R. The community richness was measured by observed species; total count of unique OTUs in the sample and by the nonparametric richness estimator Chao1; account for the number of singletons and doubletons (Chao 1984). The total community diversity (richness and evenness) was measured by Simpson's inverse diversity index (Simpson 1949), Shannon index and the phylogenetic diversity (Faith's PD); that uses phylogenetic distance to calculate diversity (Faith 1992) (Lozupone and Knight 2008).

Beta diversity, between samples diversity, was determined using phylogenetic-based Unifrac distances; that measure phylogenetic distances between samples both unweighted (presence\absence) and weighted (relative abundance) (C. Lozupone & Knight, 2005), and OTU based Bray-Curtis dissimilarity matrix (Bray and Curtis 1957, Lozupone and Knight 2005); account for both the presence/absence and abundance of OTUs. Beta diversity metrics were calculated with ordinate() function in "*phyloseq*" and were visualized by non-metric multidimensional scaling (NMDS) plots using plot_oridination() function in "*phyloseq*".

3.1.2.6 Microbial Load Quantification

Quantitative real-time PCR was performed to determine the total bacterial load in each sequenced sample. Samples were analyzed in duplicates in a 96-well plate using a thermocycler

(CFX96 Real-time system C1000 Thermocycler; BioRad Laboratories, Hercules, CA, USA). A qPCR standard curve was generated from serially diluted *Fusobacterium nucleatum* ATCC 10953 genomic DNA in a range of 10^8 to 10^1 16s copy number. Each reaction was performed in a total volume of 20 µl consisted of 2 µl of DNA or standards added to 10 µl of the master mix (TaqMan™ Fast Advanced Master Mix; Applied Biosystems, Foster City, CA, USA). Primers set that specifically target the 16S rRNA gene were added with 900 nM final concentrations for both forward primer, 5′-TCCTACGGGAGGCAGCAGT-3′, and reverse primer, 5′-GGACTACCAGGGTATCTAATCCTGTT -3′; and 200 nM of TaqMan probe, (6-FAM)-5′-CGTATTACCGCGGCTGCTGGCAC- 3′-(TAMRA), (Sigma Aldrich, St Louis, MO, USA) (Nadkarni, Martin et al. 2002). Nuclease-free water was added to bring the total volume of the reaction to 20 µl. The negative control sample was included in the run using nulcease-free water to ensure no contamination occurred. The qPCR run consisted of the following amplification conditions: 50°C for 2 minutes (UNG incubation); 95°C for 20 seconds (Polymerase activation); 40 cycles of 95°C for 3 seconds (denature) and 60°C for 30 seconds (anneal/extend). The subgingival bacterial load was calculated (BioRad CFX software V3.1; BioRad Laboratories, Hercules, CA, USA) using regression mode (Cq determination mode). A logarithmic transformation of the bacterial load data was performed.

3.1.3 Statistical Analyses

3.1.3.1 Identification of responders subgroups

Participants were clustered into groups based on the joint clinical data trajectories of gingivitis severity represented by GI and BOP in response to plaque accumulation represented by PI between Day 0 and Day 21 in the test sides. The clustering analysis was performed using the k-means for longitudinal data method in the "*kml3d*" R package (Genolini, Alacoque et al. 2015).

One-way ANOVA and Chi-square test were conducted to compare the responder groups age and gender, respectively.

3.1.3.2 Clinical and chemokine data for test and control sides

Clinical data including PI, GI, BOP and GCF volume, and immunoassay data including chemokine and MPO total amount (pg per 30-s sample) were summarized into a single average score per side at each time point. Data were reported in means and standard deviations. All statistical analyses were performed using a software (R software Version 3.5.1, R Foundation for Statistical Computing, Vienna, Austria) (Team 2018). Tables for clinical and chemokine data were created using "*expss"* package (Demin 2018). The comparisons between test and control sides over time and the changes over time within test sides in the clinical parameters and chemokine levels were performed using Generalized Estimating Equation (GEE) models (Liang and Zeger 1986). Statistical tests were performed using the function geeglm() in the "*geepack"* package (Halekoh, Højsgaard et al. 2006). A Gaussian distribution was selected for the family with an identity link and a first-order autoregressive (ar1) model for the working correlation matrix. All multiple comparisons of the estimated marginal means were performed using emmeans() function in the "*emmeans"* package in R (Lenth 2018) with false discovery rate (FDR) adjustment (Benjamini and Hochberg 1995). Multiple comparisons were performed between test and control sides during induction phase (Day 0, 4, 7, 14 and 21), and within test sides between baseline (Day 0) and different time points during induction phase (Day 4, 7, 14 and 21). Statistical significance was considered when p values were <0.05.

3.1.3.1 Clinical and chemokine data for responder groups

Clinical and mediators data for the responder groups were summarized into a single average score per group at each time point and were reported in means and standard deviations. As summarized above, statistical tests based on GEE models were used to compare clinical and chemokines data between different responder groups during induction phase.

3.1.3.2 Correlation analysis

In order to investigate the association between clinical, host and microbial data repeated measures correlation analyses were performed for the test sides. The function rmcorr()in the "*rmcorr*" package (Bakdash and Marusich 2018), based on the method proposed by Bland and Altman (Bland and Altman 1995, Bland and Altman 1995), was used to investigate the within-participants correlation for paired variables while accounting for the between-participants variance using Analysis of Covariance (ANCOVA). The rmcorr() analyzes repeated measures data without requiring averaging the data or violating assumptions of independence (Bakdash and Marusich 2018). Clinical, chemokines, MPO and bacterial load data for the test sides during induction phase were incorporated in the analyses.

3.1.3.3 Microbial data analysis

Statistical analysis of the changes in subgingival microbial composition and load longitudinally during gingivitis induction were performed using R Software, version 3.5.1(Team 2018). Logarithmic transformations (base 10) were performed for the subgingival bacterial load data prior to analysis. In a similar manner to clinical data, the difference in subgingival microbial load and alpha diversity indices between test and control sides, and between different responder groups were determined using GEE models.

Differences in microbial community composition between test and control sides or between different responder groups over time were evaluated by performing permutational analysis of variance (PERMANOVA) on the calculated beta diversity matrices (Bray-Curtis and UniFrac distances) using the function adonis() in the "*vegan*" package version 2.5-4 (Jari Oksanen, Legendre et al. 2019). Between groups multiple comparisons were performed by pairwise PERMANOVA using the function pairwise.perm.manova() from the "*RVAideMemoire*" package (Hervé 2019) with false discovery rate (FDR) adjustment (Benjamini and Hochberg 1995).

Results

3.1.4 Study implementation

A total of thirty-three subjects between the age of 18 and 35 years was screened for the study enrollment. Twenty-one subjects (mean age: 23.33 ± 4.37 years), eleven males (mean age: 21.09 ± 1.97 years) and ten females (mean age: 25.8 ± 5.03 years), met the study inclusion criteria and were enrolled. All subjects had generalized gingival health with <10 % gingival inflammation at the screening visit and GI=0 at baseline on the sites of interest. All twenty-one participants completed the study with no reported adverse events. During the study period, one subject missed one appointment at Day 7, analysis for Day 7 is limited to N=20.

3.1.5 Clinical results

3.1.5.1 Changes in clinical parameters during induction and resolution of experimental gingivitis

The study yielded the expected results when performing human gingivitis studies. There was a significant increase in the dental plaque biofilm (PI), gingival inflammation (GI), and vascularization of gingival tissue (BOP) as well as the gingival crevicular fluid volume (µl) on the

test sides. Table 2 summarizes the mean values of clinical parameters for the test and control sides during different study visits. The data showed no difference between test and control sides at baseline (Day 0) for gingival index (GI), plaque index (PI), bleeding on probing (BOP) and gingival crevicular fluid (GCF) volume. At baseline, GI and BOP values were zero for control and test sides representing the absence of inflammation. During gingivitis induction, a significant increase on the test sides was observed in all gingival inflammation indices and plaque levels from baseline peaking at Day 21 ($p<0.001$), Figure 3.2. Mean PI score at baseline was 0.12 ± 0.17 in the test sides and significantly increased to 2.03 ± 0.29 on Day 21 ($p < 0.001$). GI and BOP mean values on the test sides significantly increased from zero at baseline to 1.75 ± 0.33 and 76.98 ± 22.03, respectively, at Day 21 ($p < 0.001$). GCF mean volume on the test sides showed two-fold increase at Day 21 0.12 ± 0.06 compared to baseline measurement 0.06 ± 0.03 ($p < 0.001$). GI, BOP and PI scores on the control sides remained low during the experimental phase. Similarly, GCF values did not significantly change on the control sides during the induction phase compared to baseline levels. All clinical parameters were statistically significantly higher in the test sides compared to the control sides at all time points during plaque accumulation ($p < 0.001$), in agreement with previous work (Löe, Theilade et al. 1965, Trombelli, Tatakis et al. 2004, Offenbacher, Barros et al. 2010). Reinstitution of oral hygiene resulted in a significant decrease in plaque scores that was accompanied with a significant decrease in all clinical signs of inflammation for the test sides ($p<0.001$) during the resolution phase. All clinical indices reverted close to baseline levels by Day 35 in the test sides indicating reestablishment of gingival health.

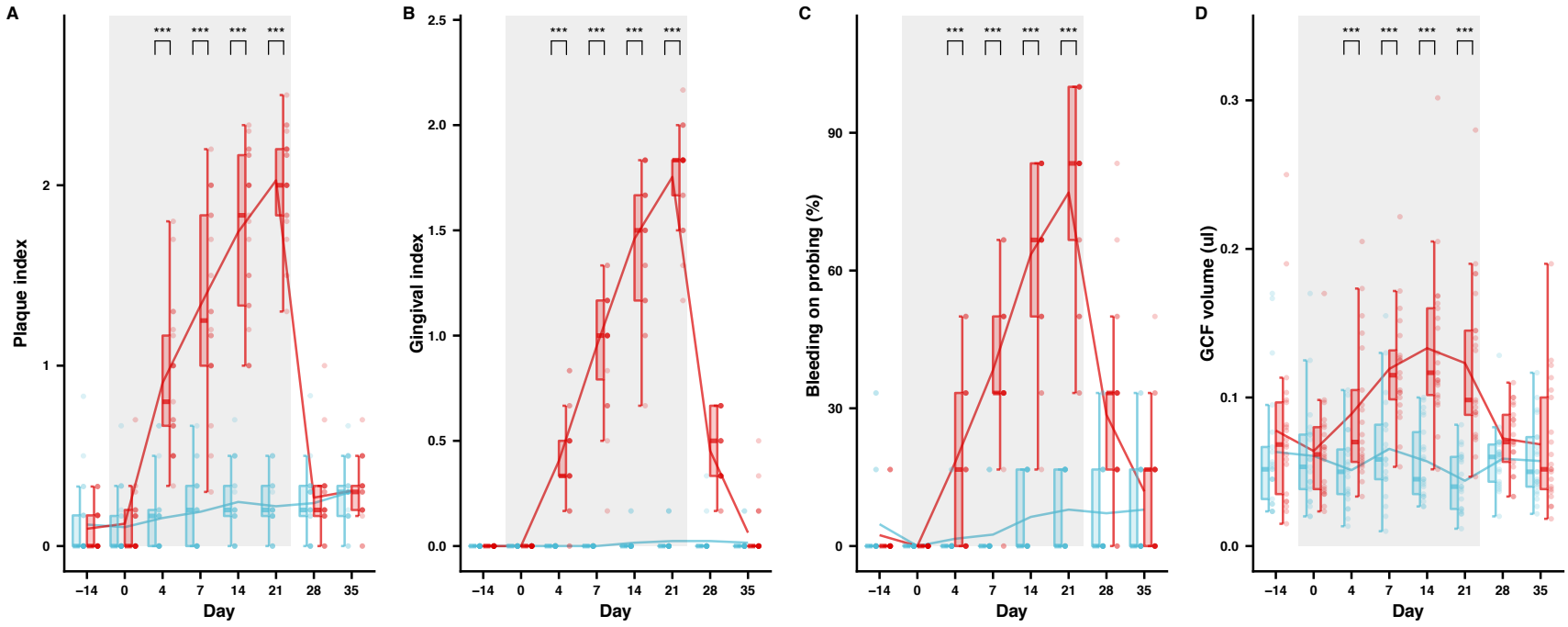

Figure 3.2: Clinical indices boxplots during induction and resolution of experimental gingivitis.
There is a significant change in the clinical parameters during the transition from health to disease.
The trend line represent the average values across time points. Blue control side and red test side. Significance *p < 0.05, **p < 0.01 or ***p < 0.001.

Table 2: Clinical indices during induction and resolution of experimental gingivitis.

Mean with standard deviation for plaque index (PI), gingival index (GI), percentage bleeding on probing (BOP) and gingival crevicular fluid volume (µl) at each visit. Statistical significant difference for test side vs control side at different visit, *$p < 0.05$, **$p < 0.01$ or ***$p < 0.001$. Statistical significant difference for the time trend on the test side; induction phase values vs Day 0, §$p < 0.05$, †$p < 0.01$ or ‡$p < 0.001$.

	Control								Test							
	Hygiene Phase	Induction Phase					Resolution Phase		Hygiene Phase	Induction Phase					Resolution Phase	
	-14	0	4	7	14	21	28	35	-14	0	4	7	14	21	28	35
PI	0.12 ± 0.22	0.1 ± 0.18	0.16 ± 0.21	0.19 ± 0.21	0.24 ± 0.2	0.22 ± 0.16	0.24 ± 0.2	0.3 ± 0.17	0.1 ± 0.12	0.12 ± 0.17	0.90 ± 0.4***‡	1.33 ± 0.54***‡	1.74 ± 0.45***‡	2.03 ± 0.29***‡	0.27 ± 0.23	0.31 ± 0.17
GI	0 ± 0	0 ± 0	0 ± 0	0 ± 0	0.02 ± 0	0.02 ± 0.05	0.02 ± 0.06	0.02 ± 0.08	0 ± 0.05	0 ± 0	0.40 ± 0***‡	0.95 ± 0.23***‡	1.46 ± 0.29***‡	1.75 ± 0.33***‡	0.45 ± 0.24	0.06 ± 0.17
BOP	4.76 ± 10.73	0 ± 0	1.59 ± 5.01	2.5 ± 6.11	6.35 ± 8.29	7.9 ± 8.5	7.14 ± 11.27	7.94 ± 11.33	2.38 ± 5.98	0 ± 0	18.25 ± 18.93***‡	38.33 ± 18.81***‡	63.49 ± 19.45***‡	76.98 ± 22.03***‡	28.57 ± 21.18	11.90 ± 14.09
GCF	0.06 ± 0.04	0.06 ± 0.04	0.05 ± 0.03	0.07 ± 0.04	0.06 ± 0.03	0.04 ± 0.02	0.06 ± 0.02	0.06 ± 0.03	0.08 ± 0.06	0.06 ± 0.03	0.09 ± 0.05***	0.12 ± 0.04***‡	0.13 ± 0.05***‡	0.12 ± 0.06***‡	0.07 ± 0.02	0.07 ± 0.04

3.1.5.2 Responders groups identification

Interestingly, variability was observed among the study subjects in the trajectories of gingivitis development. Three distinct responders groups were identified based on joint trajectories of three clinical indices representing the severity of gingival inflammation (GI and BOP) in response to plaque accumulation (PI). The identified three responder groups comprise a high responder group (28.6 %), a low responder group (28.6 %), and a slow responder group (42.9 %). The high responder group included at a total of six participants: three males and three females (mean age: 20.67 ± 0.82 years), the low responder group also included a total of six participants: four males and two females (mean age: 24.5 ± 5.47 years), and the slow group included nine participants with mean age of 24.33 ± 4.61 years including four males and five females. There were no statistical significant differences between the three groups in age ($F(2, 18) = 1.668$, $p = 0.216$) or gender ($\chi^2 = 0.73182$, $p = 0.6936$).

3.1.5.3 Changes in clinical parameters in the responder groups

Although an overall significant increase in clinical indices was evident across study participants during the induction phase, different responder groups showed distinct temporal patterns for the different clinical parameters, Figure 3.3. The analysis showed that during the induction phase, all three responder groups mean GI and BOP scores started to increase as early as Day 4 in response to biofilm build up, Table 3. The overall trends for mean GI and BOP scores among the high and slow responders are higher compared to the low responder group. By the end of the induction phase, both high and slow responders mean BOP and GI scores are statistically significantly higher compared to low responder group. The most important difference between the high and slow groups is that the slow group responded at a slower rate to plaque accumulation compared to the immediate and fast response seen in the high group. The slow group had a delayed

gingival inflammation response during first two weeks of gingivitis induction compared to the high group and only by Day 21, at the end of the experimental phase, slow responders achieved GI and BOP scores similar to the high responder group. Interestingly, groups trajectories for plaque accumulation over time showed that high and low responders groups have similar mean plaque scores which were higher compared to slow responders.

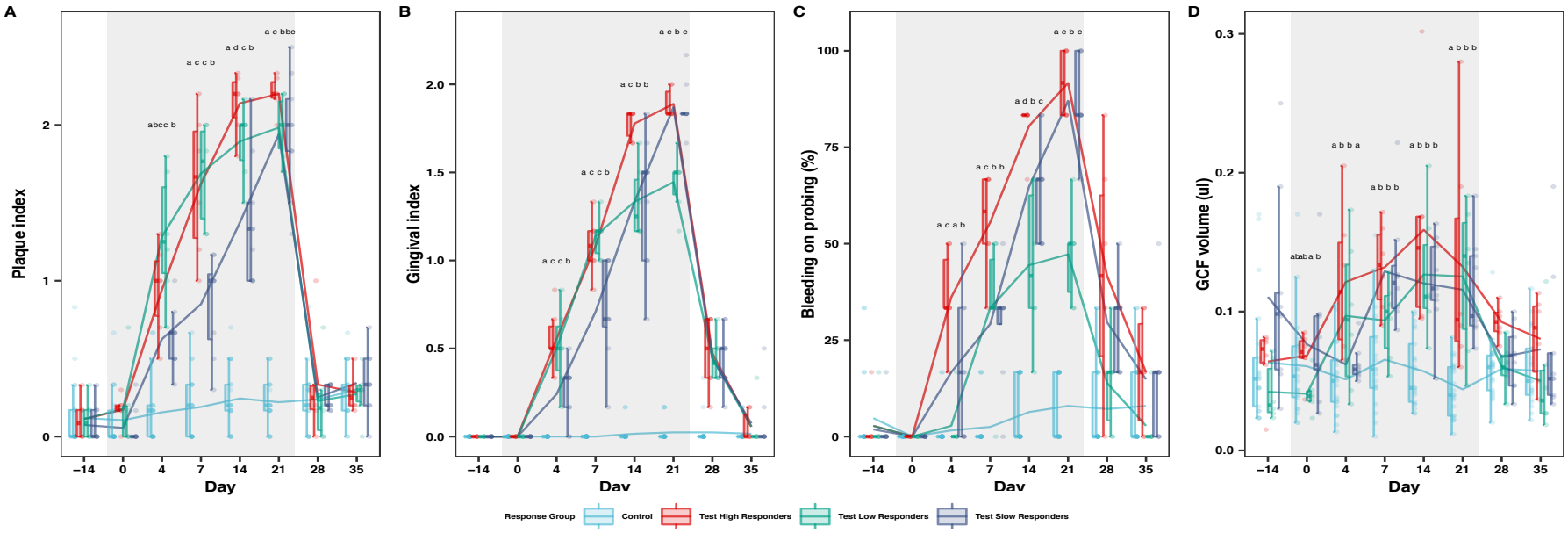

Figure 3.3: Clinical indices boxplots during induction and resolution of experimental gingivitis among the different responder groups.

There is variability in the trajectories of clinical responses among the different responder groups during the transition from health to disease.

The trend line represent the average values across time points. Blue control side, red test high responders, green test low responders, and purple test slow responders. Different letters above bars indicate significant differences between groups at each visit (a, b, c) (FDR $P< 0.05$).

Table 3: Clinical indices during induction and resolution of experimental gingivitis among the responder groups.

Mean with standard deviation for plaque index (PI), gingival index (GI), percentage bleeding on probing (BOP) and gingival crevicular fluid volume (µl) at each visit for the different responder groups. Different letters indicate significant differences between groups at each visit (a, b, c) (FDR $P < 0.05$).

	Control								Test High Responders								Test Low Responders								Test Slow Responders							
	Hygiene Phase	Induction Phase					Resolution Phase		Hygiene Phase	Induction Phase					Resolution Phase		Hygiene Phase	Induction Phase					Resolution Phase		Hygiene Phase	Induction Phase					Resolution Phase	
	-14	0	4	7	14	21	28	35	-14	0	4	7	14	21	28	35	-14	0	4	7	14	21	28	35	-14	0	4	7	14	21	28	35
PI	0.12 ± 0.22	0.1 ± 0.18a	0.16 ± 0.21a	0.19 ± 0.21a	0.24 ± 0.2a	0.22 ± 0.16a	0.24 ± 0.2	0.3 ± 0.17	0.11 ± 0.14	0.17 ± 0.1a	0.94 ± 0.3bc	1.62 ± 0.47c	2.14 ± 0.2d	2.2 ± 0.12c	0.33 ± 0.35	0.28 ± 0.12	0.11 ± 0.14	0.18 ± 0.27a	1.28 ± 0.42c	1.69 ± 0.32c	1.89 ± 0.25c	1.98 ± 0.2[b]	0.23 ± 0.26	0.27 ± 0.17	0.07 ± 0.12	0.06 ± 0.12a	0.63 ± 0.2[b]	0.85 ± 0.32b	1.37 ± 0.4b	1.94 ± 0.38bc	0.25 ± 0.08	0.34 ± 0.2
GI	0 ± 0	0 ± 0a	0 ± 0a	0 ± 0a	0.02 ± 0.05a	0.02 ± 0.06a	0.02 ± 0.08	0.02 ± 0.05	0 ± 0	0 ± 0a	0.56 ± 0.17c	1.08 ± 0.17c	1.78 ± 0.09c	1.89 ± 0.09c	0.47 ± 0.22	0.06 ± 0.09	0 ± 0	0 ± 0a	0.5 ± 0.24c	1.14 ± 0.13c	1.33 ± 0.21b	1.44 ± 0.17b	0.44 ± 0.14	0.06 ± 0.14	0 ± 0	0 ± 0a	0.24 ± 0.17b	0.71 ± 0.29b	1.33 ± 0.37b	1.87 ± 0.14c	0.44 ± 0.17	0.07 ± 0.17
BOP	4.76 ± 10.73	0 ± 0a	1.59 ± 5.01a	2.5 ± 6.11a	6.35 ± 8.29a	7.94 ± 8.53a	7.14 ± 11.27	7.94 ± 11.33	2.78 ± 6.8	0 ± 0a	36.11 ± 12.55c	55.56 ± 13.61c	80.56 ± 6.8d	91.67 ± 9.13c	41.67 ± 31.18	16.67 ± 14.91	2.78 ± 6.8	0 ± 0a	2.78 ± 6.8a	33.33 ± 18.26b	44.44 ± 20.18b	47.22 ± 12.55b	13.89 ± 12.55	2.78 ± 6.8	1.85 ± 5.56	0 ± 0a	16.67 ± 18.63b	29.17 ± 14.77b	64.81 ± 13.03c	87.04 ± 11.11c	29.63 ± 11.11	14.81 ± 15.47
GCF	0.06 ± 0.04	0.06 ± 0.04ab	0.05 ± 0.03a	0.07 ± 0.04a	0.06 ± 0.03a	0.04 ± 0.02a	0.06 ± 0.02	0.06 ± 0.03	0.06 ± 0.03	0.07 ± 0.02ab	0.12 ± 0.05b	0.13 ± 0.03b	0.16 ± 0.08b	0.13 ± 0.09b	0.09 ± 0.01	0.08 ± 0.03	0.04 ± 0.02	0.04 ± 0.01a	0.1 ± 0.06b	0.09 ± 0.03b	0.13 ± 0.05b	0.13 ± 0.05b	0.06 ± 0.02	0.05 ± 0.04	0.11 ± 0.07	0.08 ± 0.04b	0.06 ± 0.01a	0.13 ± 0.04b	0.12 ± 0.03b	0.12 ± 0.04b	0.07 ± 0.02b	0.07 ± 0.05

3.1.6 Chemokine results

Summaries of the mean values and standard deviations of the analyzed forty chemokines are presented in Table 4 and Table 5, for test and control sides, and for the different responder groups, respectively. TARC/CCL17, EOTAXIN-2/CCL24, IL-4, EOTAXIN-3/CCL26, CTACK/CCL27, I-TAC/CXCL11, and SDF-1α+β/CXCL12 had low detection level in most of the assayed samples, detected in less than 50% of all samples, and will not be included in the analysis. The following chemokines: I-309/CCL1, MCP-3/CCL7, MCP-2/CCL8, EOTAXIN/CCL11, MPIF-1/CCL23, IL-2, and IFN-γ had detection levels between 50% and 80%. All other chemokines were detected in more than 80% of all samples.

Overall, twenty three chemokines in the examined panel show significant differences between test and control sides after first week of plaque accumulation including I-309/CCL1, MCP-1/CCL2, MIP-1α/CCL3, MCP-2/CCL8, EOTAXIN/CCL11, MIP-3α/CCL20, 6CKINE/CCL21, TECK/CCL25, GRO-α/CXCL1, GRO-B/CXCL2, ENA-78/CXCL5, GCP-2/CXCL6, IP-10/CXCL10, BCA-1/CXCL13, SCYB16/CXCL16, IL-2, IL-6, IL-8/CXCL8, MIG/CXCL9, IL-16, MIF, IFN-γ, and TNF-α, that showed significant early drop in mean levels except for TECK/CCL25 and MIF which showed an initial significant increase. However, only seven chemokines showed significant differences between test and control side during the second, and third week of the induction phase (Day 14 and Day 21) including MIP-1α/CCL3, MIP-1δ/CCL15, MDC/CCL22, TECK/CCL25, GCP-2/CXCL6, IL-β, and MIF. Both MIP-1α/CCL3 and GCP-2/CXCL6 levels decreased, while MIP-1δ/CCL15, MDC/CCL22, TECK/CCL25, IL-β, and MIF increased.

3.1.6.1 Chemokine expression patterns in the different responder groups

The three responder groups presented distinct patterns of chemokine expressions during gingivitis induction and resolution, Figure 3.4. High responder group demonstrated overall higher expression levels in all assayed chemokines at baseline, and which were restored during the resolution phase following perturbations in the induction phase. On the other hand, low responders were associated with low chemokine expression profiles during the entire study compared to the other groups. The slow responders shared similarity to the high responder group chemokine profiles; however, a delayed response was evident during the initial stages of gingivitis induction.

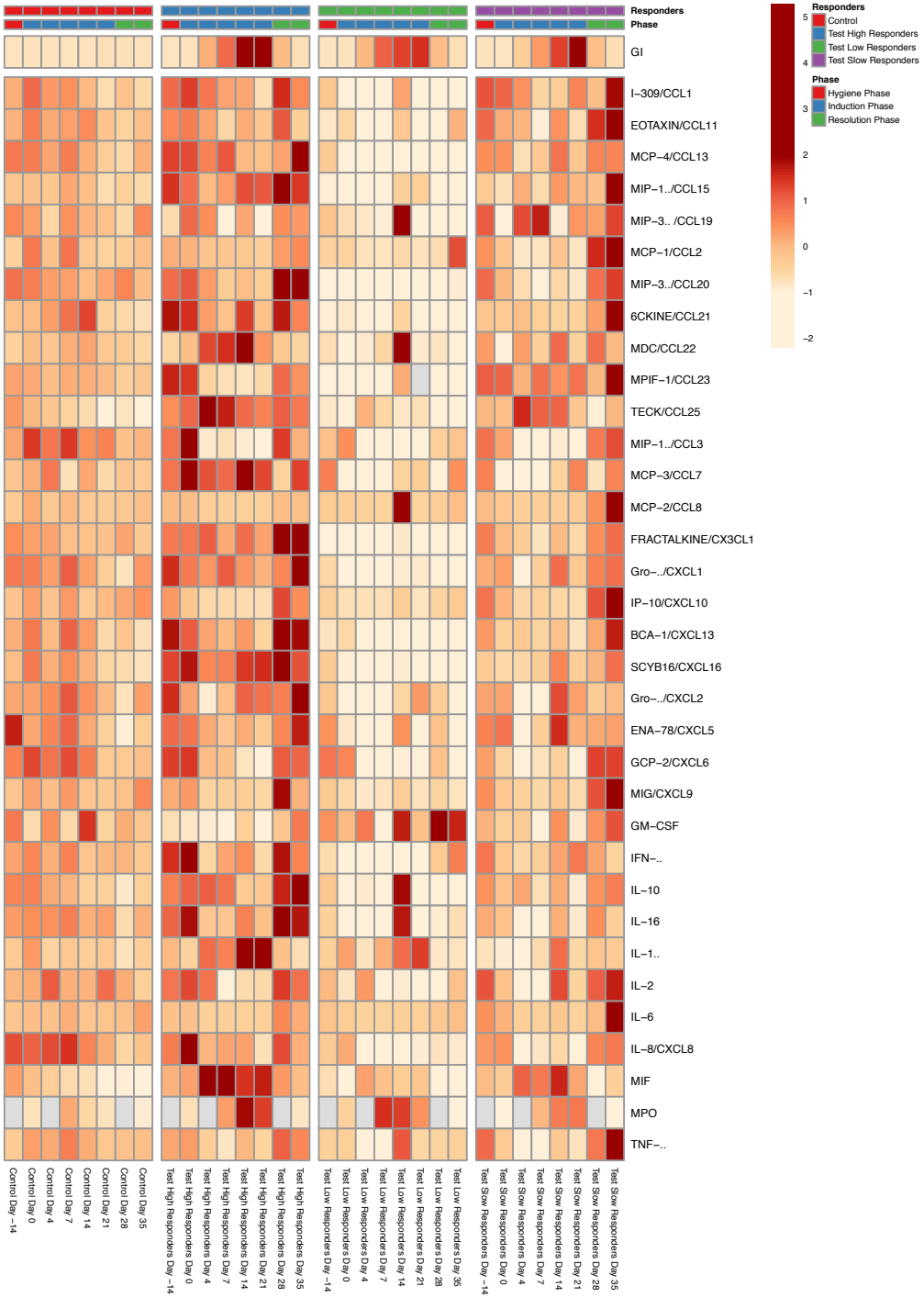

Figure 3.4: Z-score heatmap of GCF chemokine expression levels during induction and resolution of experimental gingivitis.
Heatmap shows the distinct chemokine expression patterns among the responder groups. Columns are visits and rows are chemokines. Color scale for heatmap appears in the top right, high expression in red and the low expression in orange. Color bars in the right depict annotation according to responder groups (columns).

3.1.6.2 Changes in neutrophil chemokines during induction and resolution of experimental gingivitis

The Multiplex immunoassay for gingival crevicular fluid was able to detect six different neutrophil chemokines GRO-α/CXCL1, GRO-β/CXCL2, ENA-78/CXCL5, GCP-2/CXCL6, IL-8/CXCL8, and MIF that represents the most complete analysis of neutrophil chemokine expression patterns in humans to date, Figure 3.5. Only one neutrophil chemokine, macrophage migration inhibitory factor (MIF), which is the most abundant neutrophil chemokine found in GCF, was found to significantly increase during gingivitis induction in the test sides in comparison to control sides, Figure 3.5 (A). It increased from baseline level (1962.76 ± 1275.21 pg per 30-s sample) to the first time point at Day 4 (3469.15 ± 1645.46 pg per 30-s sample), 1.8-fold increase, in the test sides and remained elevated during the entire gingivitis period. It went back to baseline levels after gingivitis resolution (Day 28) and at the end of the study (Day 35). The overall responder groups trajectories for MIF showed, although not statistically significant, high and slow responder groups trends during the induction phase are higher compared to the low responder group, Figure 3.6 (A). MIF mean value reached the highest level as early as Day 4 for the high responder group, whereas slow responders showed a delayed increase and values peaked at Day 21 at the end of the induction phase.

The next three most abundant neutrophil chemokines at baseline (GRO-α/CXCL1; test sides 111.49 ± 57.12 pg per 30-s sample and control sides 126.78 ± 63.41 pg per 30-s sample, ENA-78/CXCL5; test sides 40.96 ± 21.87 pg per 30-s sample and control sides 39.79 ± 20.89 pg per 30-s sample, and IL-8/CXCL8; test sides 185.24 ± 146.41 pg per 30-s sample and control sides 190.17 ± 126.37 pg per 30-s sample), Figure 3.5 (B, C and D). GRO-α/CXCL1 and ENA-78/CXCL5 showed transient (Day 4 and 7) decrease in GCF levels in the test sides. However, at

Day 14, while the plaque index, gingival index, and BOP sites were still increasing the amount of these two chemokines returned to baseline levels. Interestingly, at baseline, high responders levels for GRO-α/CXCL1 and ENA-78/CXCL5 were obviously separated from that of low responders but not statistically significant, Figure 3.6. During the early induction phase, Day 4 and Day 7, both low and slow responders mean levels for GRO-α/CXCL1 and ENA-78/CXCL5 were significantly decreased compared to controls, however, high responders levels remained stable through entire induction phase. In contrast, IL-8/CXCL8 showed a significant decrease from Day 0 (185.24 ± 146.41 pg per 30-s sample) to Day 4 (85.8 ± 77.66), 2.2 fold decrease, and remained decreased for the entire period of gingivitis in the test sides which was significant different compared to control sides for Day 4 and Day 7. All three responder groups showed a significant decrease in IL-8/CXCL8 during the induction phase, however, high responder mean levels remained higher compared to low and slow responder groups, Figure 3.6. Two previous reports have described the reduction in IL-8/CXCL8 during experimental gingivitis in healthy participants (Deinzer, Weik et al. 2007, Offenbacher, Barros et al. 2010) and in smokers (Matthews, Joshi et al. 2013).

The following most abundant neutrophil chemokines (Gro-β/CXCL2; test sides 4.11 ± 2.45 per 30-s sample and control sides 4.6 ± 2.81 per 30-s sample, and GCP-2/CXCL6; test sides 3.89 ± 2.55 per 30-s sample and control sides 4.98 ± 4.53 pg per 30-s sample) showed different expression patterns, Figure 3.5 (E and F). Gro-β/CXCL2 demonstrated a transient decrease within GCF for the stent area (reduced Day 4 and 7: restored to baseline at Day 14) as described for the GRO-α/CXCL1 and ENA-78/CXCL5. Again all three groups showed decrease in Gro-β/CXCL2 mean levels at Day 4 and Day 7, whereas high responders levels remained higher compared to low and slow groups, Figure 3.6.

In contrast, GCP-2/CXCL6 levels in the test sides showed a decrease for the entire period of gingivitis similar to IL-8/CXCL8. Likewise, all three groups decreased significantly during induction phase reaching similar low levels at Day 21.

Neutrophil numbers as measured by MPO showed a 1.8-fold increase in the test sides at Day 21 (from 19465.06 ± 16048.37 pg per 30-s sample at baseline to 35265.87 ± 30322.75 pg per 30-s sample at Day 21) which likely occurs when additional neutrophils enter the sulcus during gingivitis development, Figure 3.7 (A). All three responder groups showed a significant increase in MPO levels with no significant differences between the group expression patterns, Figure 3.7 (B).

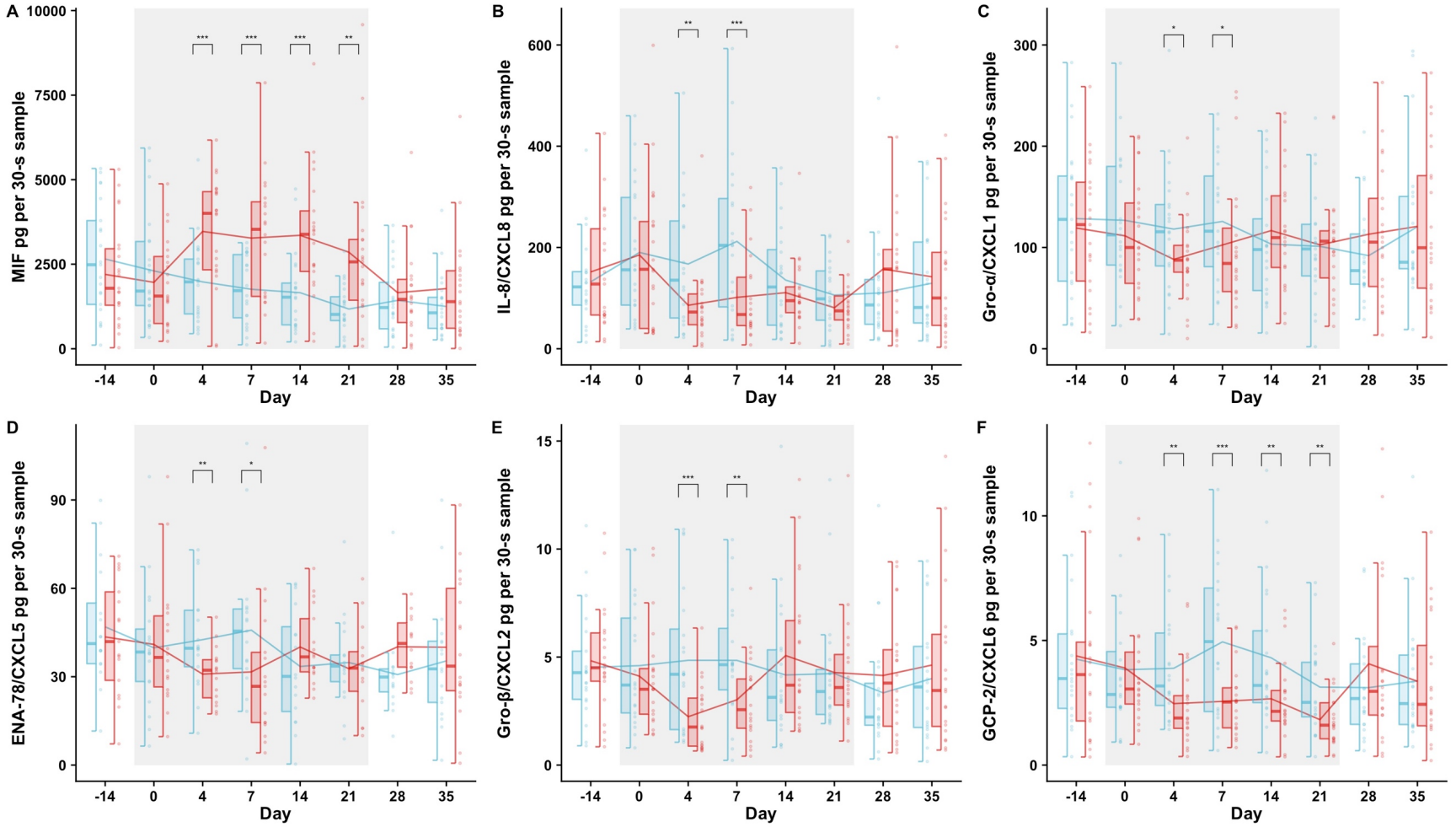

Figure 3.5: Neutrophil chemokines boxplots during induction and resolution of experimental gingivitis.
There is a significant change in neutrophil chemokine utilization patterns in the transition from health to disease. The trend line represent the average values across time points. Blue control side and red test side. Significance *p < 0.05, **p < 0.01 or ***p < 0.001

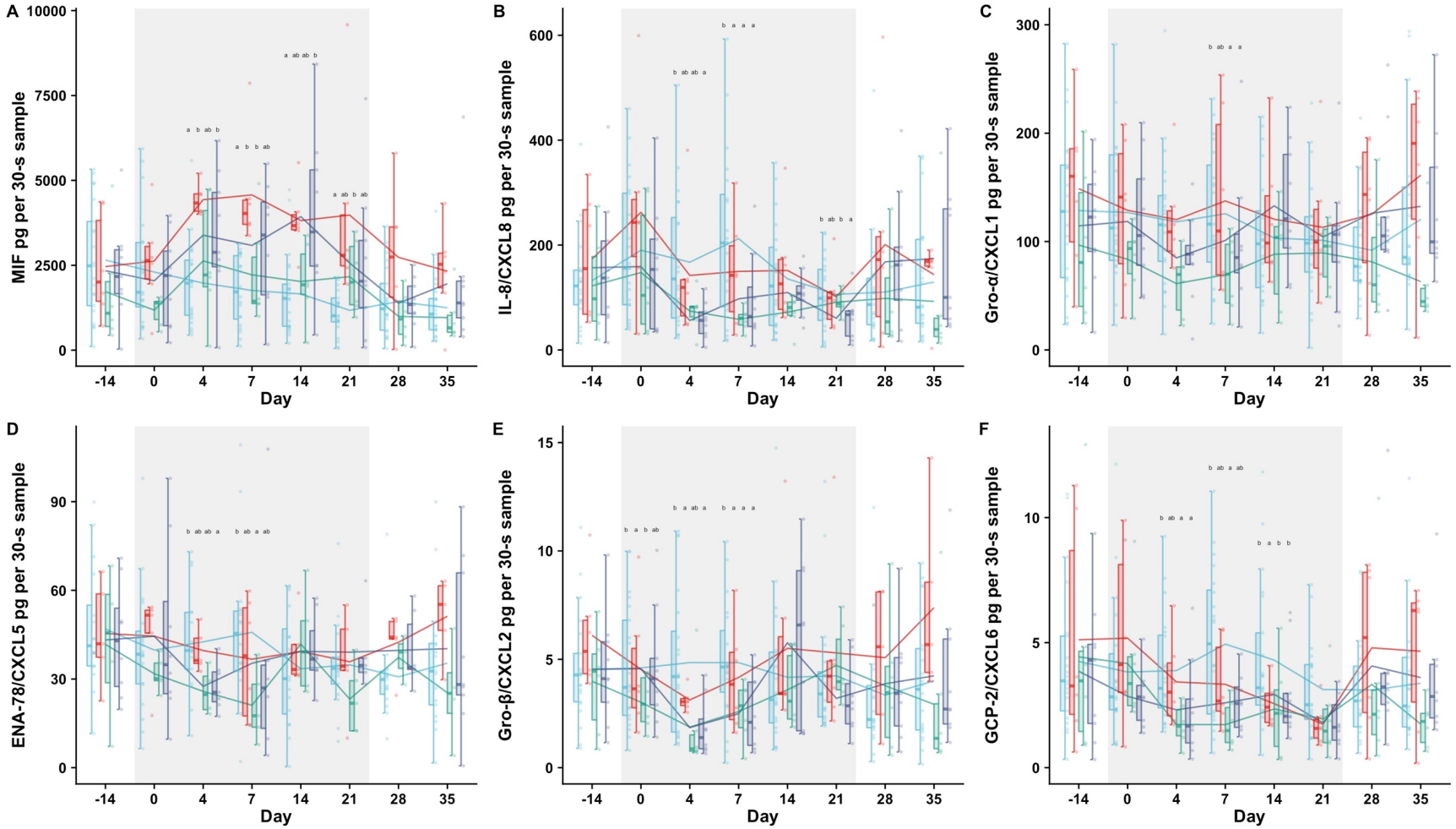

Figure 3.6: Neutrophil chemokines boxplots during induction and resolution of experimental gingivitis in the responder groups.

There is variability in the chemokines expression patterns among the different responder groups during the transition from health to disease.

The trend line represent the average values across time points. Blue control side, red test high responders, green test low responders, and purple test slow responders. Different letters above bars indicate significant differences between groups at each visit (a, b, c) (FDR $p < 0.05$).

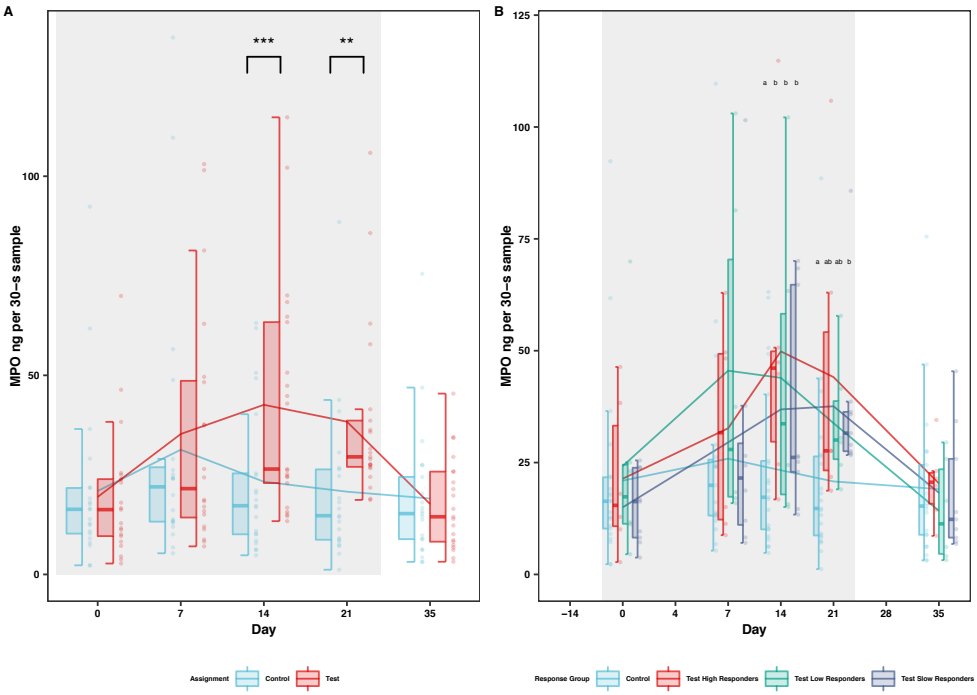

Figure 3.7: MPO boxplots during induction and resolution of experimental gingivitis.
All three responder groups showed significant increase in MPO levels during gingivitis induction.
The trend line represent the average values across time points. (A) Test and control sides; blue control side and red test side. Significance *p < 0.05, **p < 0.01 or ***p < 0.001.
(B) Responder groups; blue control side; red test high responders, green test low responders purple test slow responders. Different letters above bars indicate significant differences between groups at each visit (a, b, c) (FDR P < 0.05).

3.1.6.1 Changes in immune cell chemokines during induction and resolution of experimental gingivitis

Host chemokines which facilitate chemotaxis of host immune cells were also significantly altered in the transition from health to disease. Few chemokines showed Significant increase between test and control sides during the induction phase. Briefly, TECK/CCL25, a chemokine that facilitates chemotaxis for thymocytes, dendritic cells, and activated macrophages increased significantly at the first time point after the onset of gingivitis (Day 4) and steadily decreased afterward. All responders showed an increase in the TECK/CCL25 mean levels during the

induction phase. However, at baseline, low responders TECK/CCL25 levels were significantly lower than high responders and low responders trends remained lower than high and slow responder groups during the entire induction phase, Figure 3.8 (A).

MIP-1δ/CCL15 which is chemotactic for T cells and monocytes showed a slight increase that was significant by Day 21 between test and control sides. Different groups also showed a slight increase in MIP-1δ/CCL15 levels during the induction phase, the high responders' trends are higher than low responder groups. Similarly, MDC/CCL22, chemotactic for monocytes, dendritic cells, natural killer cells, and chronically activated T lymphocytes showed a significant increase during induction phase until Day 14 and then started to go down reaching baseline levels by Day 35. High and slow responders MDC/CCL22 showed a significant increase from baseline levels, whereas, low responders also showed a slight increase during the induction phase. The high responders' trends remained higher than low responders during the entire induction phase, with a significant difference at Day 4.

On the other hand, suppression or no change in the concentration of every other immune cell chemokines examined was observed during induction phase on the test sides. IL-16; a proinflammatory cytokine and chemotactic for T cells, monocytes, and eosinophils, MPIF-1/CCL23; chemotactic for resting T-cells and monocytes and slight chemotactic for neutrophils, SCYB16/CXCL16; chemotactic for activated T-cells, GM-CSF; hematopoietic growth factor, and IL-2; a pleiotropic cytokine and regulator of T-cells proliferation and differentiation, all showed transient initial decrease on Day 4 and Day 7 on the test sides followed by rebound to baseline level at Day 14. All three responder groups showed the initial drop for the IL-16, MPIF-1/CCL23, GM-CSF, and SCYB16/CXCL16. High responders group demonstrated higher temporal patterns for the IL-16, MPIF-1/CCL23, and SCYB16/CXCL16 compared to the low responder group; however, low responders had higher expression pattern for GM-CSF compared to high responders,

Figure 3.8. Interestingly, high and low responders IL-2 levels increased while slow responders decreased at Day 4. By Day 7 all groups showed transient reduction followed by rebound at Day 14 to baseline level.

Other immune cells chemokines including MCP-1/CCL2; chemotactic for monocytes, EOTAXIN/CCL11; chemotactic for eosinophils, MCP-4/CCL13; chemotactic for monocytes, lymphocytes, basophils, and eosinophils, MIP-3α/CCL20; chemotactic for T-cells, B-cells and dendritic cells, 6CKINE/CCL21; chemotactic for activated T-cells, MIG/CXCL9; chemotactic for activated T-cells, IP-10/CXCL10; chemotactic for T-cells and monocytes, BCA-1/CXCL13; chemotactic for B-cells, IL-6; pleiotropic cytokine, and MCP-2/CCL8; chemotactic for monocytes, lymphocytes, basophils, and eosinophils, showed a decrease through the entire induction phase followed by an increase during resolution phase reaching concentration closer to baseline levels. The three responders expression levels for the chemokines mentioned above were decreased during the entire induction phase, however, high responders demonstrated higher temporal patterns compared to the low responder group for MCP-1/CCL2, EOTAXIN/CCL11, MCP-4/CCL13, MIP-3α/CCL20, 6CKINE/CCL21, MIG/CXCL9, and BCA-1/CXCL13. Interestingly, MIG/CXCL9, IP-10/CXCL10, BCA-1/CXCL13, and IL-6 levels showed a noticeble increase during the resolution phase reaching expression levels higher than baseline for the high responder group.

MIP-3β /CCL19; chemotactic for T-cell and B-cells and IL-10; anti-inflammatory cytokine remained unchanged during the induction phase. Different groups expression patterns for IL-10 showed a slight nonsignificant drop at Day 21, followed by an increase at Day 28 of resolution phase.

3.1.6.2 Changes in inflammatory cytokine expressions during induction and resolution of experimental gingivitis

IL-1β significantly increased during gingivitis induction, 2.2 fold increase from baseline 30.29 ± 31.4 pg per 30-s sample to Day 21 65.79 ± 84.07 pg per 30-s sample was observed on the test sides. There was a significant difference in IL-1β levels between the test and control sides at Day 14 of the induction phase. All three groups showed an increase in IL-1β levels during gingivitis induction with a noticeable transient early drop at Day 4, Figure 3.8 (C). High responders showed higher IL-1β levels on Day 14 and Day 21 compared to other groups but not statistically significant.

The level of TNF-α transiently decreased during the gingivitis induction on Day 4 and Day 7 and then increased back to baseline level by Day 14 on the test sides. TNF-α was statistically significantly different between test and control sides at Day 4 and Day 7. Mean levels of TNF-α were dropped for all three groups at Day 4 and Day 7 but only slow responders levels were significantly decreased compared to control sides, Figure 3.8 (D).

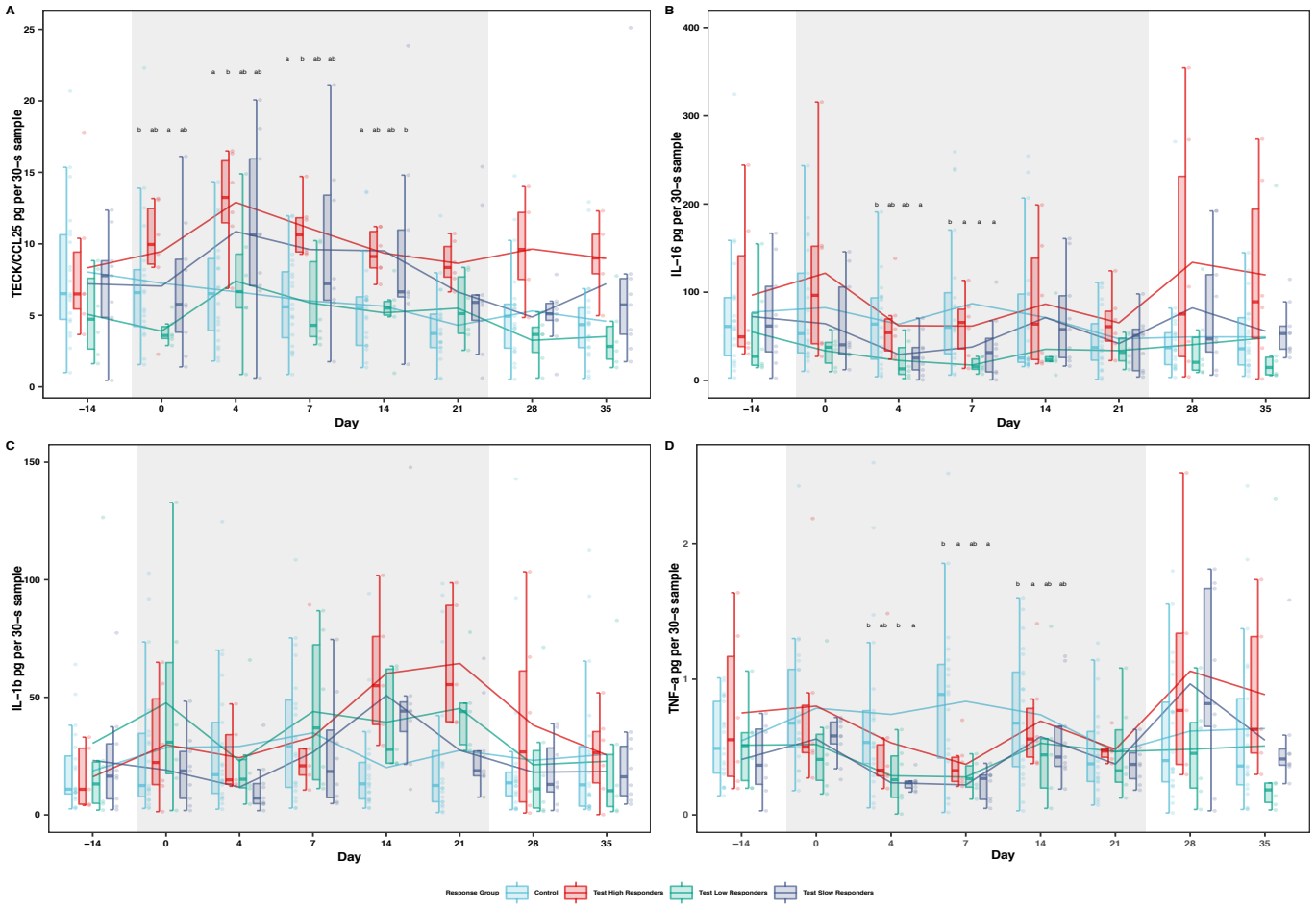

Figure 3.8: Major chemokines and cytokines boxplots during induction and resolution of experimental gingivitis among the responder groups.

There is variability in the chemokine and cytokine expression patterns among the different responder groups during the transition from health to disease.

The trend line represent the average values across time points. Blue control side, red test high responders, green test low responders, and purple test slow responders. Different letters above bars indicate significant differences between groups at each visit (a, b, c) (FDR $P < 0.05$).

Table 4: Gingival crevicular fluid mediators (mean ± SD) during induction and resolution of experimental gingivitis.
Statistical significant difference for test side vs control side, *$p < 0.05$, **$p < 0.01$ or ***$p < 0.001$. Statistical significant difference for the time trend on the test sides; induction phase values vs Day 0, §$p < 0.05$, †$p < 0.01$ or ‡$p < 0.001$.

	Control								Test							
	Hygiene Phase	Induction Phase					Resolution Phase		Hygiene Phase	Induction Phase					Resolution Phase	
	-14	0	4	7	14	21	28	35	-14	0	4	7	14	21	28	35
I-309/CCL1	1.01 ± 0.48	1.21 ± 0.44	1.07 ± 0.41	1.09 ± 0.43	0.98 ± 0.38	0.82 ± 0.44	0.96 ± 0.52	0.83 ± 0.43	1.18 ± 0.39	1.09 ± 0.41	0.97 ± 0.43	0.91 ± 0.32*	0.98 ± 0.44	0.76 ± 0.36§	0.98 ± 0.54	1.13 ± 0.69
EOTAXIN/CCL11	0.48 ± 0.24	0.54 ± 0.2	0.49 ± 0.14	0.5 ± 0.23	0.52 ± 0.2	0.45 ± 0.17	0.42 ± 0.13	0.47 ± 0.3	0.5 ± 0.15	0.48 ± 0.18	0.43 ± 0.11	0.36 ± 0.15*†	0.48 ± 0.13	0.37 ± 0.16§	0.53 ± 0.23	0.6 ± 0.63
MCP-4/CCL13	1.03 ± 0.67	1.03 ± 0.6	0.9 ± 0.6	1.02 ± 0.7	0.87 ± 0.73	0.74 ± 0.51	0.68 ± 0.48	0.87 ± 0.74	0.97 ± 0.65	0.89 ± 0.6	0.68 ± 0.39	0.77 ± 0.64	0.84 ± 0.51	0.7 ± 0.5	0.84 ± 0.62	0.93 ± 0.69
MIP-1δ/CCL15	1.4 ± 0.88	1.44 ± 0.9	1.39 ± 1.03	1.69 ± 1.15	1.48 ± 0.71	1.1 ± 0.84	1.23 ± 1.08	1.13 ± 0.88	1.58 ± 1.24	1.29 ± 0.8	1.32 ± 1.07	1.21 ± 0.85	1.81 ± 0.97†	1.7 ± 1.1*	1.73 ± 1.86	2.15 ± 3.93
MIP-3β /CCL19	0.5 ± 0.24	0.47 ± 0.17	0.39 ± 0.23	0.48 ± 0.21	0.45 ± 0.2	0.43 ± 0.25	0.39 ± 0.27	0.49 ± 0.24	0.45 ± 0.2	0.4 ± 0.18	0.48 ± 0.21	0.43 ± 0.24	0.49 ± 0.49	0.36 ± 0.21	0.43 ± 0.22	0.48 ± 0.33
MCP-1/CCL2	0.32 ± 0.23	0.94 ± 1.51	0.46 ± 0.4	0.97 ± 1.79	0.41 ± 0.42	0.27 ± 0.28	0.36 ± 0.61	0.5 ± 0.89	0.58 ± 0.78	0.44 ± 0.43	0.21 ± 0.21**	0.23 ± 0.24	0.37 ± 0.54	0.19 ± 0.22	0.84 ± 2.21	1.84 ± 5.32
MIP-3α/CCL20	1.09 ± 1.27	1.01 ± 1.15	0.87 ± 0.94	0.87 ± 1.13	0.72 ± 0.66	0.83 ± 1.07	0.98 ± 1.73	0.72 ± 0.83	0.88 ± 0.91	0.76 ± 0.79	0.52 ± 0.58	0.38 ± 0.36*	0.52 ± 0.32	0.43 ± 0.3	1 ± 1.15	1.16 ± 1.64
6CKINE/CCL21	3.02 ± 1.54	3.21 ± 1.91	3.69 ± 2.37	4.5 ± 3.22	5.18 ± 6.79	2.58 ± 1.95	2.39 ± 1.51	2.21 ± 1.38	3.6 ± 5.37	3.56 ± 3.17	2.92 ± 1.97	2.4 ± 1.56**	3.36 ± 3.32	2.48 ± 1.55	3.97 ± 3.13	4.95 ± 6.66
MDC/CCL22	0.54 ± 0.23	0.63 ± 0.41	0.6 ± 0.41	0.67 ± 0.34	0.71 ± 0.46	0.58 ± 0.23	0.57 ± 0.41	0.52 ± 0.25	0.58 ± 0.38	0.48 ± 0.24	0.73 ± 0.27†	0.68 ± 0.42§	1.11 ± 0.71*‡	0.57 ± 0.27	0.66 ± 0.36	0.53 ± 0.46
MPIF-1/CCL23	0.22 ± 0.18	0.21 ± 0.16	0.19 ± 0.12	0.21 ± 0.16	0.2 ± 0.13	0.19 ± 0.13	0.16 ± 0.13	0.18 ± 0.12	0.25 ± 0.16	0.22 ± 0.17	0.15 ± 0.14	0.16 ± 0.16	0.18 ± 0.15	0.2 ± 0.11	0.2 ± 0.16	0.27 ± 0.19
TECK/CCL25	8.03 ± 4.75	7.25 ± 4.71	6.65 ± 3.59	6.01 ± 3.18	5.64 ± 3.36	4.31 ± 2.59	5.3 ± 3.46	4.59 ± 3.22	6.91 ± 4	6.84 ± 4.22	10.46 ± 5.38***†	8.93 ± 4.78**	8.23 ± 4.79**	6.88 ± 3.52*	5.58 ± 3.37	6.54 ± 5.36
MIP-1α/CCL3	2.26 ± 2.28	3.99 ± 3.7	3.07 ± 2.83	4.01 ± 3.06	2.62 ± 2.12	2.88 ± 4	1.81 ± 1.94	2.06 ± 1.98	2.75 ± 2.36	3.39 ± 3.68	0.37 ± 0.44***‡	0.53 ± 0.81***‡	0.56 ± 0.7***‡	0.38 ± 0.23**‡	2.8 ± 3.62	2.67 ± 3.8
MCP-3/CCL7	0.52 ± 0.23	0.56 ± 0.27	0.62 ± 0.29	0.48 ± 0.31	0.56 ± 0.28	0.49 ± 0.36	0.53 ± 0.35	0.52 ± 0.29	0.61 ± 0.24	0.53 ± 0.3	0.49 ± 0.26	0.51 ± 0.29	0.58 ± 0.26	0.61 ± 0.27	0.48 ± 0.33	0.62 ± 0.39
MCP-2/CCL8	0.07 ± 0.06	0.23 ± 0.28	0.09 ± 0.06	0.18 ± 0.18	0.08 ± 0.06	0.06 ± 0.09	0.09 ± 0.1	0.15 ± 0.28	0.14 ± 0.15	0.09 ± 0.07*	0.03 ± 0.03**†	0.02 ± 0.03***†	0.51 ± 1.84	0.03 ± 0.03†	0.21 ± 0.49	0.6 ± 1.95
FRACTALKINE/CX3CL1	2.57 ± 2.08	2.42 ± 1.93	2.36 ± 1.8	2.08 ± 1.8	2.04 ± 1.49	2.01 ± 1.66	2.35 ± 2.92	1.88 ± 1.8	2.3 ± 1.72	1.99 ± 1.71	1.94 ± 1.58	1.56 ± 1.26	2.15 ± 1.1	1.72 ± 1.09	2.55 ± 2.27	2.76 ± 3.11
GRO-α/CXCL1	128.53 ± 73.55	126.78 ± 63.41	118.14 ± 62.5	136.87 ± 78.57	117.73 ± 87.18	101.1 ± 54.4	91.93 ± 46.25	120.47 ± 74.84	119.19 ± 66.38	111.49 ± 57.12	88.22 ± 44.45*	102.45 ± 69.13*	116.68 ± 57.83	102.59 ± 52.94	113.06 ± 66.6	120.84 ± 76.74
IP-10/CXCL10	1.74 ± 2.63	2.77 ± 3.67	1.79 ± 2.48	2.92 ± 3.69	1.51 ± 1.22	2.15 ± 5.11	2.6 ± 3.83	3.09 ± 5.27	2.8 ± 4.07	1.59 ± 2.01	0.82 ± 0.6*	0.92 ± 1.18**	0.99 ± 0.84	0.65 ± 0.49	3.74 ± 4.57	6.67 ± 15.36
BCA-1/CXCL13	0.53 ± 0.44	0.68 ± 0.48	0.5 ± 0.4	0.76 ± 0.73	0.59 ± 0.45	0.36 ± 0.24	0.46 ± 0.43	0.33 ± 0.16	0.61 ± 0.79	0.49 ± 0.32*	0.4 ± 0.26	0.36 ± 0.19**	0.44 ± 0.27	0.32 ± 0.17	0.59 ± 0.53	0.72 ± 1.01
SCYB16/CXCL16	0.91 ± 0.55	1.22 ± 0.85	0.99 ± 1.24	1.13 ± 0.85	0.98 ± 0.69	0.74 ± 0.72	0.7 ± 0.6	0.66 ± 0.5	1 ± 0.85	0.93 ± 0.68*	0.74 ± 0.5	0.81 ± 0.58*	1.09 ± 0.67	0.92 ± 0.76	0.98 ± 0.78	1.04 ± 1.3
Gro-β/CXCL2	4.52 ± 2.51	4.6 ± 2.81	4.85 ± 3.25	5.6 ± 4.31	4.77 ± 4.25	4.24 ± 2.94	3.34 ± 2.82	4.63 ± 4	4.83 ± 2.55	4.11 ± 2.45	2.24 ± 1.55***†	3.02 ± 1.95**	5.07 ± 3.38	4.85 ± 3.69	4.15 ± 2.84	4.63 ± 3.87
ENA-78/CXCL5	50.96 ± 26.17	39.79 ± 20.89	42.58 ± 17.11	45.81 ± 25.57	39.72 ± 31.99	34.81 ± 15.2	30.74 ± 15.08	35.36 ± 21.87	43.5 ± 19.32	40.96 ± 21.87	30.88 ± 9.48**	31.63 ± 25.68*§	44.82 ± 23.74	32.72 ± 15.1	40.16 ± 10.58	40 ± 23.94
GCP-2/CXCL6	4.25 ± 2.91	4.98 ± 4.53	4.47 ± 3.41	4.94 ± 3.01	4.3 ± 2.86	3.13 ± 1.86	3.11 ± 2.01	3.37 ± 2.47	4.38 ± 3.7	3.89 ± 2.55	2.46 ± 1.71**§	2.55 ± 1.39***§	2.66 ± 1.62**	1.82 ± 1.12**‡	4.49 ± 3.91	3.99 ± 3.8
MIG/CXCL9	9.46 ± 12.57	14.76 ± 19.51	11.17 ± 12.74	16.3 ± 23.76	9.85 ± 9.96	8.13 ± 10.75	10.35 ± 11.64	18.23 ± 43.59	14.11 ± 18.86	9.59 ± 12.41	4.48 ± 4.88**	4.65 ± 3.38*	7.89 ± 8.69	4.22 ± 3.8	22.31 ± 34.16	31.65 ± 94.67
GM-CSF	3.16 ± 1.09	2.67 ± 1.17	3.06 ± 1.05	2.67 ± 1.29	3.42 ± 0.99	2.72 ± 1.3	2.95 ± 0.92	2.82 ± 1.21	2.88 ± 1.32	2.74 ± 1.26	2.81 ± 1.2	2.35 ± 1.24	3.08 ± 1.16	2.58 ± 0.97	3.18 ± 0.71	3.32 ± 0.6
IFN-γ	0.18 ± 0.17	0.2 ± 0.18	0.17 ± 0.16	0.21 ± 0.15	0.15 ± 0.12	0.17 ± 0.21	0.17 ± 0.24	0.15 ± 0.2	0.21 ± 0.22	0.19 ± 0.21	0.11 ± 0.08**	0.14 ± 0.13*	0.15 ± 0.11	0.14 ± 0.13	0.21 ± 0.2	0.17 ± 0.15
IL-10	0.6 ± 0.36	0.6 ± 0.33	0.54 ± 0.29	0.53 ± 0.34	0.46 ± 0.28	0.46 ± 0.25	0.4 ± 0.27	0.46 ± 0.44	0.56 ± 0.3	0.5 ± 0.3	0.55 ± 0.21	0.47 ± 0.29	0.58 ± 0.39	0.39 ± 0.24	0.56 ± 0.35	0.59 ± 0.59
IL-16	77.36 ± 72.13	82.39 ± 65.22	81.09 ± 92.51	87.04 ± 78.85	71.26 ± 74.58	75.51 ± 134.71	49.34 ± 55.33	71.48 ± 108.75	74.33 ± 66.1	71.88 ± 73.24	36.75 ± 32.6*	38.79 ± 34.33***	89.18 ± 117.57	46.19 ± 30.57	85.01 ± 96.14	71.85 ± 77.55
IL-1β	34.14 ± 72.6	49.55 ± 72.11	29.11 ± 30.1	34.88 ± 29.1	31.99 ± 58.41	34.81 ± 46.48	23.18 ± 33.73	31.68 ± 40.68	30.34 ± 42.64	30.29 ± 31.4	29.19 ± 52.69	40.44 ± 41.09	74.32 ± 74.13*†	65.79 ± 84.07§	32.85 ± 44.87	28.4 ± 35.97
IL-2	0.06 ± 0.05	0.06 ± 0.04	0.08 ± 0.06	0.06 ± 0.05	0.06 ± 0.03	0.08 ± 0.1	0.06 ± 0.07	0.05 ± 0.04	0.07 ± 0.05	0.06 ± 0.06	0.05 ± 0.05	0.03 ± 0.03*	0.06 ± 0.05	0.05 ± 0.03	0.06 ± 0.08	0.08 ± 0.07
IL-6	0.56 ± 0.66	0.8 ± 1.02	0.7 ± 0.97	1.16 ± 2.08	0.58 ± 0.96	0.6 ± 1.11	0.68 ± 1.34	1.4 ± 3.73	1.12 ± 1.72	0.75 ± 0.96	0.12 ± 0.09**§	0.12 ± 0.12*§	0.3 ± 0.65	0.16 ± 0.18§	1.02 ± 1.83	5.45 ± 19.34
IL-8/CXCL8	198.31 ± 315.62	190.17 ± 126.37	200.1 ± 196.03	212.05 ± 159.42	168.7 ± 182.68	145.25 ± 191.83	110.39 ± 104.34	129.39 ± 114.3	151.67 ± 114.4	185.24 ± 146.41	85.8 ± 77.66**§	101.4 ± 85.97***§	110.76 ± 69.16§	80.94 ± 45.86†	157.42 ± 147.64	142.11 ± 121.65
MIF	2653.53 ± 1654.8	2301.22 ± 1635.17	1976.5 ± 1246.6	1758.56 ± 1011.92	1656.83 ± 1214.34	1173.52 ± 725.88	1428.84 ± 1009.37	1249.44 ± 935.98	2198.66 ± 1493.03	1962.76 ± 1275.21	3469.15 ± 1645.46***‡	3271.48 ± 1868.18***‡	3353.87 ± 1895.46***‡	2854.62 ± 2216.57**§	1658.08 ± 1378.46	1778.09 ± 1569.86
MPO	-	20953.59 ± 20899.8	-	31319.69 ± 33857.23	23283.68 ± 18527.47	20781.81 ± 19213.11	-	19071.64 ± 16984.07	-	19465.06 ± 16048.37	-	35265.87 ± 30322.75†	42599.7 ± 29030.34***‡	38365.76 ± 22271.09**‡	-	17687.41 ± 11585.47
TNF-α	0.55 ± 0.29	0.79 ± 0.51	0.74 ± 0.65	0.93 ± 0.75	0.74 ± 0.47	0.58 ± 0.64	0.62 ± 0.5	0.64 ± 0.63	0.8 ± 0.9	0.62 ± 0.44	0.34 ± 0.31**§	0.28 ± 0.15***†	0.76 ± 0.82	0.43 ± 0.22	0.84 ± 0.68	1.41 ± 3.55

Table 5: Gingival crevicular fluid mediators (mean ± SD during induction and resolution of experimental gingivitis among the responder groups.

Different letters indicate significant differences between the groups at each visit (a, b, c) (FDR P < 0.05).

	Control								Test High Responders								Test Low Responders								Test Slow Responders							
	Hygiene Phase	Induction Phase					Resolution Phase		Hygiene Phase	Induction Phase					Resolution Phase		Hygiene Phase	Induction Phase					Resolution Phase		Hygiene Phase	Induction Phase					Resolution Phase	
	-14	0	4	7	14	21	28	35	-14	0	4	7	14	21	28	35	-14	0	4	7	14	21	28	35	-14	0	4	7	14	21	28	35
I-309/CCL1	1.01 ± 0.48	1.21 ± 0.44	1.07 ± 0.41	1.09 ± 0.43[b]	0.98 ± 0.38	0.82 ± 0.44[ab]	0.96 ± 0.52	0.83 ± 0.43	1.22 ± 0.51	1.32 ± 0.38	1.18 ± 0.29	1.04 ± 0.26[b]	1.04 ± 0.35	0.82 ± 0.34[a]	1.37 ± 0.63	1.11 ± 0.62	0.92 ± 0.2	0.67 ± 0.16	0.51 ± 0.26	0.67 ± 0.19[b]	1.04 ± 0.65	0.53 ± 0.12[b]	0.54 ± 0.21	0.62 ± 0.49	1.27 ± 0.36	1.23 ± 0.32	1.09 ± 0.44	0.85 ± 0.4[a]	0.89 ± 0.38	1.14 ± 0.43[b]	0.96 ± 0.44	1.46 ± 0.77
EOTAXIN/CCL11	0.48 ± 0.24	0.54 ± 0.2	0.49 ± 0.14	0.5 ± 0.23[b]	0.52 ± 0.2	0.45 ± 0.17	0.42 ± 0.13	0.47 ± 0.3	0.53 ± 0.16	0.54 ± 0.25	0.5 ± 0.07	0.41 ± 0.12[a]	0.49 ± 0.06	0.45 ± 0.11	0.59 ± 0.13	0.43 ± 0.22	0.38 ± 0.13	0.42 ± 0.13	0.3 ± 0.07	0.31 ± 0.14[ab]	0.44 ± 0.19	0.27 ± 0.19	0.37 ± 0.1	0.48 ± 0.26	0.57 ± 0.12	0.49 ± 0.15	0.48 ± 0.08	0.37 ± 0.21[ab]	0.51 ± 0.14	0.4 ± 0.14	0.63 ± 0.32	0.83 ± 0.96
MCP-4/CCL13	1.03 ± 0.67	1.03 ± 0.6	0.9 ± 0.6	1.02 ± 0.7	0.87 ± 0.73	0.74 ± 0.51	0.68 ± 0.48	0.87 ± 0.74	1.19 ± 0.69	1.17 ± 0.69	1.01 ± 0.36	1.14 ± 0.76	0.84 ± 0.43	0.81 ± 0.52	0.91 ± 0.61	1.5 ± 0.5	0.76 ± 0.76	0.51 ± 0.25	0.38 ± 0.23	0.39 ± 0.29	0.54 ± 0.3	0.47 ± 0.21	0.54 ± 0.53	0.37 ± 0.36	0.97 ± 0.58	0.95 ± 0.63	0.66 ± 0.35	0.77 ± 0.63	1.05 ± 0.59	0.78 ± 0.62	1 ± 0.67	0.99 ± 0.68
MIP-1δ/CCL15	1.4 ± 0.88	1.44 ± 0.9	1.39 ± 1.03	1.69 ± 1.15	1.48 ± 0.71	1.1 ± 0.84	1.23 ± 1.08	1.13 ± 0.88	2.58 ± 1.84	2.15 ± 0.78	1.54 ± 0.53	1.79 ± 1.01	2.38 ± 0.94	2.33 ± 1.17	3.49 ± 2.94	2.53 ± 1.2	0.89 ± 0.37	0.78 ± 0.13	0.68 ± 0.6	0.78 ± 0.62	1.25 ± 0.93	1.26 ± 0.94	0.66 ± 0.56	0.58 ± 0.64	1.34 ± 0.56	1.04 ± 0.62	1.63 ± 1.46	1.1 ± 0.71	1.79 ± 0.89	1.57 ± 1.07	1.44 ± 0.64	2.98 ± 5.74
MIP-3β /CCL19	0.5 ± 0.24	0.47 ± 0.17[ab]	0.39 ± 0.23	0.48 ± 0.21	0.45 ± 0.2	0.43 ± 0.25	0.39 ± 0.27	0.49 ± 0.24	0.38 ± 0.23	0.53 ± 0.12[b]	0.49 ± 0.15	0.33 ± 0.25	0.46 ± 0.12	0.28 ± 0.09	0.49 ± 0.16	0.48 ± 0.15	0.42 ± 0.14	0.38 ± 0.05[a]	0.36 ± 0.2	0.35 ± 0.08	0.7 ± 0.87	0.34 ± 0.13	0.32 ± 0.16	0.32 ± 0.2	0.54 ± 0.21	0.34 ± 0.24[ab]	0.56 ± 0.25	0.6 ± 0.25	0.35 ± 0.18	0.48 ± 0.35	0.47 ± 0.29	0.57 ± 0.44
MCP-1/CCL2	0.32 ± 0.23	0.94 ± 1.51	0.46 ± 0.4[c]	0.97 ± 1.79	0.41 ± 0.42	0.27 ± 0.28	0.36 ± 0.61	0.5 ± 0.89	0.61 ± 0.75	0.59 ± 0.27	0.45 ± 0.25[bc]	0.44 ± 0.35	0.42 ± 0.43	0.34 ± 0.36	0.72 ± 1.17	0.81 ± 1.36	0.27 ± 0.27	0.28 ± 0.26	0.15 ± 0.12[ab]	0.13 ± 0.05	0.23 ± 0.26	0.15 ± 0.06	0.19 ± 0.16	1.18 ± 2.77	0.76 ± 1.01	0.44 ± 0.57	0.1 ± 0.07[a]	0.14 ± 0.12	0.43 ± 0.74	0.11 ± 0.11	1.36 ± 3.27	2.85 ± 7.7
MIP-3α/CCL20	1.09 ± 1.27	1.01 ± 1.15[b]	0.87 ± 0.94	0.87 ± 1.13[b]	0.72 ± 0.66	0.83 ± 1.07	0.98 ± 1.73	0.72 ± 0.83	1.11 ± 1.07	1.2 ± 1.08[ab]	0.88 ± 0.75	0.61 ± 0.35[b]	0.73 ± 0.32	0.6 ± 0.29	1.67 ± 1.23	1.71 ± 1.85	0.28 ± 0.37	0.31 ± 0.26[a]	0.21 ± 0.17	0.23 ± 0.32[a]	0.31 ± 0.21	0.3 ± 0.29	0.27 ± 0.37	0.37 ± 0.67	1.13 ± 0.93	0.76 ± 0.72[ab]	0.48 ± 0.55	0.33 ± 0.34[a]	0.51 ± 0.31	0.4 ± 0.3	1.11 ± 1.26	1.3 ± 1.87
6CKINE/CCL21	3.02 ± 1.54	3.21 ± 1.91	3.69 ± 2.37	4.5 ± 3.22	5.18 ± 6.79	2.58 ± 1.95	2.39 ± 1.51	2.21 ± 1.38	5.92 ± 9.41	5.47 ± 4.69	3.72 ± 2.47	3.07 ± 1.62	5.29 ± 5.3	3.1 ± 0.86	5.76 ± 4.33	4.16 ± 1.87	1.86 ± 1.68	2 ± 0.93	1.39 ± 0.65	0.95 ± 1.05	2.49 ± 2.22	1.61 ± 0.83	1.54 ± 0.66	1.76 ± 1.36	2.94 ± 1.39	2.81 ± 1.43	3.11 ± 1.67	2.66 ± 1.34	2.56 ± 1.47	2.57 ± 2.17	3.72 ± 2.12	6.89 ± 9.52
MDC/CCL22	0.54 ± 0.23	0.63 ± 0.41	0.6 ± 0.41[a]	0.67 ± 0.34	0.71 ± 0.46	0.58 ± 0.23	0.57 ± 0.41	0.52 ± 0.25	0.52 ± 0.29	0.63 ± 0.27	0.95 ± 0.14[b]	1.01 ± 0.43	1.35 ± 0.45	0.74 ± 0.2	0.59 ± 0.22	0.52 ± 0.33	0.49 ± 0.52	0.41 ± 0.15	0.44 ± 0.17[a]	0.52 ± 0.32	1.27 ± 1.23	0.43 ± 0.08	0.45 ± 0.26	0.26 ± 0.16	0.73 ± 0.34	0.41 ± 0.24	0.72 ± 0.23[ab]	0.55 ± 0.37	0.87 ± 0.44	0.53 ± 0.36	0.85 ± 0.44	0.65 ± 0.61
MPIF-1/CCL23	0.22 ± 0.18	0.21 ± 0.16	0.19 ± 0.12	0.21 ± 0.16	0.2 ± 0.13	0.19 ± 0.13	0.16 ± 0.13	0.18 ± 0.12	0.34 ± 0.12	0.32 ± 0.1	0.15 ± 0.16	0.13 ± 0.08	0.13 ± 0.11	0.14 ± 0.12	0.28 ± 0.23	0.23 ± 0.15	0.09 ± 0.07	0.05 ± 0.04	0.07 ± 0.08	0.07 ± 0.07	0.21 ± 0.01	NaN ± NA	0.04 ± 0.02	0.08 ± 0.05	0.29 ± 0.17	0.28 ± 0.2	0.2 ± 0.14	0.27 ± 0.24	0.23 ± 0.2	0.26 ± 0.07	0.2 ± 0.11	0.41 ± 0.19
TECK/CCL25	8.03 ± 4.75	7.25 ± 4.71[b]	6.65 ± 3.59[a]	6.01 ± 3.18[a]	5.64 ± 3.36[a]	4.31 ± 2.59	5.3 ± 3.46	4.59 ± 3.22	8.32 ± 5.16	9.47 ± 4.03[ab]	12.9 ± 3.63[b]	11.09 ± 2.12[b]	9.35 ± 1.67[ab]	8.64 ± 1.57	9.63 ± 3.64	8.97 ± 2.79	5.07 ± 3.03	3.9 ± 0.96[a]	7.4 ± 4.73[ab]	5.88 ± 3.37[ab]	5.18 ± 2.35[ab]	5.49 ± 2.45	3.25 ± 1.67	3.52 ± 2.37	7.21 ± 3.69	7.04 ± 4.7[ab]	10.86 ± 6.2[ab]	9.6 ± 6.18[ab]	9.51 ± 6.52[b]	6.63 ± 4.67	4.88 ± 1.92	7.21 ± 7.05
MIP-1α/CCL3	2.26 ± 2.28	3.99 ± 3.7	3.07 ± 2.83[b]	4.01 ± 3.06[b]	2.62 ± 2.12[b]	2.88 ± 4[b]	1.81 ± 1.94	2.06 ± 1.98	3.08 ± 2.9	5.62 ± 6.09	0.72 ± 0.71[a]	0.94 ± 1.44[a]	0.63 ± 0.58[a]	0.41 ± 0.11[ab]	3.93 ± 5.93	2.1 ± 2.35	1.77 ± 1.81	2.65 ± 2.44	0.18 ± 0.1[a]	0.2 ± 0.19[a]	0.35 ± 0.31[ab]	0.44 ± 0.39[ab]	1.36 ± 1.2	1.7 ± 2.78	3.18 ± 2.36	2.31 ± 0.76	0.27 ± 0.13[a]	0.48 ± 0.23[a]	0.65 ± 0.96[a]	0.31 ± 0.17[a]	3.01 ± 2.71	3.7 ± 5.07
MCP-3/CCL7	0.52 ± 0.23	0.56 ± 0.27	0.62 ± 0.29	0.48 ± 0.31	0.56 ± 0.28	0.49 ± 0.36	0.53 ± 0.35	0.52 ± 0.29	0.62 ± 0.33	0.74 ± 0.31	0.66 ± 0.22	0.63 ± 0.31	0.73 ± 0.21	0.67 ± 0.3	0.5 ± 0.46	0.67 ± 0.41	0.61 ± 0.24	0.4 ± 0.29	0.4 ± 0.28	0.43 ± 0.23	0.5 ± 0.31	0.51 ± 0.43	0.45 ± 0.28	0.59 ± 0.42	0.61 ± 0.19	0.42 ± 0.24	0.39 ± 0.23	0.44 ± 0.3	0.5 ± 0.25	0.6 ± 0.06	0.47 ± 0.24	0.6 ± 0.44
MCP-2/CCL8	0.07 ± 0.06	0.23 ± 0.28[b]	0.09 ± 0.06[b]	0.18 ± 0.18[b]	0.08 ± 0.06[b]	0.06 ± 0.09[b]	0.09 ± 0.1	0.15 ± 0.28	0.17 ± 0.21	0.15 ± 0.09[ab]	0.04 ± 0.04[ab]	0.03 ± 0.05[a]	0.03 ± 0.02[a]	0.02 ± 0.011[a]	0.15 ± 0.18	0.15 ± 0.24	0.06 ± 0.07	0.04 ± 0.03[a]	0.01 ± 0[a]	0.01 ± 0.01[a]	1.82 ± 3.55[ab]	0.01 ± 0.01[a]	0.04 ± 0.04	0.16 ± 0.3	0.17 ± 0.14	0.08 ± 0.05[a]	0.03 ± 0.02[a]	0.03 ± 0.02[a]	0.04 ± 0.07[ab]	0.05 ± 0.05[ab]	0.34 ± 0.72	1.09 ± 2.84
FRACTALKINE/CX3CL1	2.57 ± 2.08	2.42 ± 1.93	2.36 ± 1.8	2.08 ± 1.8	2.04 ± 1.49	2.01 ± 1.66	2.35 ± 2.92	1.88 ± 1.8	2.79 ± 1.68	2.81 ± 2.2	3.06 ± 1.79	2.3 ± 1.14	2.94 ± 1.2	2.37 ± 1.03	4.38 ± 2.71	4.23 ± 3.26	1.16 ± 1.16	1 ± 0.71	0.97 ± 0.69	0.94 ± 1.14	1.4 ± 0.74	1.19 ± 0.61	0.98 ± 0.95	1 ± 1.4	2.74 ± 1.85	2.13 ± 1.63	1.83 ± 1.52	1.48 ± 1.29	2.12 ± 0.95	1.64 ± 1.25	2.57 ± 2.01	2.93 ± 3.49
Gro-α/CXCL1	128.53 ± 73.55	126.78 ± 63.41	118.14 ± 62.5	136.87 ± 78.57[b]	117.73 ± 87.18	101.1 ± 54.4	91.93 ± 46.25	120.47 ± 74.84	148.75 ± 78.17	128.84 ± 71.21	120.24 ± 47.53	137.48 ± 86.79[ab]	120.63 ± 63.22	113.11 ± 65.23	125.21 ± 73.43	161.22 ± 88.72	96.77 ± 71.49	83.61 ± 32.52	61.2 ± 30.46	69.32 ± 36.02[a]	88.32 ± 47.96	89.53 ± 30.13	81.32 ± 54.4	63.07 ± 45.45	114.43 ± 54.26	118.51 ± 58.84	84.9 ± 40.23	101.03 ± 68.32[a]	132.97 ± 59.26	104.28 ± 59.71	126.12 ± 69.36	132.43 ± 68.07
IP-10/CXCL10	1.74 ± 2.63	2.77 ± 3.67	1.79 ± 2.48	2.92 ± 3.69[b]	1.51 ± 1.22[b]	2.15 ± 5.11	2.6 ± 3.83	3.09 ± 5.27	2.95 ± 5.59	1.62 ± 1.03	0.87 ± 0.42	0.83 ± 0.49[a]	0.76 ± 0.34[a]	0.74 ± 0.58	4.85 ± 6.16	3.2 ± 5.07	1.2 ± 1.65	0.68 ± 0.32	0.62 ± 0.3	0.67 ± 0.67[a]	1.3 ± 1.39[ab]	0.47 ± 0.27	1.08 ± 0.56	1.5 ± 2.34	3.9 ± 4.14	2.26 ± 2.99	0.9 ± 0.85	1.19 ± 1.78[a]	0.97 ± 0.72[ab]	0.72 ± 0.56	4.59 ± 4.41	12.06 ± 22.23
BCA-1/CXCL13	0.53 ± 0.44	0.68 ± 0.48[b]	0.5 ± 0.4	0.76 ± 0.73[b]	0.59 ± 0.45[b]	0.36 ± 0.24	0.46 ± 0.43	0.33 ± 0.16	0.95 ± 1.31	0.77 ± 0.42[ab]	0.56 ± 0.22	0.51 ± 0.16[ab]	0.59 ± 0.33[ab]	0.38 ± 0.1	1.14 ± 0.19	0.97 ± 0.93	0.31 ± 0.32	0.36 ± 0.2[a]	0.17 ± 0.1	0.18 ± 0.11[a]	0.24 ± 0.16[a]	0.26 ± 0.16	0.21 ± 0.2	0.23 ± 0.27	0.59 ± 0.54	0.4 ± 0.21[a]	0.43 ± 0.27	0.38 ± 0.16[a]	0.46 ± 0.21[ab]	0.31 ± 0.21	0.55 ± 0.58	0.91 ± 1.29
SCYB16/CXCL16	0.91 ± 0.55	1.22 ± 0.85	0.99 ± 1.24	1.13 ± 0.85	0.98 ± 0.69[ab]	0.74 ± 0.72	0.7 ± 0.6	0.66 ± 0.5	1.44 ± 1.11	1.63 ± 0.82	1.17 ± 0.51	1.19 ± 0.64	1.49 ± 0.58[a]	1.53 ± 1.07	1.71 ± 0.63	1.39 ± 0.4	0.81 ± 0.89	0.58 ± 0.36	0.35 ± 0.28	0.42 ± 0.28	0.59 ± 0.32[ab]	0.51 ± 0.14	0.38 ± 0.37	0.37 ± 0.49	0.82 ± 0.56	0.71 ± 0.37	0.72 ± 0.42	0.81 ± 0.54	1.16 ± 0.74[b]	0.79 ± 0.55	0.97 ± 0.75	1.28 ± 1.83
Gro-β/CXCL2	4.52 ± 2.51	4.6 ± 2.81[b]	4.85 ± 3.25[b]	5.6 ± 4.31[b]	4.77 ± 4.25	4.24 ± 2.94	3.34 ± 2.82	4.63 ± 4	6.1 ± 2.57	4.54 ± 2.95[a]	3.12 ± 0.52[a]	4.16 ± 2.51[a]	5.5 ± 4.06	5.3 ± 4.12	5.08 ± 3.22	7.38 ± 4.26	3.98 ± 2.4	3.02 ± 1.25[b]	1.87 ± 2.22[ab]	2.59 ± 1.4[a]	3.6 ± 1.74	4.72 ± 1.82	3.78 ± 3.24	2.92 ± 3.58	4.55 ± 2.59	4.56 ± 2.71[ab]	1.85 ± 1.36[a]	2.49 ± 1.69[a]	5.76 ± 3.74	4.63 ± 4.59	3.87 ± 2.58	4.24 ± 3.38
ENA-78/CXCL5	50.96 ± 26.17	39.79 ± 20.89	42.58 ± 17.11[b]	45.81 ± 25.57[b]	39.72 ± 31.99	34.81 ± 15.2	30.74 ± 15.08	35.36 ± 21.87	45.4 ± 17.44	44.49 ± 15.36	39.64 ± 7.24[ab]	36.7 ± 20.68[ab]	39.34 ± 11.84	35.84 ± 17.09	42.43 ± 10.5	51.22 ± 13.67	41.71 ± 26.58	31.79 ± 5.83	25.83 ± 8.14[ab]	21.11 ± 12.15[a]	41.81 ± 16.94	23.21 ± 11.71	37.27 ± 8.39	25.37 ± 17.65	43.21 ± 19.29	44.48 ± 30.41	27.51 ± 7.89[a]	35.32 ± 37.5[ab]	50.14 ± 32.62	39.09 ± 13.87	39.7 ± 12.82	40.27 ± 28.67
GCP-2/CXCL6	4.25 ± 2.91	4.98 ± 4.53	4.47 ± 3.41[b]	4.94 ± 3.01[b]	4.3 ± 2.86[b]	3.13 ± 1.86	3.11 ± 2.01	3.37 ± 2.47	5.12 ± 4.55	5.18 ± 3.63	3.43 ± 1.8[ab]	3.33 ± 1.75[ab]	2.56 ± 0.94[a]	1.74 ± 0.86	4.79 ± 3.46	4.65 ± 3.02	4.43 ± 4.45	4.17 ± 2.58	1.73 ± 0.82[a]	1.72 ± 0.96[a]	2.35 ± 1.97[b]	1.95 ± 1.61	3.33 ± 3.78	1.75 ± 0.92	3.86 ± 2.87	2.86 ± 1.15	2.31 ± 1.94[a]	2.6 ± 1.13[ab]	2.93 ± 1.84[b]	1.79 ± 1	5.06 ± 4.5	5.05 ± 4.96
MIG/CXCL9	9.46 ± 12.57	14.76 ± 19.51[b]	11.17 ± 12.74[b]	16.3 ± 23.76	9.85 ± 9.96[b]	8.13 ± 10.75	10.35 ± 11.64	18.23 ± 43.59	13.74 ± 17.59	16.18 ± 19.05[ab]	5.61 ± 2.71[ab]	6.7 ± 2.97	7.28 ± 3.71[a]	5.33 ± 4.59	34.73 ± 19.42	12.81 ± 10.01	8.31 ± 9.57	4.74 ± 4.75[a]	1.18 ± 1.33[a]	2.33 ± 1.76	7.22 ± 9.99[ab]	2.95 ± 1.95	5.76 ± 6.48	2.39 ± 4.37	17.57 ± 23.89	8.44 ± 9.62[ab]	6.35 ± 6.91[a]	4.87 ± 3.84	8.74 ± 10.79[ab]	4.31 ± 4.29	25.99 ± 45.33	65.38 ± 143.83
GM-CSF	3.16 ± 1.09	2.67 ± 1.17	3.06 ± 1.05	2.67 ± 1.29	3.42 ± 0.99	2.72 ± 1.3	2.95 ± 0.92	2.82 ± 1.21	2.64 ± 1.23	2.59 ± 1.38	2.56 ± 1.38	2.36 ± 1.03	2.74 ± 1.11	2.41 ± 0.84	2.82 ± 0.26	3.16 ± 0.6	3.05 ± 1.91	2.89 ± 1.65	3.17 ± 1.6	2.16 ± 1.52	3.51 ± 1.72	2.85 ± 1.57	3.81 ± 0.84	3.48 ± 0.49	2.93 ± 0.98	2.75 ± 0.98	2.77 ± 0.86	2.51 ± 1.31	3.06 ± 0.79	2.57 ± 0.78	3.05 ± 0.65	3.32 ± 0.7

	Control								Test High Responders								Test Low Responders								Test Slow Responders							
	Hygiene Phase	Induction Phase					Resolution Phase		Hygiene Phase	Induction Phase					Resolution Phase		Hygiene Phase	Induction Phase					Resolution Phase		Hygiene Phase	Induction Phase					Resolution Phase	
	-14	0	4	7	14	21	28	35	-14	0	4	7	14	21	28	35	-14	0	4	7	14	21	28	35	-14	0	4	7	14	21	28	35
IFN-γ	0.18 ± 0.17	0.2 ± 0.18^{ab}	0.17 ± 0.16	0.21 ± 0.15	0.15 ± 0.12	0.17 ± 0.21	0.17 ± 0.24	0.15 ± 0.2	0.27 ± 0.28	0.37 ± 0.28^{b}	0.12 ± 0.07	0.18 ± 0.13	0.2 ± 0.11	0.12 ± 0.06	0.3 ± 0.31	0.21 ± 0.17	0.12 ± 0.17	0.07 ± 0.09^{ab}	0.04 ± 0.05	0.01 ± 0.01	0.05 ± 0.04	0.07 ± 0.07	0.14 ± 0.13	0.21 ± 0.3	0.22 ± 0.22	0.14 ± 0.16^{a}	0.12 ± 0.1	0.13 ± 0.14	0.18 ± 0.1	0.22 ± 0.18	0.18 ± 0.09	0.13 ± 0.11
IL-10	0.6 ± 0.36	0.6 ± 0.33	0.54 ± 0.29	0.53 ± 0.34	0.46 ± 0.28	0.46 ± 0.25	0.4 ± 0.27	0.46 ± 0.44	0.6 ± 0.35	0.65 ± 0.38	0.66 ± 0.12	0.63 ± 0.33	0.48 ± 0.19	0.48 ± 0.32	0.74 ± 0.35	0.83 ± 0.43	0.48 ± 0.42	0.35 ± 0.29	0.4 ± 0.21	0.35 ± 0.34	0.77 ± 0.66	0.28 ± 0.19	0.38 ± 0.36	0.28 ± 0.21	0.58 ± 0.18	0.5 ± 0.22	0.55 ± 0.23	0.42 ± 0.21	0.54 ± 0.28	0.39 ± 0.19	0.57 ± 0.33	0.61 ± 0.73
IL-16	77.36 ± 72.13	82.39 ± 65.22	81.09 ± 92.51^{b}	87.04 ± 78.85^{b}	71.26 ± 74.58	75.51 ± 134.71	49.34 ± 55.33	71.48 ± 108.75	96.57 ± 89.04	121.62 ± 110.53	62.03 ± 41.66^{ab}	61.61 ± 36.63^{a}	86.55 ± 76.21	65.29 ± 35.47	133.84 ± 145.86	119.53 ± 107.71	55.01 ± 56.58	33.53 ± 18.22	22.54 ± 22.6^{ab}	17.33 ± 8.12^{a}	118.82 ± 207.19	33.76 ± 17.03	40.48 ± 45.6	48.19 ± 85.02	72.38 ± 57.54	64.3 ± 50.45	29.38 ± 23.69^{a}	37.78 ± 36.76^{a}	71.18 ± 55.41	41.74 ± 30.93	82.15 ± 72.28	55.84 ± 29.22
IL-1β	34.14 ± 72.6	49.55 ± 72.11	29.11 ± 30.1	34.88 ± 29.1	31.99 ± 58.41	34.81 ± 46.48	23.18 ± 33.73	31.68 ± 40.68	41.05 ± 62.18	29.81 ± 25.51	61.62 ± 92.49	55.42 ± 61.59	104.85 ± 112.6	116.96 ± 131.14	38.13 ± 41.17	25.42 ± 18.6	30.43 ± 47.88	47.61 ± 48.45	22.89 ± 22.18	43.94 ± 33.78	62.29 ± 59.24	72.11 ± 68.16	21.31 ± 26.92	22.78 ± 31.16	23.15 ± 23.47	19.06 ± 14.96	11.78 ± 11.28	26.59 ± 25.2	61.99 ± 51.41	27.46 ± 19.19	37.02 ± 58.13	34.13 ± 48.42
IL-2	0.06 ± 0.05	0.06 ± 0.04	0.08 ± 0.06^{b}	0.06 ± 0.05^{b}	0.06 ± 0.03	0.08 ± 0.1	0.06 ± 0.07	0.05 ± 0.04	0.08 ± 0.07	0.08 ± 0.09	0.08 ± 0.07^{ab}	0.03 ± 0.02^{ab}	0.05 ± 0.03	0.05 ± 0.03	0.09 ± 0.13	0.08 ± 0.05	0.06 ± 0.03	0.04 ± 0.04	0.07 ± 0.05^{ab}	0.03 ± 0.02^{ab}	0.04 ± 0.05	0.04 ± 0.03	0.02 ± 0.02	0.06 ± 0.04	0.08 ± 0.06	0.06 ± 0.03	0.03 ± 0.03^{a}	0.03 ± 0.04^{a}	0.08 ± 0.06	0.05 ± 0.05	0.08 ± 0.04	0.09 ± 0.11
IL-6	0.56 ± 0.66	0.8 ± 1.02	0.7 ± 0.97^{b}	1.16 ± 2.08^{b}	0.58 ± 0.96	0.6 ± 1.11^{b}	0.68 ± 1.34	1.4 ± 3.73	0.73 ± 0.87	0.64 ± 0.66	0.14 ± 0.12^{a}	0.18 ± 0.19^{a}	0.18 ± 0.17	0.16 ± 0.15^{ab}	1.88 ± 3.07	1.19 ± 1.26	0.58 ± 0.61	0.28 ± 0.25	0.06 ± 0.03^{a}	0.06 ± 0.03^{a}	0.17 ± 0.2	0.18 ± 0.28^{b}	0.42 ± 0.48	0.76 ± 1.35	1.74 ± 2.47	1.08 ± 1.28	0.14 ± 0.08^{a}	0.13 ± 0.06^{a}	0.51 ± 1.04	0.11 ± 0.06^{a}	0.86 ± 1.35	10.46 ± 28.27
IL-8/CXCL8	198.31 ± 315.62	190.17 ± 126.37	200.1 ± 196.03^{b}	212.05 ± 159.42^{b}	168.7 ± 182.68	145.25 ± 191.83^{b}	110.39 ± 104.34	129.39 ± 114.3	173.54 ± 123.99	262.32 ± 190.11	142.03 ± 122.99^{ab}	149.74 ± 107.38^{a}	151.58 ± 106.49	101.71 ± 61.66^{ab}	200.73 ± 212.37	143.58 ± 69.73	122.25 ± 97.06	147.6 ± 126.67	74.1 ± 39.78^{ab}	58.42 ± 21.67^{a}	71.9 ± 33.24	90.93 ± 22.91^{b}	98.26 ± 97.61	92.57 ± 139.88	156.71 ± 127.22	158.94 ± 121.15	56.12 ± 34.22^{a}	97.38 ± 88.8^{a}	109.47 ± 42.37	60.44 ± 41.02^{a}	167.99 ± 127.25	174.16 ± 136.87
MIF	2653.53 ± 1654.8	2301.22 ± 1635.17	1976.5 ± 1246.6^{a}	1758.56 ± 1011.92^{a}	1656.83 ± 1214.34^{a}	1173.52 ± 725.88^{a}	1428.84 ± 1009.37	1249.44 ± 935.98	2460.85 ± 1548.07	2626.45 ± 1441.95	4431.64 ± 463.18^{b}	4573.03 ± 1662.6^{b}	3816.1 ± 1000.83^{ab}	3979.51 ± 2860.34^{ab}	2734.22 ± 2036.01	2326.51 ± 1433.06	1723.95 ± 1655.89	1177.9 ± 423.52	2629.95 ± 1801.81^{ab}	2217.85 ± 1518.35^{b}	2023.17 ± 1143.34^{ab}	2164.48 ± 1072.86^{b}	993.63 ± 726.06	959.65 ± 741.6	2340.34 ± 1455.37	2043.53 ± 1361.63	3386.96 ± 1837.15^{b}	3085.55 ± 1846.32^{ab}	3932.86 ± 2381.9^{b}	2564.79 ± 2247.08^{ab}	1383.62 ± 738.69	1958.1 ± 1941.52
MPO	NaN ± NA	20953.59 ± 20899.8	NaN ± NA	31319.69 ± 33857.23	23283.68 ± 18527.47^{a}	20781.81 ± 19213.11^{a}	NaN ± NA	19071.64 ± 16984.07	NaN ± NA	21399.47 ± 17149.66	NaN ± NA	32665.61 ± 23599.14	49845.51 ± 34589.17^{b}	44099.98 ± 34226.59^{ab}	NaN ± NA	20325.83 ± 8743.77	NaN ± NA	24230.29 ± 23696.65	NaN ± NA	45531.92 ± 37635.43	43934.57 ± 33995.24^{b}	33810.06 ± 13921.47^{ab}	NaN ± NA	14207.45 ± 11520.28	NaN ± NA	14998.64 ± 8174.34	NaN ± NA	29516.53 ± 30858.74	36879.25 ± 23649.95^{b}	37580.07 ± 18595.44^{b}	NaN ± NA	18248.44 ± 13790.17
TNF-α	0.55 ± 0.29	0.79 ± 0.51	0.74 ± 0.65^{b}	0.93 ± 0.75^{b}	0.74 ± 0.47^{b}	0.58 ± 0.64	0.62 ± 0.5	0.64 ± 0.63	0.75 ± 0.6	0.8 ± 0.71	0.53 ± 0.48^{ab}	0.37 ± 0.18^{a}	0.69 ± 0.39^{a}	0.48 ± 0.1	1.06 ± 0.92	0.89 ± 0.61	0.51 ± 0.32	0.52 ± 0.41	0.29 ± 0.24^{b}	0.28 ± 0.12^{ab}	1.09 ± 1.46^{ab}	0.47 ± 0.36	0.48 ± 0.39	0.51 ± 0.9	1.03 ± 1.27	0.56 ± 0.16	0.24 ± 0.06^{a}	0.22 ± 0.12^{a}	0.58 ± 0.35^{ab}	0.37 ± 0.15	0.97 ± 0.67	2.3 ± 5.26

3.1.6.3 Correlations between chemokines and clinical parameters during gingivitis induction

The repeated measures correlation coefficients between clinical indices, chemokines, MPO, and subgingival bacterial load for the test side during induction phase are shown in the correlogram in Figure 3.9, where variables are arranged based on hierarchical clustering.

The highest positive correlations ($r > 0.8$ and $p < 0.001$) were seen between plaque accumulation (PI and bacterial load) and gingival inflammation(GI and BOP), MIF and TECK/CCL25, Gro-α/CXCL1 and MCP-4/CCL13, and Fractalkine/CX3CL1 and CCL20. The highest negative correlations ($r > -0.6$ and $p < 0.001$.) were seen between PI and MIP-1α/CCL3, and between bacterial load and MIP-1α/CCL3.

Gingival inflammation severity denoted by GI and BOP were both positively correlated with PI, GCF, bacterial load, MPO, MIP-1δ/CCL15, Gro-β/CXCL2, and SCYB16 / CXCL16. However, GI and BOP exhibited negative correlation trends with most assayed chemokines, in particular statistical significant negative correlation was observed with IP-10/CXCL10, MIP-1α/CCL3, IL-6, GCP-2/CXCL6 and BCA-1/CXCL13.

Microbial plaque accumulation denoted by PI and bacterial load showed positive correlations with GI, BOP, GCF, MPO, Gro-β/CXCL2 and MDC/CCL22, and were negatively correlated with several chemokines including IP-10/CXCL10, MIP-1α/CCL3, IL-6, GCP-2/CXCL6, MIP-3α/CCL20, BCA-1/CXCL13, and IL-8/CXCL8.

MPO, which is a marker for neutrophil activation, was positively correlated with PI, GI, GCF, BOP, bacterial load, MIP-1δ/CCL15, SCYB16 / CXCL16, MDC/CCL22 and with the neutrophil chemokine Gro-β/CXCL2; whereas MPO was negatively correlated with IL-6 and neutrophil chemokine GCP-2/CXCL6. Major neutrophil chemoattractant MIF and IL-8/CXCL8 and the

potent inflammatory mediators IL-1β and TNF-α showed a strong positive correlation with almost every other examined chemokines. MIF showed overall positive correlations with gingivitis and plaque but was not statistically significant. However, IL- β showed a significant correlation with plaque accumulation (PI and bacterial load) and gingival inflammation (GI and BOP). Interestingly, IL-8/CXCL8 exhibited negative correlations with gingivitis severity and plaque.

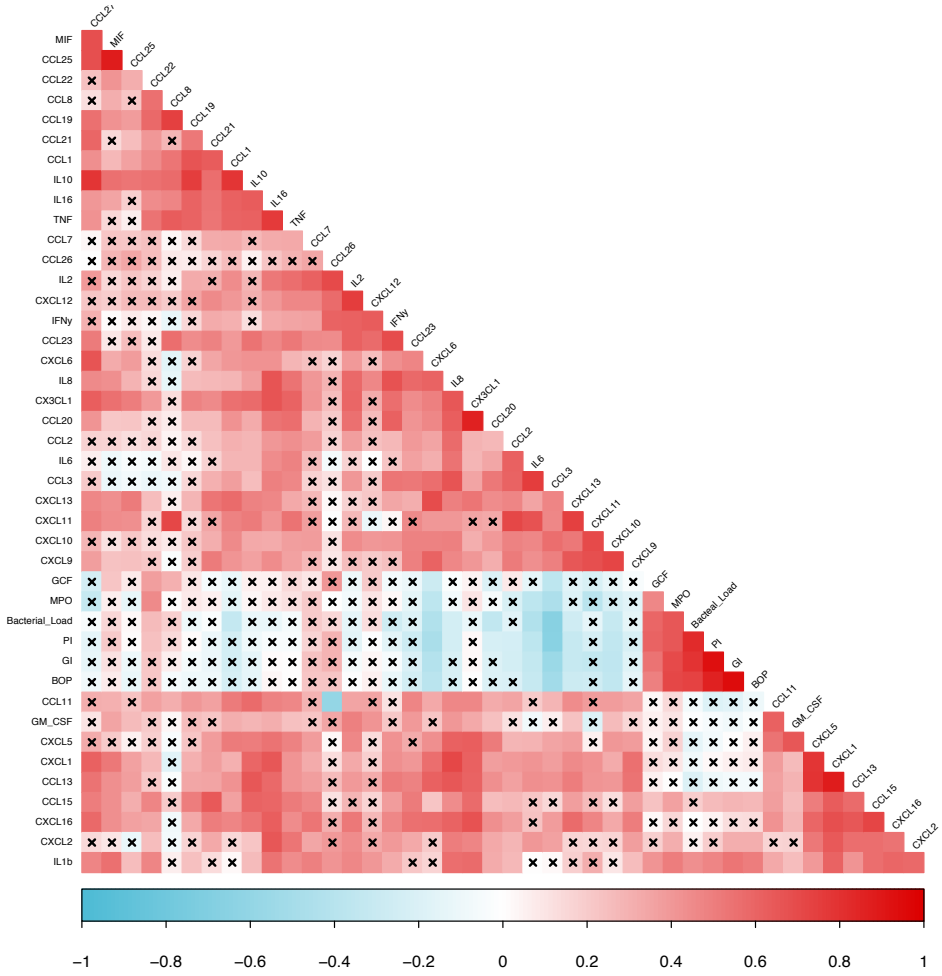

Figure 3.9: Correlation between clinical indices and chemokines in the test side during induction phase of experimental gingivitis.
Correlogram based on hierarchical clustering showing the repeated measures correlation coefficients between clinical indices, chemokines, MPO and bacterial load during entire induction phase. Correlation coefficients are expressed by color scale from red to blue. Red designate a positive correlation while blue color designate a negative correlation. Non-significant correlations according to the significance level of 0.05 are marked with an X.

3.1.6.4 Correlations between chemokines and clinical parameters in the responder groups during gingivitis induction

That different responder groups displayed distinct chemokines expression patterns. Overall correlation analysis of entire study groups may not reflect the key difference in the individual groups. Correlation analysis between clinical parameters and chemokines expression at the group level showed some interesting results. MPO was highly correlated with the clinical parameters in all three groups. Similarly, IL-1β showed positive correlations in all three groups, although higher correlation coefficients were seen in the high responder groups in comparison to slow responders. MIF was positively associated with gingivitis severity and plaque in all three groups; however significant correlation was only seen in the high and low responder groups. GCP-2/CXCL6 showed negative associations with GI and BOP in all three groups. Interestingly, MPO was positively correlated with neutrophil chemokines GRO-α/CXCL1 and GRO-β/CXCL2 in the low responder groups only.

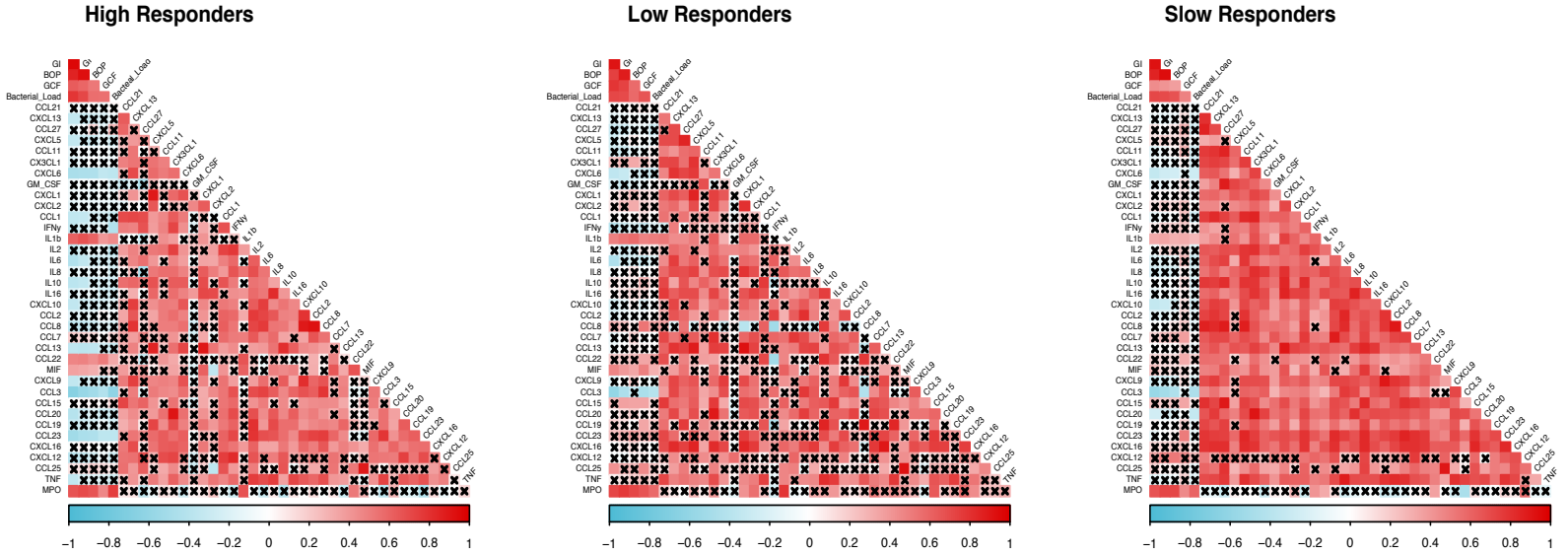

Figure 3.10: Correlation between clinical indices and chemokines among responder groups during induction phase of experimental gingivitis.

Correlogram based on hierarchical clustering showing the repeated measures correlation coefficients between clinical indices, chemokines, MPO and bacterial load during entire induction phase. Correlation coefficients are expressed by color scale from red to blue. Red designate a positive correlation while blue color designate a negative correlation. Non-significant correlations according to the significance level of 0.05 are marked with an X.

3.1.7 Microbial results

3.1.7.1 Bacterial load of the subgingival plaque

There were no significant differences in bacterial load between control and test sides on Day -14 and Day 0 visits. During gingivitis induction, the total bacterial load increased significantly from baseline as early as Day 4 and continued to be high until the peak of induction at Day 21. The microbial load was significantly higher in the test side compared to control sides during the entire induction phase ($p<0.001$). After resuming oral hygiene, bacterial load decreased from Day 21 to Day 35, Figure 3.11 (A). Interestingly, groups trajectories for bacterial load showed higher bacterial load mean levels for the high and low responders groups compared to slow responders during the induction phase, similar to the temporal pattern of plaque scores, Figure 3.11, (B).

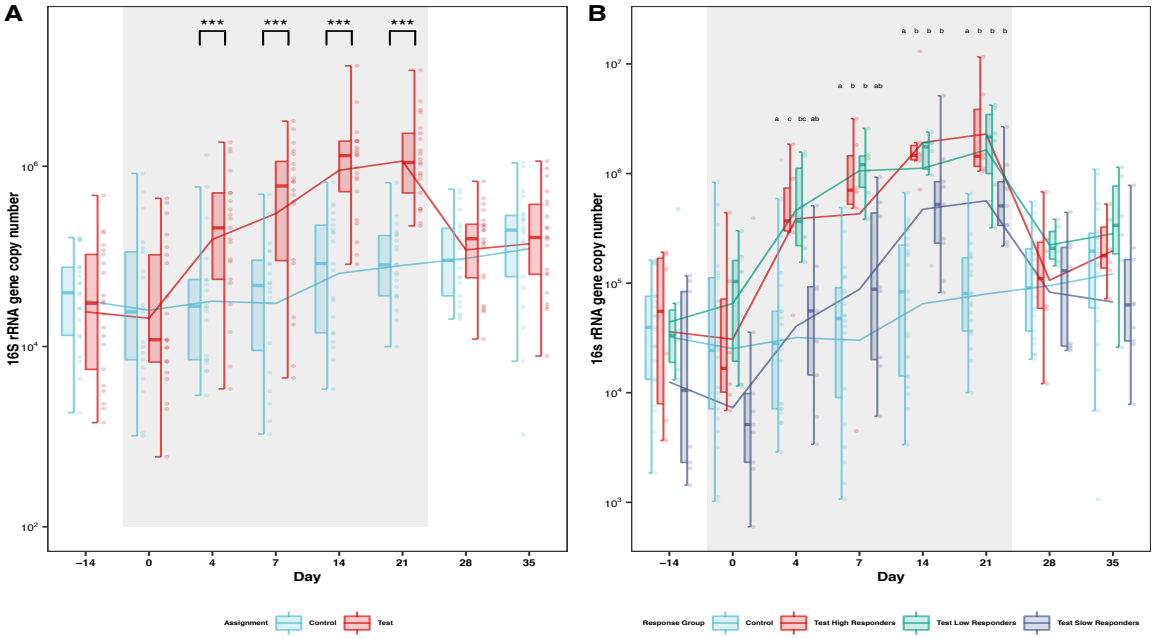

Figure 3.11: Bacterial load in subgingival plaque during induction and resolution of experimental gingivitis.
The trend line represent the average values across time points. (A)Test and control sides: Blue control side and red test side. Significance *p < 0.05, **p < 0.01 or ***p < 0.001.
(B) Responder groups. Blue control side, red test high responders, green test low responders, and purple test slow responders. Different letters above bars indicate significant differences between groups at each visit (a, b, c) (FDR P < 0.05).

3.1.7.2 Sequencing summary

The bacterial 16S rRNA gene V3-V4 region sequencing resulted in a total of 11,885 identified amplicon sequence variants (ASVs) across all subjects and all time points. A total of 2,209,852 reads was obtained from sequencing with an average of 6,616.323 (± 2,797.687) reads per sample, the maximum and minimum reads per sample were 30,666 and 2,621, respectively, Figure 3.12. In addition, 20.69% of the OTUs are doubletons or singletons. In the subgingival plaque samples, a total of 10 phyla, 24 classes, 36 orders, 59 families, 111 genera, and 421 species were identified.

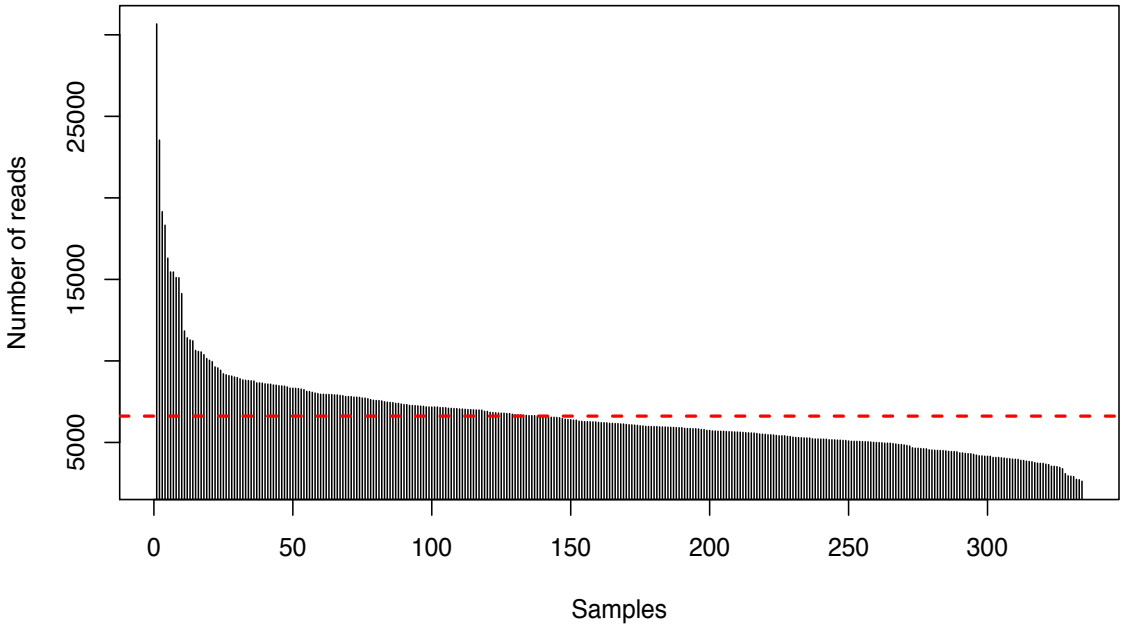

Figure 3.12: Sum of reads per sample.

3.1.7.3 Alpha diversity of the subgingival bacterial communities

To evaluate the changes in the diversity within the microbial communities during gingivitis induction, alpha diversity was calculated using five different metrics across different time points, Table 6 and Table 7. At baseline, there were no significant differences in any of alpha diversity indices between control and test sides. In general, all alpha diversity metrics showed a significant increase during the experimental phase corresponding to increased disease severity as measured by GI, Figure 3.13. Alpha diversity scores in all metrics increased as early as Day 4 in the test sides and by Day 14 all measured diversity indices were significantly higher compared to baseline on the test sides, Table 6. At the groups level, different responders showed a significant increase in all measured alpha diversity metrics during the induction phase, Figure 3.14. Interestingly, high responder group displayed a noticeable drop in all measured alpha diversity metrics on Day 7.

Between-group analysis showed that species richness values as measured by the observed number of species and Chao1 richness estimator were significantly higher in the test sides compared to control sides during experimental gingivitis, Figure 3.13 (A, B). Different responder groups subgingival microbiome showed an increase in richness scores with no statistical differences between the groups. Only slow responders showed significantly higher species number and Choa1 index scores at Day 7 compared to controls, Figure 3.14 (A, B). In addition, community diversity estimated by Shannon diversity index and Simpson's Inverse index revealed that test sides comprised significantly more diverse communities than control sides as plaque accumulated, Figure 3.13 (C, D). Community diversities for different responder groups were significantly increased compared to control during the induction phase. Shannon index and Simpson's Index were significantly higher for high and slow responders after two weeks of gingivitis in comparison to controls, Figure 3.14 (C, D).

The phylogenetic diversity (PD) index also showed that the microbial communities associated with diseased test sides are more diverse than communities associated with the control healthy sides, Figure 3.13 (E). Temporal patterns for PD index showed a significant increase in all three responder groups compared to control during the induction phase, Figure 3.14 (E). However, there was an evident lag in the slow responders PD index at Day 4 compared to high and low responder groups. After the first week of gingivitis, all responder groups showed a similar increase in PD index scores peaking at Day 21. After oral hygiene reinstitution, all alpha diversity metrics scores decreased during resolution phase returning to baseline levels at Day 35.

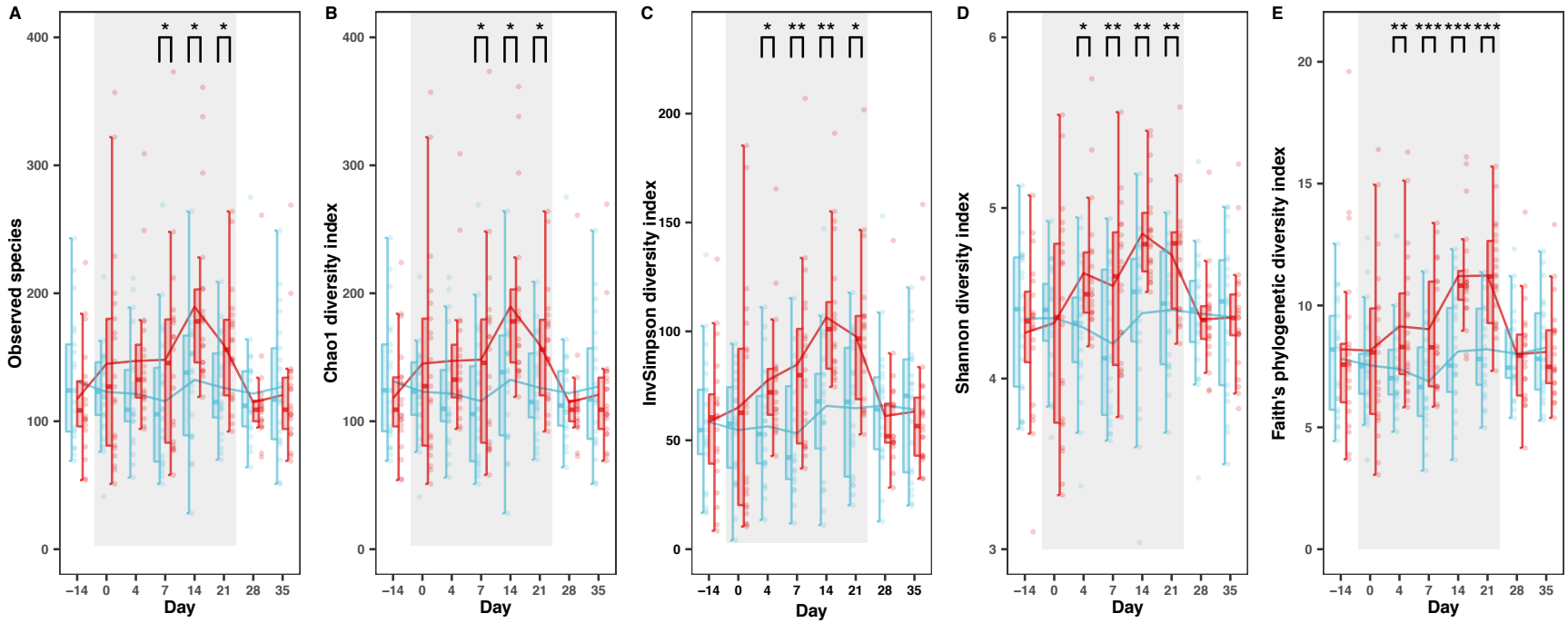

Figure 3.13: Richness and diversity metrics of the subgingival microbial communities during the induction and resolution of experimental gingivitis.
All alpha diversity metrics showed a significant increase during gingivitis induction.
(A) Observed, (B) Chao1 diversity (C) Simpson's inverse diversity (D) Shannon diversity (E) Faith's phylogenetic diversity.
Blue control side and red test side. Significance*$p < 0.05$, **$p < 0.01$ or ***$p < 0.001$.

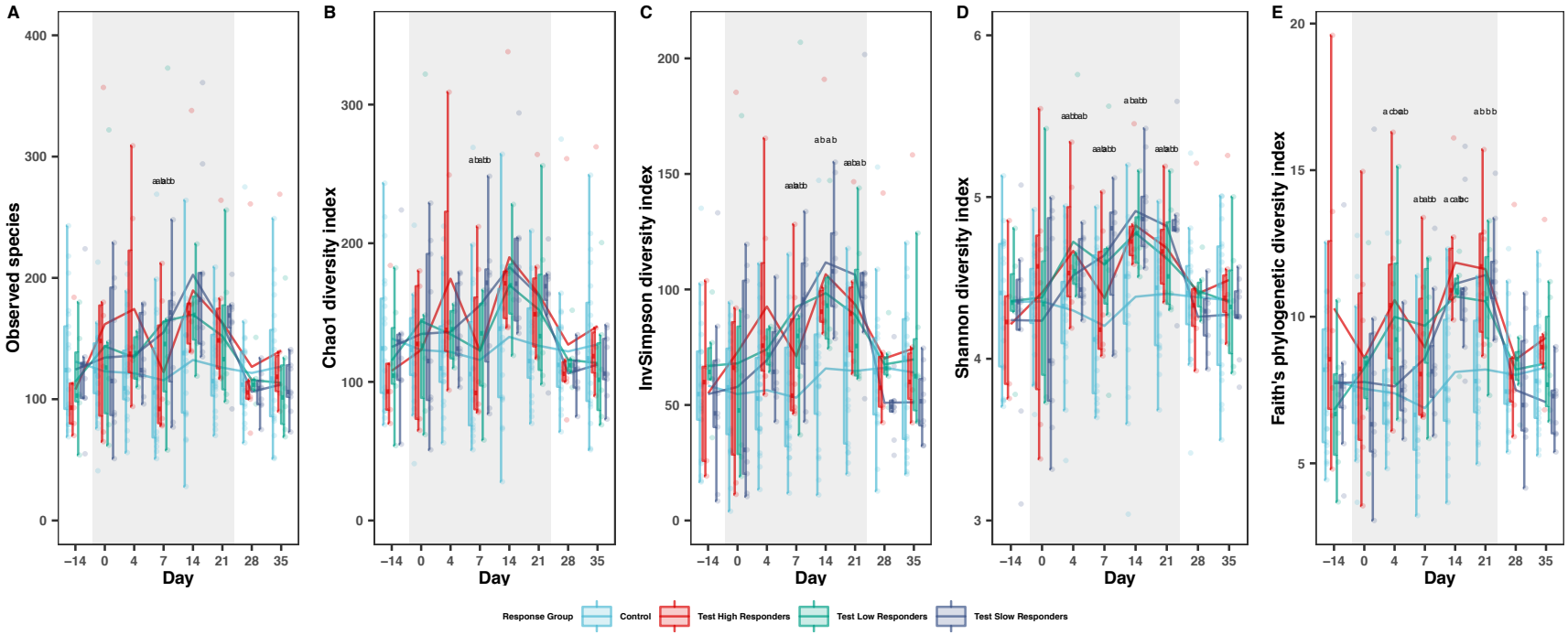

Figure 3.14: Richness and diversity metrics of the subgingival microbial communities among responder groups during the induction and resolution of experimental gingivitis.
The subgingival microbial communities showed an increase in alpha diversity scores in all responder groups during the induction of gingivitis. At Day 7, high responders showed a drop in all diversity measures indicating a significant shift in the microbial community.
(A) Observed, (B) Chao1 diversity (C) Simpson's inverse diversity (D) Shannon diversity (E) Faith's phylogenetic diversity.
Blue control side, red test high responders, green test low responders, and purple test slow responders. Different letters above bars indicate significant differences between groups at each visit (a, b, c) (FDR $P < 0.05$).

Table 6: Alpha diversity indices (mean ± SD) during induction and resolution of experimental gingivitis.
Statistical significant difference for test side vs control sides, *$p < 0.05$, **$p < 0.01$ or ***$p < 0.001$. Statistical significant difference for the time trend on the test sides; induction phase values vs Day 0, §$p < 0.05$, †$p < 0.01$ or ‡$p < 0.001$.

	Control								Test							
	Hygiene Phase	Induction Phase					Resolution Phase		Hygiene Phase	Induction Phase					Resolution Phase	
	-14	0	4	7	14	21	28	35	-14	0	4	7	14	21	28	35
Shannon diversity	4.35 ± 0.43	4.26 ± 0.53	4.3 ± 0.38	4.2 ± 0.44	4.38 ± 0.5	4.4 ± 0.35	4.38 ± 0.38	4.36 ± 0.46	4.35 ± 0.59	4.33 ± 0.66	4.62 ± 0.38*§	4.54 ± 0.46**	4.85 ± 0.28**‡	4.72 ± 0.34**†	4.35 ± 0.27	4.36 ± 0.34
Chao1 diversity	131.23 ± 50.14	123.04 ± 36.71	121.57 ± 43.48	115.74 ± 56.61	132.47 ± 51.83	126.07 ± 38.16	121.96 ± 44.06	127.02 ± 52.66	142.66 ± 120.84	145.06 ± 82.26	161.78 ± 84.33*	148.1 ± 75.05*	189.63 ± 65.79***§	171.2 ± 70.17**	114.85 ± 37.66	120.68 ± 45.17
Simpson's inverse diversity	58.38 ± 30.45	54.68 ± 25.09	56.41 ± 26.26	53.15 ± 28.59	65.8 ± 32.96	64.72 ± 30.02	66.08 ± 29.81	64.09 ± 30.8	70.03 ± 61.36	65.04 ± 52.69	85.87 ± 46.71*§	84.74 ± 41.06**	106.45 ± 30.98**‡	97.76 ± 34.81*†	61.16 ± 23.69	63.15 ± 29.97
Faith's phylogenetic diversit	7.69 ± 2.35	7.41 ± 2.14	7.26 ± 1.82	6.74 ± 2.11	7.97 ± 2.41	8.05 ± 1.99	7.87 ± 1.87	8.12 ± 2.12	8.08 ± 3.74	8.01 ± 3.53	9.04 ± 2.89**	8.89 ± 2.43***	11.08 ± 2.18***‡	11.1 ± 2.13***‡	7.83 ± 2.1	7.96 ± 1.94
Observed species	130.95 ± 49.92	122.9 ± 36.7	121.43 ± 43.41	115.6 ± 56.55	132.33 ± 51.72	126 ± 38.18	121.62 ± 44.1	126.95 ± 52.59	142.05 ± 120.67	144.86 ± 82.2	161.67 ± 84.07	148 ± 74.97*	189.48 ± 65.74*§	171.1 ± 70.11*	114.76 ± 37.67	120.48 ± 45.02

Table 7: Alpha diversity indices (mean ± SD) during induction and resolution of experimental gingivitis among the responder groups.
Different letters indicate significant differences between groups at each visit (a, b, c) (FDR $P < 0.05$).

	Control								Test High Responders								Test Low Responders								Test Slow Responders							
	Hygiene Phase	**Induction Phase**					**Resolution Phase**		**Hygiene Phase**	**Induction Phase**					**Resolution Phase**		**Hygiene Phase**	**Induction Phase**					**Resolution Phase**		**Hygiene Phase**	**Induction Phase**					**Resolution Phase**	
	-14	0	4	7	14	21	28	35	-14	0	4	7	14	21	28	35	-14	0	4	7	14	21	28	35	-14	0	4	7	14	21	28	35
Shannon diversity	4.35 ± 0.43	4.26 ± 0.53^{a}	4.3 ± 0.38^{a}	4.2 ± 0.44^{a}	4.38 ± 0.5^{a}	4.4 ± 0.35^{a}	4.38 ± 0.38	4.36 ± 0.46	4.51 ± 0.84	4.41 ± 0.8^{a}	4.67 ± 0.44^{ab}	4.38 ± 0.43^{ab}	4.82 ± 0.32^{b}	4.68 ± 0.31^{ab}	4.4 ± 0.44	4.49 ± 0.41	4.36 ± 0.34	4.38 ± 0.63^{a}	4.72 ± 0.52^{b}	4.58 ± 0.59^{ab}	4.78 ± 0.24^{ab}	4.62 ± 0.35^{ab}	4.42 ± 0.16	4.35 ± 0.41	4.24 ± 0.56	4.24 ± 0.65^{a}	4.52 ± 0.21^{ab}	4.64 ± 0.41^{b}	4.91 ± 0.3^{b}	4.82 ± 0.36^{b}	4.26 ± 0.19	4.27 ± 0.24
Chao1 diversity	131.23 ± 50.14	123.04 ± 36.71^{a}	121.57 ± 43.48^{a}	115.74 ± 56.61^{a}	132.47 ± 51.83^{a}	126.07 ± 38.16^{a}	121.96 ± 44.06	127.02 ± 52.66	196.18 ± 219.78	161.98 ± 106.65^{a}	174.42 ± 84.88^{a}	122.35 ± 58.83^{ab}	189.89 ± 74.78a	163.27 ± 55.05^{a}	126.87 ± 67.36	140.11 ± 65.6	115.39 ± 44.77	143.87 ± 93.23^{a}	187.74 ± 131.92^{a}	164.37 ± 109.91^{ab}	169.75 ± 37.47^{a}	152.15 ± 60.44^{a}	115.94 ± 18.9	113.58 ± 48.67	125.17 ± 44.88	134.58 ± 63.53^{a}	136.04 ± 32.09^{a}	155.2 ± 57.74^{b}	202.71 ± 77.21^{a}	189.2 ± 86.3^{a}	106.12 ± 17.09	112.47 ± 23.12
Simpson's inverse diversity	58.38 ± 30.45	54.68 ± 25.09^{ab}	56.41 ± 26.26^{a}	53.15 ± 28.59^{a}	65.8 ± 32.96^{a}	64.72 ± 30.02^{a}	66.08 ± 29.81	64.09 ± 30.8	96.11 ± 105.12	72.89 ± 63.39^{a}	92.64 ± 42.73^{a}	71.05 ± 33.83^{ab}	106.59 ± 41.92^{b}	93.57 ± 29.93^{b}	70.12 ± 36.83	74.5 ± 42.5	66.9 ± 20.75	68.01 ± 58.88^{a}	103.86 ± 73.35^{a}	92.5 ± 59.04^{ab}	98.41 ± 27.21^{a}	89.06 ± 34.13^{a}	67.55 ± 13.44	69.74 ± 30.81	54.72 ± 38.13	57.82 ± 46.37^{a}	69.38 ± 19.18^{a}	89.2 ± 32.16^{b}	111.71 ± 27.53^{b}	106.36 ± 39.86^{b}	50.93 ± 15.29	51.19 ± 15.28
Faith's phylogenetic diversit	7.69 ± 2.35	7.41 ± 2.14^{a}	7.26 ± 1.82^{a}	6.74 ± 2.11^{a}	7.97 ± 2.41^{a}	8.05 ± 1.99^{a}	7.87 ± 1.87	8.12 ± 2.12	10.19 ± 5.48	8.49 ± 4.23^{a}	10.43 ± 3.52^{c}	8.81 ± 2.85^{b}	11.74 ± 2.31^{c}	11.51 ± 2.67^{b}	8.37 ± 2.79	9.14 ± 2.16	6.66 ± 2.49	8.1 ± 2.59^{a}	9.89 ± 3.27^{bc}	9.53 ± 2.41^{ab}	10.54 ± 1.45^{ab}	10.4 ± 2.17^{b}	8.03 ± 1.06	8.29 ± 2.05	7.61 ± 2.7	7.64 ± 3.93^{a}	7.54 ± 1.38^{ab}	8.46 ± 2.34^{b}	11 ± 2.59^{bc}	11.29 ± 1.86^{b}	7.34 ± 2.22	6.94 ± 1.28
Observed species	130.95 ± 49.92	122.9 ± 36.7^{a}	121.43 ± 43.41^{a}	115.6 ± 56.55^{a}	132.33 ± 51.72^{a}	126 ± 38.18^{a}	121.62 ± 44.1	126.95 ± 52.59	196 ± 219.35	161.83 ± 106.73^{a}	174.33 ± 84.85^{a}	122.33 ± 58.81^{ab}	189.67 ± 74.76a	163.17 ± 55.07^{a}	126.67 ± 67.5	140 ± 65.39	114.5 ± 44.23	143.67 ± 93.22^{a}	187.5 ± 131.33^{a}	164.17 ± 109.83^{ab}	169.67 ± 37.46^{a}	152 ± 60.57^{a}	115.83 ± 18.65	113.5 ± 48.51	124.44 ± 44.81	134.33 ± 63.24^{a}	136 ± 32.08^{a}	155.12 ± 57.64^{b}	202.56 ± 77.13^{a}	189.11 ± 86.12^{a}	106.11 ± 17.08	112.11 ± 22.87

3.1.7.4 Temporal changes in beta diversity of the subgingival plaque microbiome

Comparisons of the subgingival microbial community membership and structure between the different groups were achieved using different beta diversity metrics, Bray-Curtis dissimilarity, and UniFrac distances, and were visualized by Non-metric multidimensional scaling (NMDS). A distinct shift in the microbial community composition was evident in the test sides corresponding to the progression of gingival inflammation, Figure 3.15.

PERMANOVA based tests of the Bray-Curtis and UniFrac distances showed that there is a significant difference in the microbiome composition ($p<0.001$) between test and control sides during gingivitis induction. There was no clear separation between test and control sites at baseline, however, the microbial communities of the test and control sides start to separate after gingivitis induction with significant separations at Day 7, Day 14, and Day 21 (PERMNOVA, Bray and UniFrac distances, $p<0.01$), Figure 3.15. After prophylaxis at Day 21, the control and test sides microbial communities go back to a state where they become more similar at Day 28 and Day 35.

Beta diversity analyses for the microbial communities in the different responder groups showed an early separation of the high responder group from the control sides after the first week of plaque accumulation. A complete separation between the high responders and control sides microbiome was observed after the third week of gingivitis (PERMNOVA, Bray-Curtis and UniFrac distances $p<0.05$), Figure 3.16. Similarly, the low and slow responders showed significant differences in the microbial community composition compared to the control sides at Day 21, $p<0.05$. In addition, pairwise PERMNOVA showed a significant difference in the microbial communities between the high and slow responder groups at Day 21 (Bray-Curtis distances, $p<0.05$).

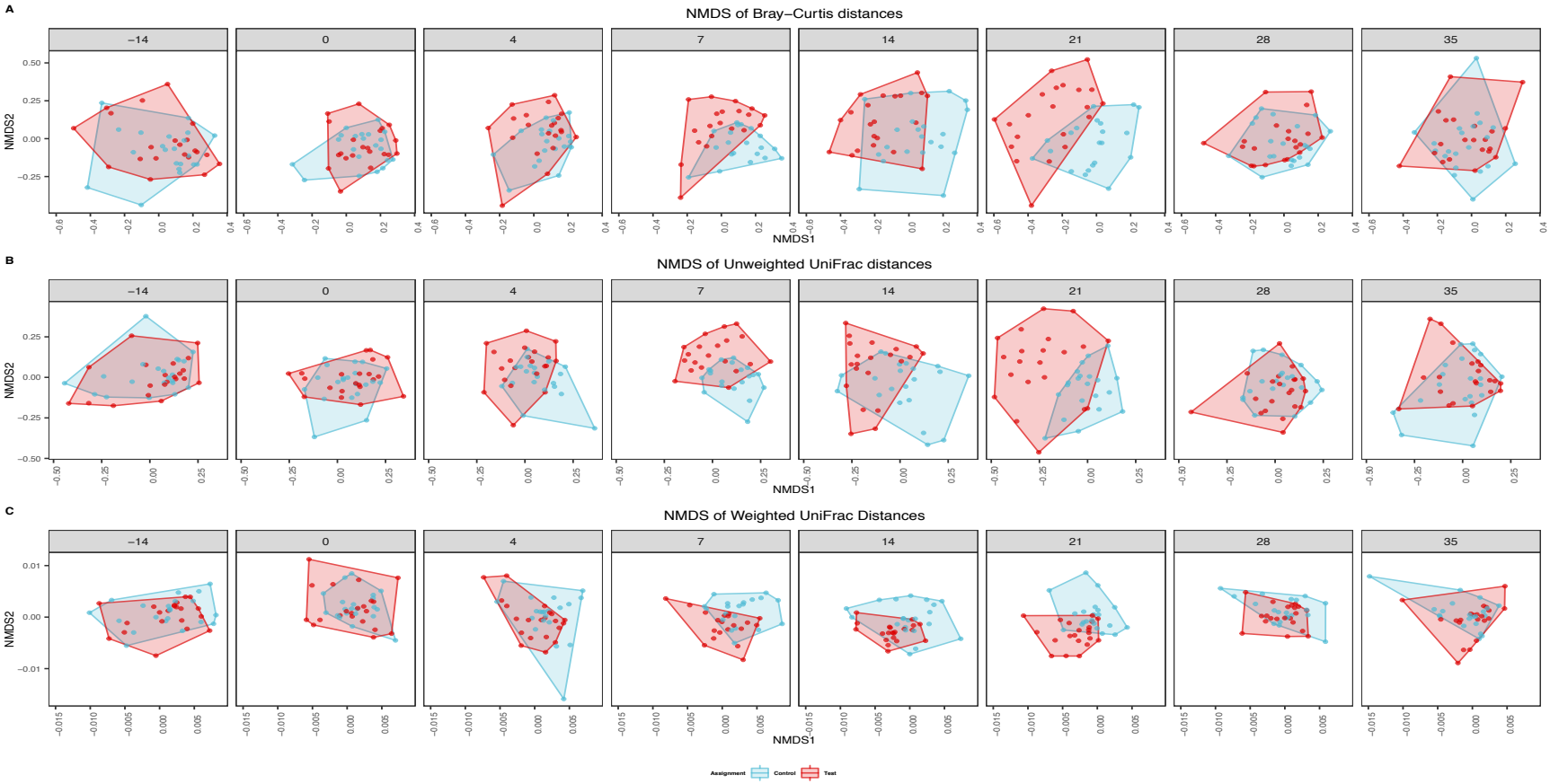

Figure 3.15: Beta diversity analysis of subgingival microbiome during induction and resolution of experimental gingivitis.
A distinct shift in the microbial community composition was evident in the test sides corresponding to the progression of gingival inflammation
Non-metric multidimensional scaling (NMDS) plots based on (A) Bray–Curtis, (B) unweighted UniFrac, and (C) weighted UniFrac distances. Blue control side and red test side.

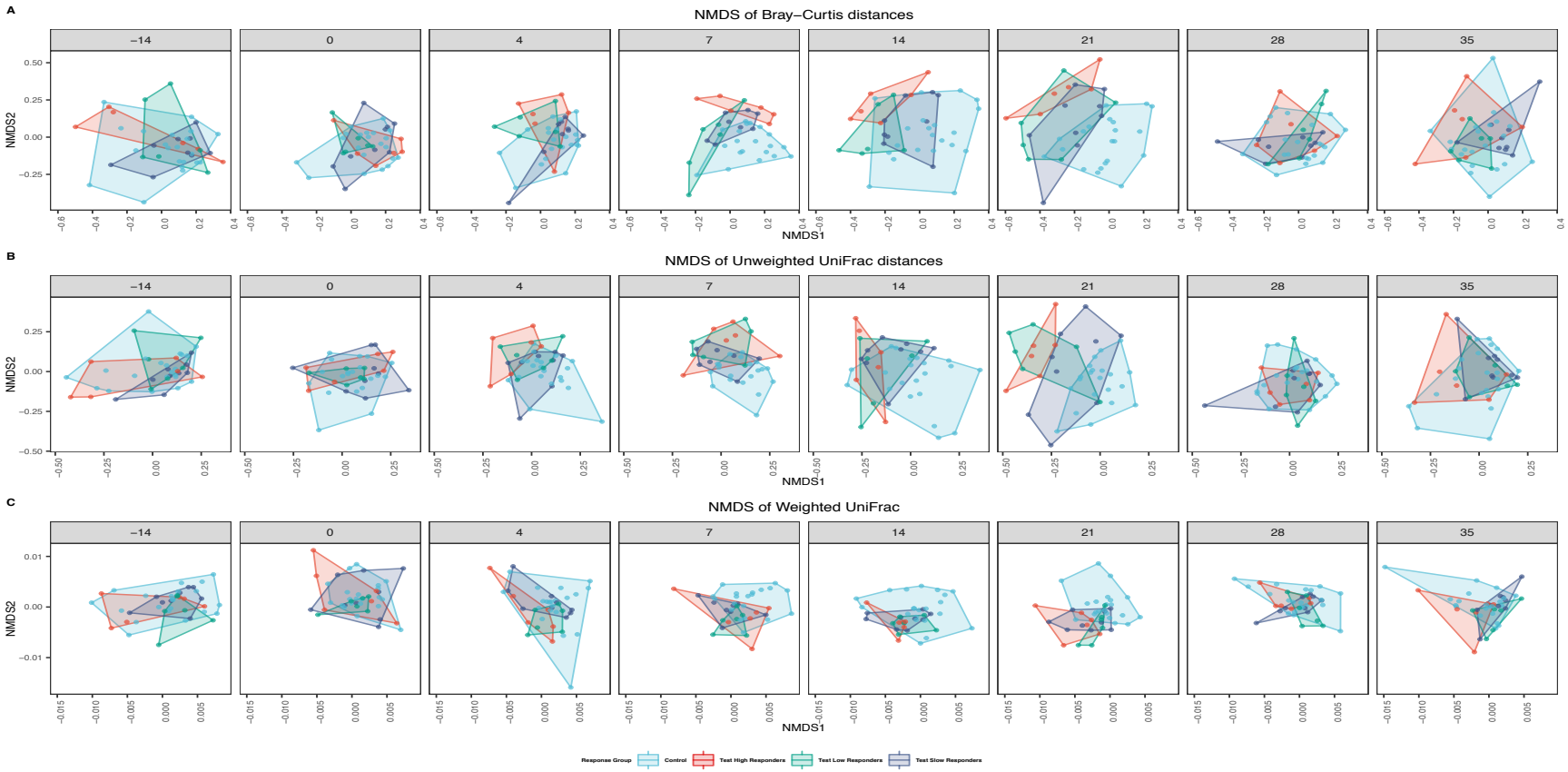

Figure 3.16: Beta diversity analysis of subgingival microbiome among the responder groups during induction and resolution of experimental gingivitis.
PERMNOVA showed significant difference in the microbial communities between high and slow responder groups at Day 21 (Bray-Curtis distances, $p<0.05$).
Non-metric multidimensional scaling NMDS plots based on (A) Bray–Curtis, (B) unweighted UniFrac, and (C) weighted UniFrac distances. Blue control side, red test high responders, green test low responders, and purple test slow responders.

3.1.7.5 Microbial composition of the subgingival plaque

At baseline, five phyla represented an average of 97% of the total microbial composition for the subgingival plaque. Firmicutes was the most abundant phylum in both control and test sides (Control 42.57 % vs Test 40.97 %), followed by Actinobacteria (Control 16.16% vs Test 16.39%), Bacteroidetes (Control 15.22% vs Test 14.69%), Proteobacteria (Control 15.03% vs Test 14.35%), in addition to Fusobacteria (Control 8.57% vs Test 11.02%). Saccharibacteria (TM7), Spirochaetes, Absconditabacteria (SR1), Gracilibacteria (GN02), and Synergistetes represented the remaining 3%. Changes in relative abundances over time at the phylum level are shown in Figure 3.17. The induction phase was characterized by a significant drop in Firmicutes, and Actinobacteria coupled to an increase in Bacteroidetes and Fusobacteria relative abundance in the test sides. Interestingly, Proteobacteria showed an initial increase in relative abundance at Day 4, followed by a decrease until Day 21. On the other hand, a similar increase was seen during the induction phase in the low abundant phyla including Saccharibacteria (TM7), Spirochaetes, Absconditabacteria (SR1), Gracilibacteria (GN02) as well as Synergistetes. After oral hygiene reinstitution, different phyla relative abundances returned to baseline levels.

Firmicutes relative abundances showed an immediate drop for high and low responders at Day 4, but slow responders showed a delayed drop. Slow responder group had low Bacteroidetes average relative abundance at baseline 11.38% compared to high and slow responders, 17.47% and 16.88%, respectively. Additionally, during the induction phase, the slow responder group showed an initial lag in Bacteroidetes relative abundance compared to other groups until Day 14 and Day 21, Figure 3.18. The high and slow responders showed an immediate increase in Gracilibacteria (GN02) and Absconditabacteria (SR1) relative abundances compared to low responders. Following gingivitis induction, the high and low responders showed a three-fold increase in Saccharibacteria (TM7) (6.1% and 5.7%, correspondingly) reaching a higher level

compared to slow responders 4.2%. High responders reached peak levels for Spirochetes relative abundance at Day 14 (3.3%) compared to low and slow groups that reached peak levels at Day 21, 3.1% and 3.2%, respectively.

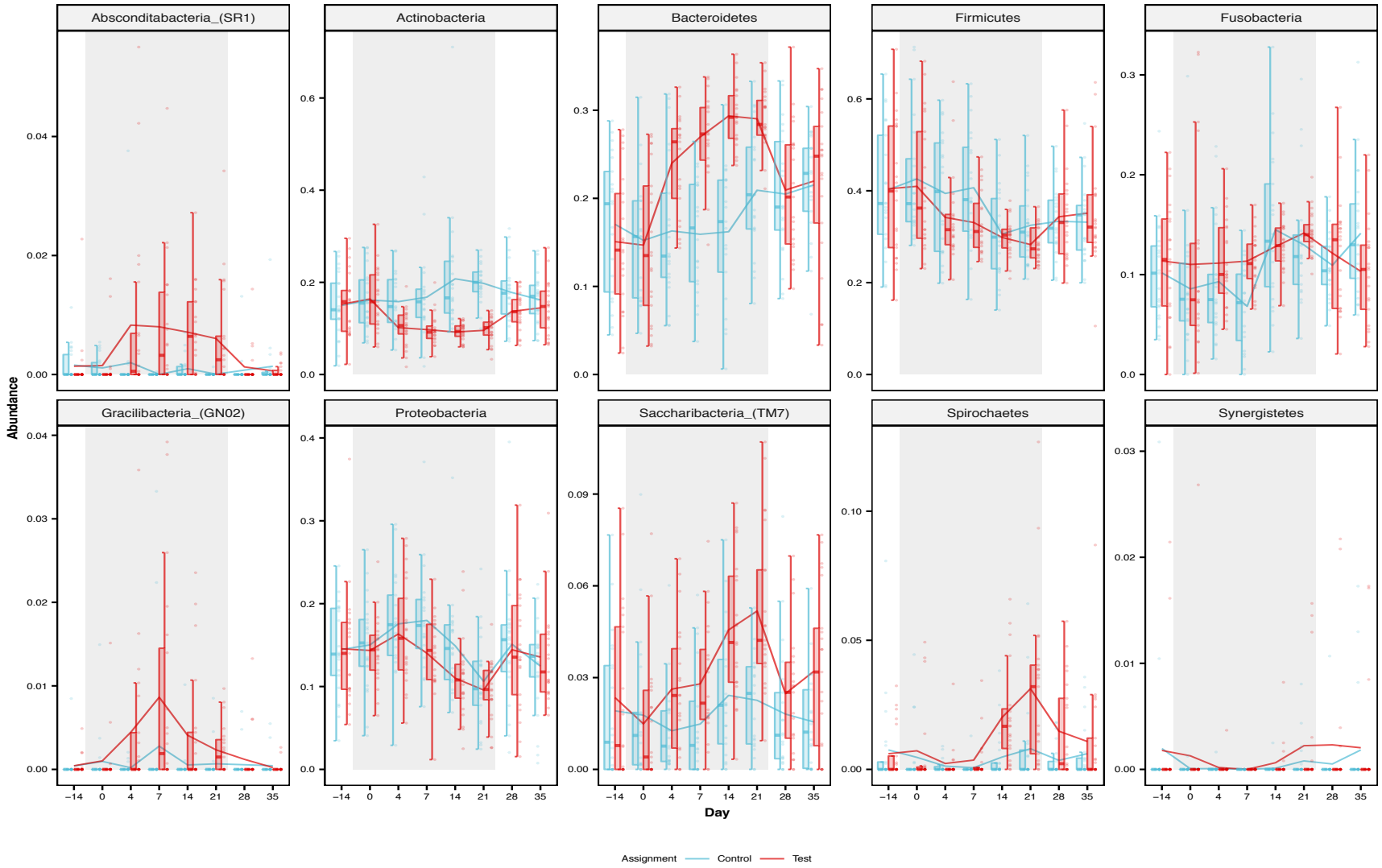

Figure 3.17: Relative abundances of the microbial communities at the phylum level during induction and resolution of experimental gingivitis.
Induction phase was characterized by a significant drop in Firmicutes, and Actinobacteria coupled to increased Bacteroidetes and Fusobacteria relative abundances in the test sides. Blue control side and red test side.

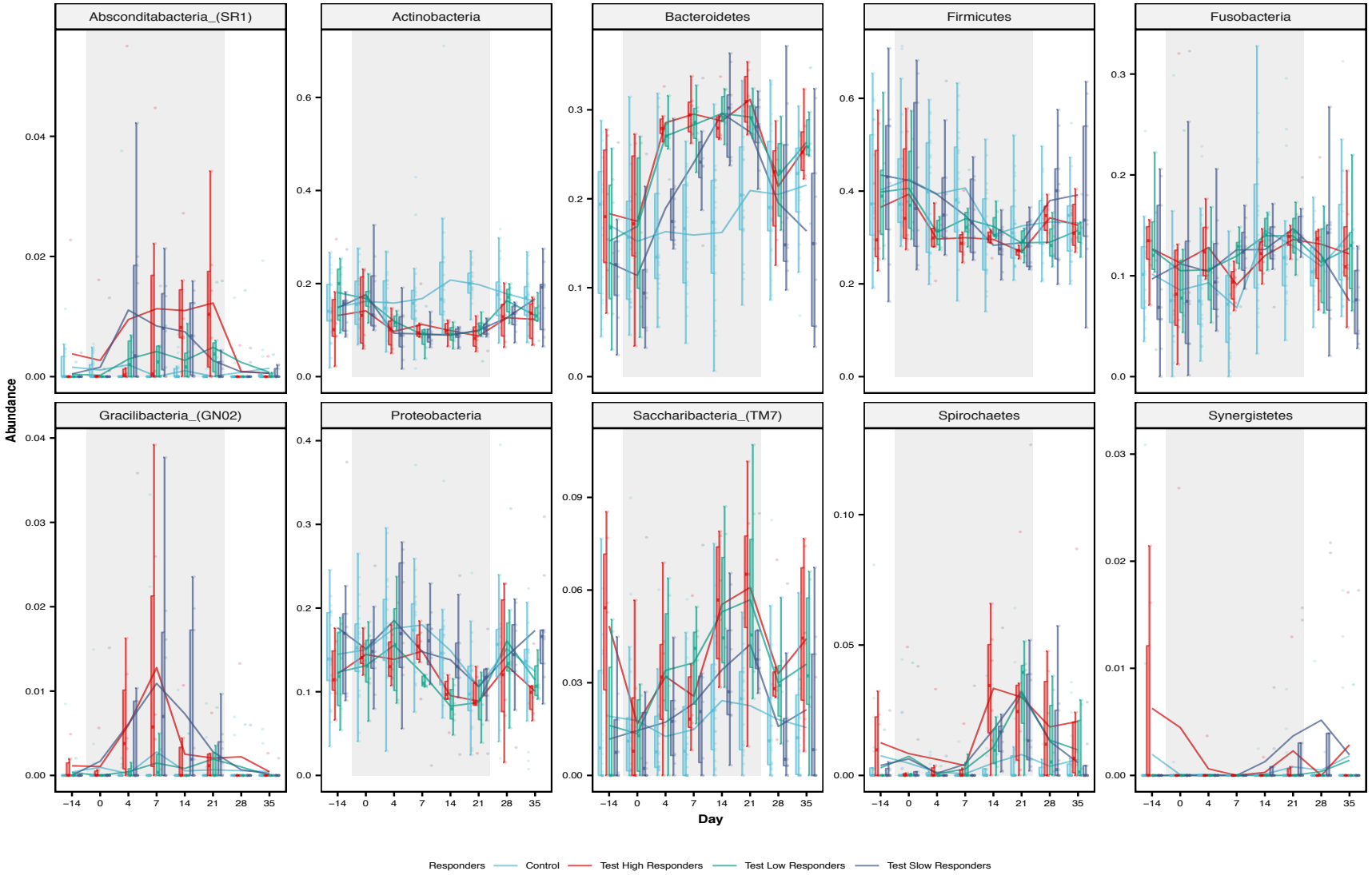

Figure 3.18: Relative abundances of the microbial communities at the phylum level among the responder groups during induction and resolution of experimental gingivitis.
Slow responder group showed an initial delay in the microbial community shift. Blue control side, red test high responders, green test low responders, and purple test slow responders.

The relative abundance profiles of the bacterial community revealed differences in the predominant genera associated with health and disease states, Figure 3.19. Genera associated with health which exhibited higher abundances at baseline (Day 0) were *Streptococcus, Fusobacterium, Actinomyces, Rothia, Haemophilus,* and *Granulicatella.* During gingivitis induction, shifts in the relative abundances of several genera were distinct. Major Gram-negative periodontal pathogen genera *Treponema and Porphyromonas* showed an increase in relative abundances in the test sides. Additionally, other disease associated genera including *Prevotella, Leptotrichia, Selenomonas, Capnocytophaga, and Saccharibacteria_(TM7)_[G-1]* were more abundant in the test sides at the peak of induction at Day 21. Correspondingly, health-associated genera exhibited a marked drop during plaque accumulation, among these were *Streptococcus, Actinomyces, Rothia* and *Haemophilus.*

The responder groups trajectories showed that high responders had higher *Porphyromonas, Fusobacterium* and *Granulicatella* and lower *Actinomyces* relative abundances at baseline Figure 3.20. Interestingly, the slow responders were associated with elevated *Streptococcus and Rothia,* and lower *Prevotella* and *Veillonella* relative abundances during healthy state at baseline. *Prevotella and Parvimonas* showed elevated abundance at baseline in the low responders compared to other groups. Correspondingly, shifts in the genera relative abundances during gingivitis induction revealed distinct ecological succession patterns in the responder groups, Figure 3.21. During gingivitis induction, *Aggregatibacter, Selenomonas* and *Treponema* showed a notable increase in the high responder group compared to other groups. Moreover, the low responders showed higher abundances of *Prevotella and Parvimonas* during the entire induction phase. Interestingly, the slow responders showed a delayed decline of *Streptococcus* and a delayed increase in *Prevotella, Saccharibacteria_(TM7)_[G-1], Selenomonas* and *Campylobacter* compared to other groups.

At the species level, a total of 5 species were present in the majority of subjects ≥ 50% at abundances of 0.1% in either the healthy or gingivitis sites during the induction phase. Core microbiome species in the subgingival microbiome included *Veillonella dispar, Fusobacterium nucleatum_subsp._polymorphum, Streptococcus spp.;Streptococcus sanguinis, Streptococcus tigurinus,* and *Streptococcus intermedius*, in agreement with previous reports (Griffen, Beall et al. 2012, Abusleme, Dupuy et al. 2013).

At baseline, the most abundant species associated with health in all samples included *Streptococcus spp. Streptococcus sanguinis, Streptococcus tigurinus and Streptococcus intermedius; Fusobacterium spp Fusobacterium nucleatum subsp. animalis* and *Fusobacterium nucleatum_subsp._vincentii,* and *Rothia spp. Rothia aeria, Rothia mucilaginosa* and *Rothia dentocariosa.* In addition, *Neisseria mucosa, Haemophilus parainfluenzae*, *Veillonella dispar*, *Lautropia mirabilis, Granulicatella adiacens, Gemella haemolysans, Veillonella parvula, Actinomyces naeslundii and Corynebacterium matruchotii* were among the abundant species in health, in accordance to previous reports (Griffen, Beall et al. 2012, Abusleme, Dupuy et al. 2013).

Interestingly, at baseline, high responders showed elevated relative abundances of *Fusobacterium sp._HMT_203, Alloprevotella sp._HMT_473, Peptidiphaga sp._HMT_183, Granulicatella elegans,* and Veillonella sp._HMT_780 among which taxa that displayed associations with periodontitis, (Diaz, Hoare et al. 2016). At the peak of induction (Day 21*), Saccharibacteria spp; Saccharibacteria_(TM7)_[G-1] bacterium_HMT_952 and Saccharibacteria_(TM7)_[G-1] bacterium_HMT_346, Tannerella sp._HMT_286, Selenomonas sp._HMT_892,* and *Leptotrichia sp._HMT_417* were more predominant in the high responders in comparison to the slow group, whereas, the low responders showed higher abundances in periodontitis-associated tax including *Prevotella sp.* and *Dialister invisus*. The low and slow responders displayed a higher level of previously reported core microbiome species

Fusobacterium nucleatum_subsp._vincentii and *Prevotella nigrescens* compared to the high group at Day 21 (Griffen, Beall et al. 2012, Abusleme, Dupuy et al. 2013). After disease resolution, the subgingival microbial composition shifted back to resemble the healthy state at baseline.

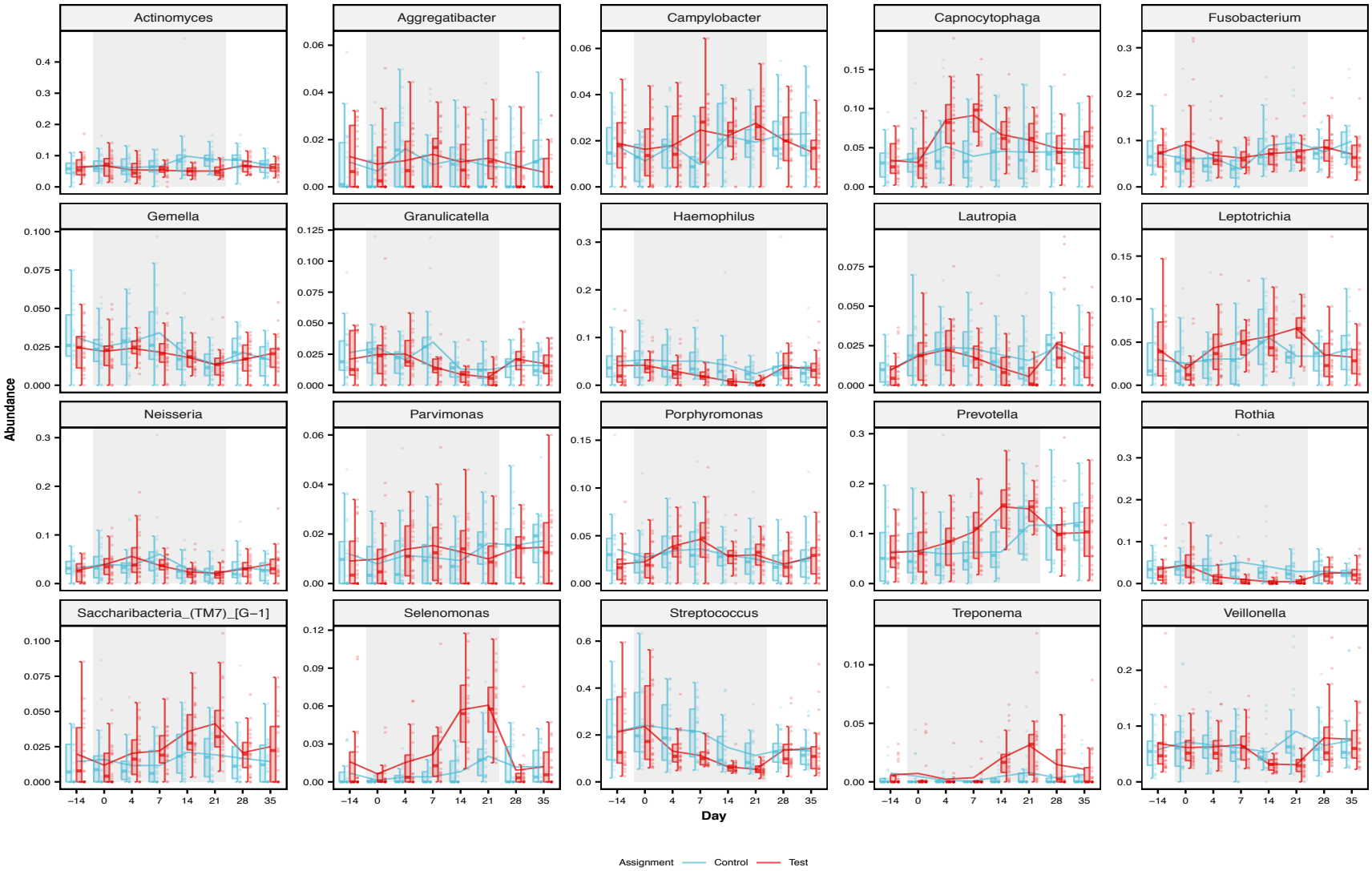

Figure 3.19: Relative abundances of the top twenty genera during induction and resolution of experimental gingivitis. The induction phase was associated with a significant drop in health-associated genera and increase in known periodontitis-associated genera. Blue control side and red test side.

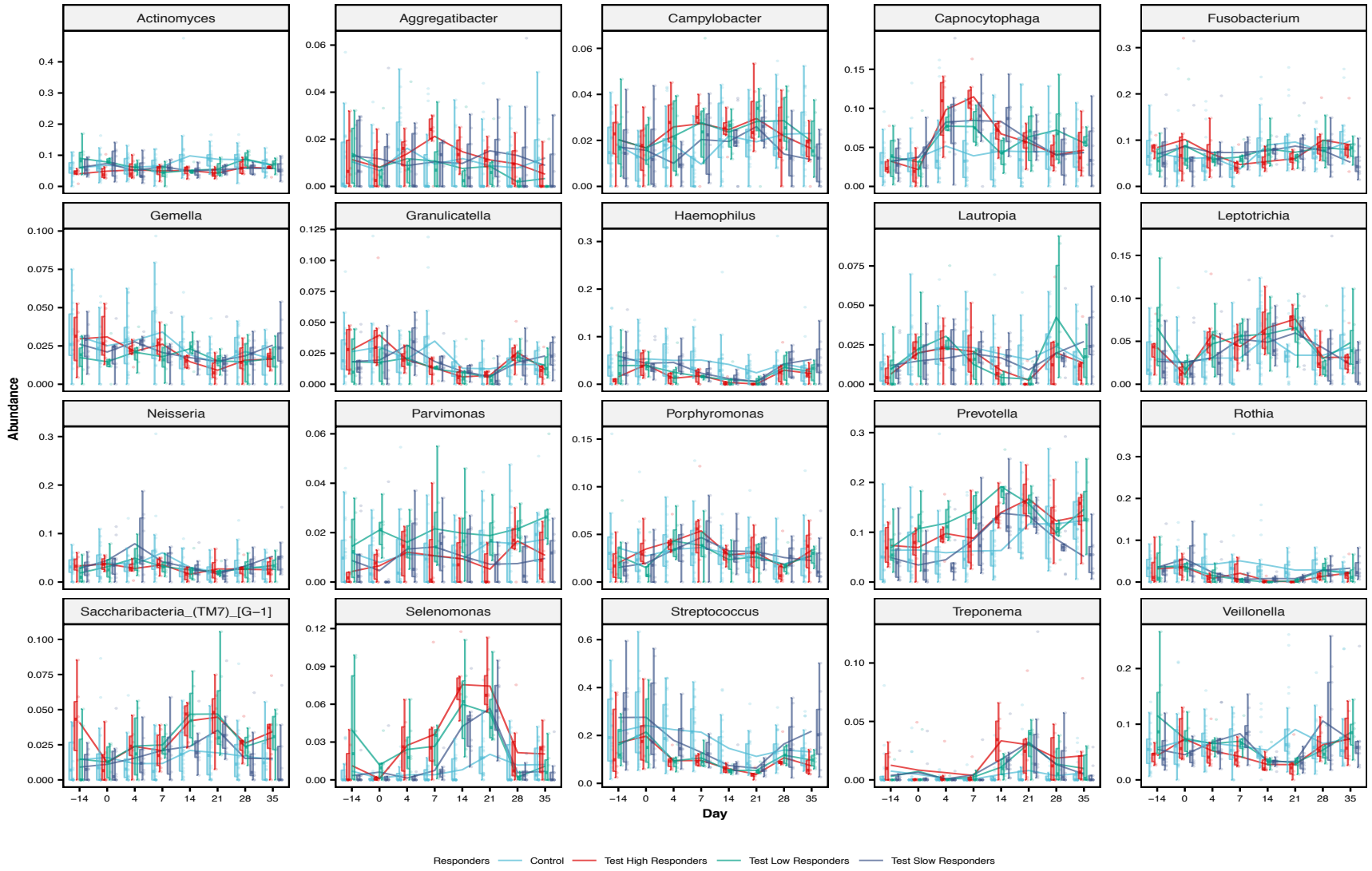

Figure 3.20: Relative abundances of the top twenty genera among responder groups during induction and resolution of experimental gingivitis.
Slow responder group showed an initial delay in *Streptococcus* relative abundances drop compared to the high and low responders. Blue control side, red test high responders, green test low responders, and purple test slow responders.

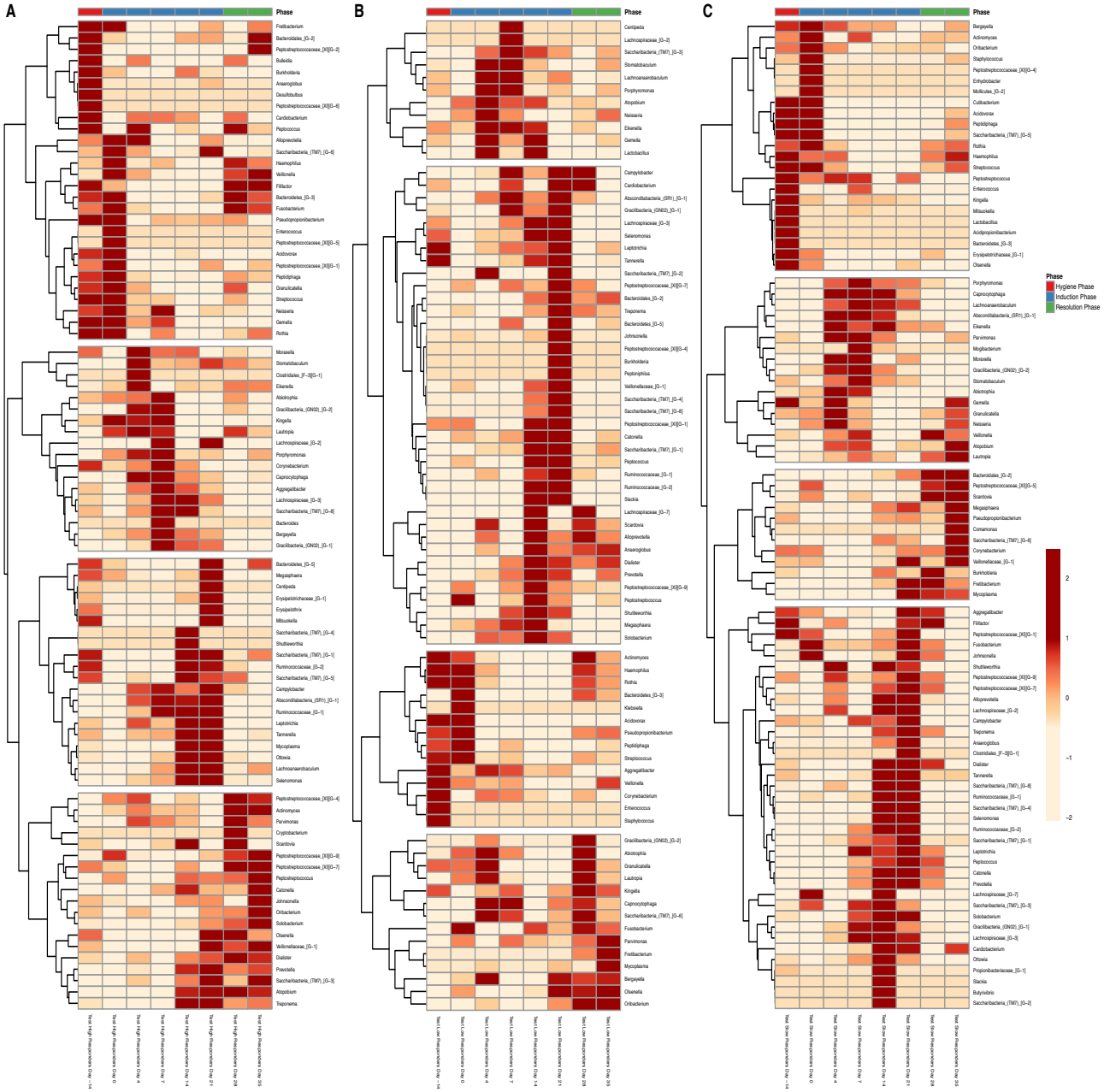

Figure 3.21: Z-score heatmap of the relative abundances at the genus level among the responder groups during induction and resolution of experimental gingivitis.
Heatmap shows distinct ecological succession patterns in the different responder groups during gingivitis induction.
(A) Test high responders, (B) test lower responders, (C) test slow responders. Each row corresponds to a genus and each column represent a study visit. Color scale for heatmap appears in the top right with the most abundant genus in red and the least abundant in orange.

Discussion

This study aimed to investigate microbial succession patterns, as well as host mediator changes during the transition from clinical health to gingivitis. The data obtained showed evident changes in the microbial composition and diversity corresponding to the progression of gingival inflammation during experimental gingivitis. In addition, a significant shift in host homeostasis occurs upon the onset of gingivitis with the majority of the response being suppression of host chemotactic factors for neutrophils as well as immune cells. Three groups were identified based on variations in clinical response patterns; these variations suggest that the microbiome composition and host response may account for the difference in future disease susceptibility.

The study successfully induced gingivitis after 21 days of abstinence from oral hygiene at the test sites as evidenced by a significant increase in gingival inflammation parameters ($p < 0.001$), Figure 3.2. These data are consistent with numerous previous studies and demonstrate that without brushing there is a rapid increase in gingival inflammation (Löe, Theilade et al. 1965, Trombelli, Tatakis et al. 2004, Offenbacher, Barros et al. 2010). Variability in clinical responses to plaque accumulation in experimental gingivitis studies has been described. Trombelli *et al.* identified "low" and "high" responders based on gingival inflammation severity in response to plaque accumulation during gingivitis induction (Trombelli, Tatakis et al. 2004). Two other studies described three types of responses during gingivitis induction, "susceptible" group which showed substantial gingival inflammation, "resistant" group to gingivitis and an "intermediate" group (Wiedemann, Lahrsow et al. 1979, Van der Weijden, Timmerman et al. 1994). However, methods used to identify clinical responses patterns in these reports did not account for the longitudinal nature of experimental gingivitis study. In this study, joint clinical data trajectories were used to define variation in clinical responses. Three groups were identified based on the degree of gingival inflammation measured by GI and BOP in response to plaque accumulation represented by PI.

These groups were defined as the high responder group (28.6 %), low responder group (28.6 %), and slow responder group (42.9 %). The high responders developed gingival inflammation at a faster rate in comparison to the slow group. The slow responders showed delayed gingivitis in parallel with a delay in plaque index during the first two weeks of gingivitis induction. After 3 weeks of plaque accumulation, high and slow responder reached similar gingival inflammation levels which was significantly higher compared to the low responder group, Figure 3.3. A recent study applied group trajectories modeling to identify variation in clinical response in experimental gingivitis, however only two groups were identified "fast" and "slow" responders (Nascimento, Danielsen et al. 2019).

The data demonstrate that during the initial transition from clinical health to gingivitis a significant shift in chemokine utilization patterns occurs. There is a significant increase in MIF, the most abundant neutrophil chemokine found in clinically healthy tissue, and a significant decrease or slight increase in the concentration of every other neutrophil chemokine examined. Some of the observed supressions in the other neutrophil chemokines were transient and surprisingly regained basal level concentrations before the clinical parameters improved whereas the levels of other chemokines remained depressed until the resolution phase of the study. A decrease in select neutrophil chemokines after the induction of human gingivitis has been reported previously (Deinzer, Weik et al. 2007, Offenbacher, Barros et al. 2010, Kumar 2019) however the extent of the reduction, the increase in MIF, and the restoration of basal levels of select chemokines before the resolution of the clinical symptoms has not been previously reported in a single study. The exact cause of the observed drop in chemokine levels is not fully understood; it has been attributed to *P. gingivalis* mediated chemokine paralysis and increased chemokines degradation (Darveau, Belton et al. 1998, Offenbacher, Barros et al. 2010).

The groups' identification based on temporal clinical response patterns allowed a more accurate and revealing picture of the host response to bacterial biofilm accumulation. The three responder groups exhibited distinct patterns of chemokine expressions during gingivitis induction, Figure 3.4. An overall higher chemokine expression levels were detected in the high responder group compared to low responders in accordance with the observed clinical responses. MIF increased in all three groups during gingivitis induction, high responders exhibited a higher trend than the other groups. Higher MIF levels in the high responder groups compared to low responders at baseline proposes an intrinsic susceptibility in these individuals to periodontitis development. MIF showed a similar increase during gingivitis induction in young adults although older adults in the study showed a reduction in MIF levels (Nonnenmacher, Helms et al. 2009). IL-8/CXCL8 showed a significant decrease at Day 4 and remained suppressed the entire induction phase in all responder groups; however high responders MIF levels remained higher than the other groups. Interestingly, both the low and slow responders mean levels for GRO-α/CXCL1 and ENA-78/CXCL5 showed an initial reduction, whereas, the high responders mean levels remained stable.

The large variability in healthy neutrophil chemokine levels was noted in the previous study described in chapter 2. Neutrophil numbers as measured by MPO showed a 1.8-fold increase in the test sides at Day 21 (from 19465.06 ± 16048.37 pg per 30-s sample at baseline to 35265.87 ± 30322.75 pg per 30-s sample at Day 21) which likely occurs when additional neutrophils enter the sulcus during gingivitis development, Figure 3.7 (A). All three responders groups showed no differences in MPO levels at baseline and similarly increased during the induction phase despite differences in the neutrophil chemokines expression patterns.

Gingivitis induction was associated with alteration in host inflammatory cytokines, an increase in IL-β and a decrease in TNF-α was observed consistent with other reports (Deinzer, Weik et al. 2007, Offenbacher, Barros et al. 2010, Scott, Milward et al. 2012). High responders

exhibited a higher trend of IL-1β levels on Day 14 and Day 21, however, it was not statistically significant. Thus IL-1β might not be a good marker to differentiate between the responder groups in the study. Taken together, the above results may indicate that the host alters neutrophil recruitment in times of disease and bring neutrophil through different mechanisms. The data suggest that neutrophil migration during episodes of gingivitis may come under the control of other neutrophil chemoattractants not measured in this study such as complement proteins C5a and C3a, the bacterial protein translation initiation sequence fMLP, the anti-microbial peptide LL-37, or as of yet unknown neutrophil chemoattractants (Sadik, Kim et al. 2011).

The study utilized high-throughput sequencing of the16S rRNA gene using Illumina MiSeq platform to characterize the subgingival plaque microbial community. A total of 10 phyla, 111 genera, and 421 were identified in the subgingival plaque, in agreement with the previously reported number of species in plaque (Paster, Boches et al. 2001, Griffen, Beall et al. 2012, Abusleme, Dupuy et al. 2013). The longitudinal comparison of the subgingival microbiome revealed significant shifts in the microbial composition from the health to the disease state. Health is associated with low diversity community dominated by the health-associated species; however, increased diversity in disease is associated with the emergence of periodontitis-associated species and more even distribution of the predominant species in the community.

During gingivitis induction, all alpha diversity metrics (within sample diversity) showed a significant increase corresponding to increased subgingival microbial load, Figure 3.13, Figure 3.14, and Figure 3.11. The increase in species richness (observed number of species and Chao1 richness), and community evenness (Shannon diversity index and Simpson's Inverse index) was evident as early as Day 4 and continued to increase entire induction phase in all responder groups. Interestingly, high responders had higher alpha diversity score compared to other groups at Day 4 which was followed by a sudden drop in all alpha diversity metrics at Day 7, indicating the

depletion of health associated species and emergence of new dominant species (Matthews, Joshi et al. 2013). This early community shift could explain the rapid development of gingivitis in the high responder group. However, slow responders who showed a distinct delay in plaque index and subgingival microbial load during the first week of the induction phase, also displayed a delay in Faith's phylogenetic diversity but higher species richness at Day 7. Low Faith's phylogenetic diversity is associated with lower phylogenetic variation across the species. This observation indicates that slow responders presented the least changes in the species that dominate subgingival communities initially, which was reflected by the delay of gingivitis onset.

The NMDS plot showed evident changes in the microbial composition and structure corresponding to the progression of gingival inflammation following oral hygiene withdraw, Figure 3.16. On the basis of the responder groups, beta diversity analysis of microbial communities showed early separation of the high responder group communities from the control sides as early as first week and complete separation into a tight cluster after third week of gingivitis (PERMNOVA, Bray-Curtis and UniFrac distances $p<0.05$), Figure 3.15 (A and B). This is an indication that as the high responder microbiome increase in diversity with plaque accretion, the community is becoming similar among the subjects in this group, sharing common pathogenic bacteria. Similarly, an evident separation between high and slow responders microbiome at Day 21 (Bray-Curtis distances, $p<0.05$) indicates that their microbial community structure is different. After oral hygiene reinstitution, microbial communities of the subjects across different groups were spread apart with no noticeable clustering similar to baseline (Day 0), which may reflect the individual differences in health-associated subgingival microbiome.

On the basis of abundance profile, the subgingival microbiome was dominated by facultatively anaerobic or aerobic organisms in health state and anaerobes in the diseased state. Genera that were abundant at baseline *Streptococcus, Actinomyces, Rothia, and Haemophilus*

showed a significant drop at Day 4 and then showed a sustained decrease during gingivitis induction, Figure 3.19. These genera have been associated with health and showed to be early colonizers; similar findings were reported in experimental gingivitis studies (Kistler, Booth et al. 2013, Huang, Li et al. 2014). In parallel, the genera *Treponema, Porphyromonas, Prevotella, Selenomonas, Leptotrichia, Capnocytophaga and Saccharibacteria_(TM7)_[G-1]* showed continued increase throughout the progression of the disease and a significant decrease after oral hygiene reinstitution. Among members of these genera are major Gram-negative taxa that have been associated with periodontitis and a similar increase in their abundances has been reported (Kistler, Booth et al. 2013, Huang, Li et al. 2014).

Community succession during the shift is shown to be dependent on interspecies interactions. The responder groups showed distinct ecological succession patterns which could justify the differences in clinical responses. Slow responder group maintain higher relative abundances of *Streptococcus and Rothia* and lower abundances of *Prevotella* and *Veillonella* compared to other groups. Maintenance of high *Streptococcus* in the slow responder group and delayed growth of Bacteriodetes and Proteobacteria was evident until Day 14. *Streptococcus sanguinis,* a representative of the core microbiome in health, has shown to play a protective role by delaying the colonization of periodontal pathogens such as *Porphyromonas gingivalis* (Bacteriodetes) and *Aggregatibacter actinomycetemcomitans (*Proteobacteria) (Stingu, Eschrich et al. 2008). In multi-species biofilms, *Aggregatibacter actinomycetemcomitans,* was responsible for the protection *Porphyromonas gingivalis* by diminishing H2O2 produced by *Streptococcus sanguinis (Zhu, Macleod et al. 2019).* The slow responders associated with a higher relative abundance of *Streptococcus sanguinis* at baseline 5.2% compared to 1.1% and 2.1% in the high and low groups, respectively. The presence of *Streptococcus sanguinis* might have played a role in the delay of the microbiome shift seen in the slow responders, as evident by higher alpha

diversity scores at Day 7 compared to other groups. Moreover, high responders displayed a transient increase in *Aggregatibacter* on Day 7 when the microbial diversity showed a significant drop, demonstrating a critical time for pathogen colonization and community shift. It has bee shown that periodontal disease is associated with shifts of the complex microbial community rather than by a single pathogen (Diaz, Hoare et al. 2016). Understanding details about ecological succession in the transition from health to disease could lead to new methods to prevent and impede the progression of periodontal disease.

Although the analyses in this study were conducted with high temporal resolutions, one limitation of the study is the small sample size, future studies will be necessary to confirm these findings. Besides, pooling of subgingival microbial samples may result in lost site-specific data (Socransky and Haffajee 2005). Another possible limitation in the study design is the continuous disruption of the subgingival plaque biofilm since plaque samples were collected from the same sites at each study visit. The findings of the study were in agreement with previously published work, however differences in the results could be attributed to difference in the different target population, sample collection technique (paper point vs curettes), sample pooling (single vs multiple sites), method of DNA extraction, selection of different regions of the 16S rRNA gene, sequencing technology, or downstream bioinformatics analysis.

In summary, plaque accumulation is associated with variable clinical responses that are characterized by differential shifts in the subgingival microbiome and varying chemokines profiles. This study provides preliminary data for future studies that evaluate a wide range of gingival crevicular fluid mediators and their relationship to subgingival microbiomes in gingival health and disease.

CHAPTER 4 . SUMMARY AND FUTURE DIRECTIONS

Maintenance of clinically healthy gingival tissue is an active process. Understanding how the host regulates immune cells migration in non-diseased gingiva is significant in that it will begin to define a key mechanism for the maintenance of gingival health. The microbiome has an influential role in modulating the host immune response. Therefore, full assessments of host-microbial interplay are crucial for a better understanding of the gingival homeostasis and identification of potential biomarkers for disease prediction. The overall goal of this thesis is to gain comprehensive knowledge about the relationship between the subgingival microbiome and the chemokines expression patterns in gingival health and disease.

Most of the studies reporting gingival crevicular fluid mediators compared periodontal health and disease; nevertheless, a comprehensive definition of gingival health is crucial to diagnose and treat diseases. The study in chapter 2 detected 40 different chemokines in the GCF of the healthy adolescent for the first time using a multiplex bead immunoassay, many of which can be a potential marker for the diagnosis and monitoring of periodontal disease. Findings of the study highlight the variation in chemokines profiles and the number of neutrophils (as measured by myeloperoxidase) in the gingival crevicular fluid. The findings showed strong correlations between the number of neutrophils and neutrophil chemokines, rendering confidence that relevant chemokine markers are detected. Interestingly, macrophage inhibitory factor (MIF), a neutrophil chemokine, was the most abundant chemokine by far in all the samples examined. Future studies are needed to elucidate on the role of MIF in the gingival homeostasis. The study also highlighted the interindividual variation in subgingival microbiomes using next-generation sequencing. In the study, the two groups identified based on chemokines expression did not cluster based on

microbiome composition, Figure 2.12. The uniqueness of the microbial community and the host response among individuals in health emphasize the notion that health is an active and dynamic process and not just that absence of disease. This study represents the first most complete analysis of combined chemokines and microbiome profiles found in the clinically healthy condition. The finding suggests that variation in microbiome and chemokines profiles may contribute to individual variability in periodontal disease susceptibility.

Dental plaque is insufficient to explain gingivitis development fully; host variability also contributes to gingival inflammation. In chapter 3, the study successfully induced gingivitis after 21 days of abstinence from oral hygiene in the test sites, as evidenced by a significant increase in gingival inflammation parameters. This study employed strict health criteria and determined by an initial exam of the natural state of gingivitis for each study participant. This lead to the identification of "low," "slow," and high" gingivitis responders. Defining the groups based on temporal clinical response patterns, allowing a more accurate and revealing picture of the host response to bacterial biofilm accumulation. The different clinical responders demonstrated distinct ecological succession and chemokines expression patterns, which may suggest deferential susceptibility to future diseases. Biofilm overgrowth during the induction phase was associated with a significant shift in the microbial composition corresponding to the progression of gingival inflammation. The slow responder groups showed a delay in the clinical presentation of the disease compared to the high group, a similar lag in the community shift was evident at the initial phase of the disease. The slow responders' microbiome had a higher abundance of *Streptococcus* at baseline, which might have played a protective role in the ecological succession. The data suggest that understanding the microbial interaction in the subgingival microbiome may help develop new strategies to prevent or treat periodontal disease. The chemokine analysis showed that only MIF

significantly increased during the induction phase of the study, whereas all of the other neutrophil chemokines decreased either initially after gingivitis induction or during the entire induction phase of gingivitis. The detection of high MIF expression during the study may suggest its important role in gingival health and disease. In addition, observed high MIF in the high responders compared to a lower level in the low responders at baseline and after disease resolution may suggest that investigation of the predictive validity of baseline MIF is warranted.

Furthermore, it was found that only one immune cell chemotactic factor increased during the onset of gingivitis while all the other immune cell chemotaxis factors decreased or were unchanged. To the best of our knowledge, this is the first demonstration that immune cell chemotaxis molecules are significantly altered during the initial phases of gingivitis. The significant alteration (either increase or decrease) of GCF levels of several host chemotactic factors suggests that a diagnostic for gingivitis may be feasible. This data must be interpreted however in the context that these numbers are from twenty-one subjects where there is a large amount of variability in the clinically healthy levels of these chemokines.

Overall, the data from these studies provide a potential biomarker for gingivitis initiation that could be incorporated into a diagnostic to predict potentially active disease sites. Future studies to gain comprehensive knowledge regarding the functional potential of the subgingival microbial communities and their interaction with the host through the integration of advanced technology such as metagenomic, metatranscriptomic, metabolomics is warranted.

REFERENCES

Abusleme, L., A. K. Dupuy, N. Dutzan, N. Silva, J. A. Burleson, L. D. Strausbaugh, J. Gamonal and P. I. Diaz (2013). "The subgingival microbiome in health and periodontitis and its relationship with community biomass and inflammation." ISME J **7**(5): 1016-1025.

Ainamo, J. and I. Bay (1975). "Problems and proposals for recording gingivitis and plaque." International dental journal **25**(4): 229-235.

Attström, R. and H. E. Schroeder (1979). "Effect of experimental neutropenia on initial gingivitis in dogs." European journal of oral sciences **87**(1): 7-23.

Bakdash, J. and L. Marusich (2018). rmcorr: Repeated measures correlation. R package version 0.3. 0.

Bakker, O. B., R. Aguirre-Gamboa, S. Sanna, M. Oosting, S. P. Smeekens, M. Jaeger, M. Zorro, U. Vosa, S. Withoff, R. T. Netea-Maier, H. Koenen, I. Joosten, R. J. Xavier, L. Franke, L. A. B. Joosten, V. Kumar, C. Wijmenga, M. G. Netea and Y. Li (2018). "Integration of multi-omics data and deep phenotyping enables prediction of cytokine responses." Nat Immunol **19**(7): 776-786.

Benjamini, Y. and Y. Hochberg (1995). "Controlling the false discovery rate: a practical and powerful approach to multiple testing." Journal of the royal statistical society. Series B (Methodological): 289-300.

Bland, J. M. and D. G. Altman (1995). "Calculating correlation coefficients with repeated observations: Part 1--Correlation within subjects." BMJ **310**(6977): 446.

Bland, J. M. and D. G. Altman (1995). "Calculating correlation coefficients with repeated observations: Part 2--Correlation between subjects." BMJ **310**(6980): 633.

Bolyen, E., J. R. Rideout, M. R. Dillon, N. A. Bokulich, C. Abnet, G. A. Al-Ghalith, H. Alexander, E. J. Alm, M. Arumugam and F. Asnicar (2018). QIIME 2: Reproducible, interactive, scalable, and extensible microbiome data science, PeerJ Preprints.

Borregaard, N. (2010). "Neutrophils, from marrow to microbes." Immunity **33**(5): 657-670.

Bosshardt, D. D. and N. P. Lang (2005). "The junctional epithelium: from health to disease." Journal of dental research **84**(1): 9-20.

Bray, J. R. and J. T. Curtis (1957). "An ordination of the upland forest communities of southern Wisconsin." Ecological monographs **27**(4): 325-349.

Burrell, R. C. and J. D. Walters (2008). "Distribution of systemic clarithromycin to gingiva." Journal of periodontology **79**(9): 1712-1718.

Callahan, B. J., P. J. McMurdie, M. J. Rosen, A. W. Han, A. J. A. Johnson and S. P. Holmes (2016). "DADA2: High-resolution sample inference from Illumina amplicon data." Nature Methods **13**: 581.

Callahan, B. J., K. Sankaran, J. A. Fukuyama, P. J. McMurdie and S. P. Holmes (2016). "Bioconductor Workflow for Microbiome Data Analysis: from raw reads to community analyses." F1000Res **5**: 1492.

Cao, C. F. and Q. T. Smith (1989). "Crevicular fluid myeloperoxidase at healthy, gingivitis and periodontitis sites." J Clin Periodontol **16**(1): 17-20.

Carneiro, L. G., H. Nouh and E. Salih (2014). "Quantitative gingival crevicular fluid proteome in health and periodontal disease using stable isotope chemistries and mass spectrometry." Journal of clinical periodontology **41**(8): 733-747.

Carrassi, A., S. Abati, G. Santarelli and G. Vogel (1989). "Periodontitis in a Patient with Chronic Neutropenia*." Journal of periodontology **60**(6): 352-357.

Chao, A. (1984). "Nonparametric estimation of the number of classes in a population." Scandinavian Journal of statistics: 265-270.

Chapple, I. L., G. Landini, G. S. Griffiths, N. C. Patel and R. S. Ward (1999). "Calibration of the Periotron 8000 and 6000 by polynomial regression." J Periodontal Res **34**(2): 79-86.

Chen, T., W. H. Yu, J. Izard, O. V. Baranova, A. Lakshmanan and F. E. Dewhirst (2010). "The Human Oral Microbiome Database: a web accessible resource for investigating oral microbe taxonomic and genomic information." Database (Oxford) **2010**: baq013.

Ciantar, M. and D. J. Caruana (1998). "Periotron 8000: calibration characteristics and reliability." J Periodontal Res **33**(5): 259-264.

Darveau, R. P. (2010). "Periodontitis: a polymicrobial disruption of host homeostasis." Nat Rev Microbiol **8**(7): 481-490.

Darveau, R. P., C. M. Belton, R. A. Reife and R. J. Lamont (1998). "Local chemokine paralysis, a novel pathogenic mechanism for Porphyromonas gingivalis." Infect Immun **66**(4): 1660-1665.

Davanian, H., H. Stranneheim, T. Båge, M. Lagervall, L. Jansson, J. Lundeberg and T. Yucel-Lindberg (2012). "Gene expression profiles in paired gingival biopsies from periodontitis-affected and healthy tissues revealed by massively parallel sequencing." PloS one **7**(9): e46440.

Deas, D. E., S. A. Mackey and H. T. McDonnell (2003). "Systemic disease and periodontitis: manifestations of neutrophil dysfunction." Periodontology 2000 **32**(1): 82-104.

Deinzer, R., U. Weik, V. Kolb-Bachofen and A. Herforth (2007). "Comparison of experimental gingivitis with persistent gingivitis: differences in clinical parameters and cytokine concentrations." J Periodontal Res **42**(4): 318-324.

Delima, A. J. and T. E. Van Dyke (2003). "Origin and function of the cellular components in gingival crevice fluid." Periodontology 2000 **31**(1): 55-76.

Demin, G. (2018). expss: Tables with Labels and Some Useful Functions from Spreadsheets and 'SPSS' Statistics. R package version 0.8.10.

Dewhirst, F. E., T. Chen, J. Izard, B. J. Paster, A. C. Tanner, W. H. Yu, A. Lakshmanan and W. G. Wade (2010). "The human oral microbiome." J Bacteriol **192**(19): 5002-5017.

Diaz, P. I., A. Hoare and B. Y. Hong (2016). "Subgingival Microbiome Shifts and Community Dynamics in Periodontal Diseases." J Calif Dent Assoc **44**(7): 421-435.

Eke, P. I., B. A. Dye, L. Wei, G. D. Slade, G. O. Thornton-Evans, W. S. Borgnakke, G. W. Taylor, R. C. Page, J. D. Beck and R. J. Genco (2015). "Update on prevalence of periodontitis in adults in the United States: NHANES 2009 to 2012." Journal of periodontology **86**(5): 611-622.

Emingil, G., G. Atilla and A. Hüseyinov (2004). "Gingival crevicular fluid monocyte chemoattractant protein-1 and RANTES levels in patients with generalized aggressive periodontitis." Journal of clinical periodontology **31**(10): 829-834.

Ertugrul, A. S., H. Sahin, A. Dikilitas, N. Alpaslan and A. Bozoglan (2013). "Comparison of CCL28, interleukin-8, interleukin-1β and tumor necrosis factor-alpha in subjects with gingivitis,

chronic periodontitis and generalized aggressive periodontitis." Journal of periodontal research **48**(1): 44-51.

Faith, D. P. (1992). "Conservation evaluation and phylogenetic diversity." Biological conservation **61**(1): 1-10.

Gamonal, J., A. Acevedo, A. Bascones, O. Jorge and A. Silva (2000). "Levels of interleukin-1β,-8, and-10 and RANTES in gingival crevicular fluid and cell populations in adult periodontitis patients and the effect of periodontal treatment." Journal of periodontology **71**(10): 1535-1545.

Garant, P. R. (1976). "An electron microscopic study of the periodontal tissues of germfree rats and rats monoinfected with Actinomyces naeslundii." Journal of periodontal research **(15)**(15): 3-79.

Garlet, G. P., W. Martins, B. R. Ferreira, C. M. Milanezi and J. S. Silva (2003). "Patterns of chemokines and chemokine receptors expression in different forms of human periodontal disease." Journal of periodontal research **38**(2): 210-217.

Garnick, J. J., R. Pearson and D. Harrell (1979). "The evaluation of the Periotron." Journal of periodontology **50**(8): 424-426.

Genolini, C., X. Alacoque, M. Sentenac and C. Arnaud (2015). "kml and kml3d: R Packages to Cluster Longitudinal Data." Journal of Statistical Software **65**(4): 1-34.

Graves, D. (2008). "Cytokines that promote periodontal tissue destruction." J Periodontol **79**(8 Suppl): 1585-1591.

Graves, D. T. and D. Cochran (2003). "The contribution of interleukin-1 and tumor necrosis factor to periodontal tissue destruction." Journal of periodontology **74**(3): 391-401.

Greer, A., K. Irie, A. Hashim, B. G. Leroux, A. M. Chang, M. A. Curtis and R. P. Darveau (2016). "Site-Specific Neutrophil Migration and CXCL2 Expression in Periodontal Tissue." J Dent Res **95**(8): 946-952.

Griffen, A. L., C. J. Beall, J. H. Campbell, N. D. Firestone, P. S. Kumar, Z. K. Yang, M. Podar and E. J. Leys (2012). "Distinct and complex bacterial profiles in human periodontitis and health revealed by 16S pyrosequencing." ISME J **6**(6): 1176-1185.

Griffen, A. L., C. J. Beall, J. H. Campbell, N. D. Firestone, P. S. Kumar, Z. K. Yang, M. Podar and E. J. Leys (2012). "Distinct and complex bacterial profiles in human periodontitis and health revealed by 16S pyrosequencing." The ISME journal **6**(6): 1176-1185.

Hajishengallis, G. (2015). "Periodontitis: from microbial immune subversion to systemic inflammation." Nat Rev Immunol **15**(1): 30-44.

Halekoh, U., S. Højsgaard and J. Yan (2006). "The R package geepack for generalized estimating equations." Journal of Statistical Software **15**(2): 1-11.

Hart, T. C., L. Shapira and T. E. Van Dyke (1994). "Neutrophil Defects as Risk Factors for Periodontal Diseases*." Journal of periodontology **65**(5s): 521-529.

Heasman, P. A., J. G. Collins and S. Offenbacher (1993). "Changes in crevicular fluid levels of interleukin-1β, leukotriene B4, prostaglandin E2, thromboxane B2 and tumour necrosis factor α in experimental gingivitis in humans." Journal of periodontal research **28**(4): 241-247.

Hervé, M. (2019). RVAideMemoire: Testing and Plotting Procedures for Biostatistics. R package version 0.9-72.

Heymann, R., J. Wroblewski, C. Terling, T. Midtvedt and B. Obrink (2001). "The characteristic cellular organization and CEACAM1 expression in the junctional epithelium of rats and mice are genetically programmed and not influenced by the bacterial microflora." Journal of periodontology **72**(4): 454-460.

Hosokawa, Y., I. Hosokawa, K. Ozaki, H. Nakae and T. Matsuo (2008). "CC chemokine ligand 17 in periodontal diseases: expression in diseased tissues and production by human gingival fibroblasts." J Periodontal Res **43**(4): 471-477.

Huang, S., R. Li, X. Zeng, T. He, H. Zhao, A. Chang, C. Bo, J. Chen, F. Yang and R. Knight (2014). "Predictive modeling of gingivitis severity and susceptibility via oral microbiota." The ISME journal **8**(9): 1768-1780.

Human Microbiome Project, C. (2012). "Structure, function and diversity of the healthy human microbiome." Nature **486**(7402): 207-214.

Ishihara, Y., T. Nishihara, T. Kuroyanagi, N. Shirozu, E. Yamagishi, M. Ohguchi, M. Koide, N. Ueda, K. Amano and T. Noguchi (1997). "Gingival crevicular interleukin-1 and interleukin-1 receptor antagonist levels in periodontally healthy and diseased sites." J Periodontal Res **32**(6): 524-529.

Jari Oksanen, F. G. B., Michael Friendly, Roeland Kindt, Pierre, D. M. Legendre, Peter R. Minchin, R. B. O'Hara, Gavin L. Simpson, and M. H. H. S. Peter Solymos, Eduard Szoecs and Helene Wagner (2019). Vegan: Community Ecology Package. R package version 2.5-4.

Kebschull, M., R. Demmer, J. H. Behle, A. Pollreisz, J. Heidemann, P. B. Belusko, R. Celenti, P. Pavlidis and P. N. Papapanou (2009). "Granulocyte chemotactic protein 2 (gcp-2/cxcl6) complements interleukin-8 in periodontal disease." J Periodontal Res **44**(4): 465-471.

Kebschull, M., R. Demmer, J. H. Behle, A. Pollreisz, J. Heidemann, P. B. Belusko, R. Celenti, P. Pavlidis and P. N. Papapanou (2009). "Granulocyte chemotactic protein 2 (gcp-2/cxcl6) complements interleukin-8 in periodontal disease." Journal of periodontal research **44**(4): 465-471.

Kembel, S. W., P. D. Cowan, M. R. Helmus, W. K. Cornwell, H. Morlon, D. D. Ackerly, S. P. Blomberg and C. O. Webb (2010). "Picante: R tools for integrating phylogenies and ecology." Bioinformatics **26**(11): 1463-1464.

Kilian, M., I. L. C. Chapple, M. Hannig, P. D. Marsh, V. Meuric, A. M. L. Pedersen, M. S. Tonetti, W. G. Wade and E. Zaura (2016). "The oral microbiome–an update for oral healthcare professionals." British dental journal **221**(10): 657-666.

Kinane, D. F. (2001). "Causation and pathogenesis of periodontal disease." Periodontology 2000 **25**(1): 8-20.

Kinney, J. S., T. Morelli, M. Oh, T. M. Braun, C. A. Ramseier, J. V. Sugai and W. V. Giannobile (2014). "Crevicular fluid biomarkers and periodontal disease progression." Journal of clinical periodontology **41**(2): 113-120.

Kistler, J. O., V. Booth, D. J. Bradshaw and W. G. Wade (2013). "Bacterial community development in experimental gingivitis." PLoS One **8**(8): e71227.

Kuczynski, J., C. L. Lauber, W. A. Walters, L. W. Parfrey, J. C. Clemente, D. Gevers and R. Knight (2012). "Experimental and analytical tools for studying the human microbiome." Nature Reviews Genetics **13**(1): 47.

Kumar, P. S., A. L. Griffen, M. L. Moeschberger and E. J. Leys (2005). "Identification of candidate periodontal pathogens and beneficial species by quantitative 16S clonal analysis." J Clin Microbiol **43**(8): 3944-3955.

Kumar, S. (2019). "Evidence-Based Update on Diagnosis and Management of Gingivitis and Periodontitis." Dent Clin North Am **63**(1): 69-81.

Lahti, L. (2019). microbiome R package.

Lee, E., Y. H. Yang, Y. P. Ho, K. Y. Ho and C. C. Tsai (2003). "Potential role of vascular endothelial growth factor, interleukin-8 and monocyte chemoattractant protein-1 in periodontal diseases." The Kaohsiung journal of medical sciences **19**(8): 406-415.

Lee, J., G. Cacalano, T. Camerato, K. Toy, M. W. Moore and W. I. Wood (1995). "Chemokine binding and activities mediated by the mouse IL-8 receptor." Journal of immunology (Baltimore, Md.: 1950) **155**(4): 2158-2164.

Lenth, R. (2018). "Emmeans: Estimated marginal means, aka least-squares means." R Package Version **1**(2).

Liang, K.-Y. and S. L. Zeger (1986). "Longitudinal data analysis using generalized linear models." Biometrika **73**(1): 13-22.

Listgarten, M. A. and J. B. Heneghan (1971). "Chronic inflammation in the gingival tissue of germ-free dogs." Archives of Oral Biology **16**(10): 1207-1213.

Löe, H. and J. Silness (1963). "Periodontal disease in pregnancy I. Prevalence and severity." Acta Odontologica Scandinavica **21**(6): 533-551.

Löe, H., E. Theilade and S. B. Jensen (1965). "Experimental gingivitis in man." Journal of periodontology **36**(3): 177-187.

Loesche, W. J. and S. A. Syed (1978). "Bacteriology of human experimental gingivitis: effect of plaque and gingivitis score." Infect Immun **21**(3): 830-839.

Lozupone, C. and R. Knight (2005). "UniFrac: a new phylogenetic method for comparing microbial communities." Appl Environ Microbiol **71**(12): 8228-8235.

Lozupone, C. A. and R. Knight (2008). "Species divergence and the measurement of microbial diversity." FEMS microbiology reviews **32**(4): 557-578.

Marsh, P. D. (1994). "Microbial ecology of dental plaque and its significance in health and disease." Advances in Dental Research **8**(2): 263-271.

Matthews, C. R., V. Joshi, M. de Jager, M. Aspiras and P. S. Kumar (2013). "Host–bacterial interactions during induction and resolution of experimental gingivitis in current smokers." Journal of periodontology **84**(1): 32-40.

Mayadas, T. N., X. Cullere and C. A. Lowell (2014). "The multifaceted functions of neutrophils." Annual review of pathology **9**: 181-218.

McMurdie, P. J. and S. Holmes (2013). "phyloseq: an R package for reproducible interactive analysis and graphics of microbiome census data." PLoS One **8**(4): e61217.

Metsalu, T. ((2019)). clustvis: R package for visualizing clustering of multivariate data using PCA

and heatmap.

Meyle, J. (1994). "Leukocyte adhesion deficiency and prepubertal periodontitis." Periodontology 2000 **6**(1): 26-36.

Mocsai, A. (2013). "Diverse novel functions of neutrophils in immunity, inflammation, and beyond." The Journal of experimental medicine **210**(7): 1283-1299.

Moore, W. E., L. V. Holdeman, R. M. Smibert, I. J. Good, J. A. Burmeister, K. G. Palcanis and R. R. Ranney (1982). "Bacteriology of experimental gingivitis in young adult humans." Infect Immun **38**(2): 651-667.

Morimoto, T., J. Nishihira and T. Kohgo (2003). "Immunohistochemical localization of macrophage migration inhibitory factor (MIF) in human gingival tissue and its pathophysiological functions." Histochem Cell Biol **120**(4): 293-298.

Nadkarni, M. A., F. E. Martin, N. A. Jacques and N. Hunter (2002). "Determination of bacterial load by real-time PCR using a broad-range (universal) probe and primers set." Microbiology **148**(Pt 1): 257-266.

Nascimento, G. G., B. Danielsen, V. Baelum and R. Lopez (2019). "Identification of inflammatory response patterns in experimental gingivitis studies." Eur J Oral Sci **127**(1): 33-39.

Niederman, R., T. Westernoff, C. Lee, L. L. Mark, N. Kawashima, M. Ullman-Culler, F. E. Dewhirst, B. J. Paster, D. D. Wagner and T. Mayadas (2001). "Infection-mediated early-onset

periodontal disease in P/E-selectin-deficient mice." Journal of clinical periodontology **28**(6): 569-575.

Nonnenmacher, C., K. Helms, M. Bacher, R. M. Nusing, C. Susin, R. Mutters, L. Flores-de-Jacoby and R. Mengel (2009). "Effect of age on gingival crevicular fluid concentrations of MIF and PGE2." Journal of dental research **88**(7): 639-643.

Nourshargh, S., P. L. Hordijk and M. Sixt (2010). "Breaching multiple barriers: leukocyte motility through venular walls and the interstitium." Nat Rev Mol Cell Biol **11**(5): 366-378.

Nussbaum, G. and L. Shapira (2011). "How has neutrophil research improved our understanding of periodontal pathogenesis?" Journal of clinical periodontology **38 Suppl 11**: 49-59.

Offenbacher, S., S. Barros, L. Mendoza, S. Mauriello, J. Preisser, K. Moss, M. de Jager and M. Aspiras (2010). "Changes in gingival crevicular fluid inflammatory mediator levels during the induction and resolution of experimental gingivitis in humans." J Clin Periodontol **37**(4): 324-333.

Panezai, J., A. Ghaffar, M. Altamash, K. G. Sundqvist, P. E. Engstrom and A. Larsson (2017). "Correlation of serum cytokines, chemokines, growth factors and enzymes with periodontal disease parameters." PLoS One **12**(11): e0188945.

Park, O. J., H. Yi, J. H. Jeon, S. S. Kang, K. T. Koo, K. Y. Kum, J. Chun, C. H. Yun and S. H. Han (2015). "Pyrosequencing Analysis of Subgingival Microbiota in Distinct Periodontal Conditions." J Dent Res **94**(7): 921-927.

Paster, B. J., S. K. Boches, J. L. Galvin, R. E. Ericson, C. N. Lau, V. A. Levanos, A. Sahasrabudhe and F. E. Dewhirst (2001). "Bacterial diversity in human subgingival plaque." J Bacteriol **183**(12): 3770-3783.

Porter, J. R. (1976). "Antony van Leeuwenhoek: tercentenary of his discovery of bacteria." Bacteriological Reviews **40**(2): 260-269.

Preiss, D. S. and J. Meyle (1994). "Interleukin-1beta Concentration of Gingival Crevicular Fluid." J Periodontol **65**(5): 423-428.

Preshaw, P. M. and J. J. Taylor (2011). "How has research into cytokine interactions and their role in driving immune responses impacted our understanding of periodontitis?" J Clin Periodontol **38 Suppl 11**: 60-84.

Price, M. N., P. S. Dehal and A. P. Arkin (2010). "FastTree 2–approximately maximum-likelihood trees for large alignments." PloS one **5**(3): e9490.

Ramfjord, S. P. (1959). "Indices for prevalence and incidence of periodontal disease." The Journal of Periodontology **30**(1): 51-59.

Rawlinson, A., M. H. Dalati, S. Rahman, T. F. Walsh and A. L. Fairclough (2000). "Interleukin-1 and IL-1 receptor antagonist in gingival crevicular fluid." J Clin Periodontol **27**(10): 738-743.

Rindom Schiött, C. and H. Löe (1970). "The origin and variation in number of leukocytes in the human saliva." Journal of periodontal research **5**(1): 36-41.

Rousseeuw, P. J. (1987). "Silhouettes: a graphical aid to the interpretation and validation of cluster analysis." Journal of computational and applied mathematics **20**: 53-65.

Rovai, L. E., H. R. Herschman and J. B. Smith (1998). "The murine neutrophil-chemoattractant chemokines LIX, KC, and MIP-2 have distinct induction kinetics, tissue distributions, and tissue-specific sensitivities to glucocorticoid regulation in endotoxemia." Journal of leukocyte biology **64**(4): 494-502.

Sadik, C. D., N. D. Kim and A. D. Luster (2011). "Neutrophils cascading their way to inflammation." Trends in immunology **32**(10): 452-460.

Sahingur, S. E. and W. A. Yeudall (2015). "Chemokine function in periodontal disease and oral cavity cancer." Frontiers in immunology **6**: 214.

Sallay, K., M. Listgarten, F. Sanavi, I. Ring and A. Nowotny (1984). "Bacterial invasion of oral tissues of immunosuppressed rats." Infection and immunity **43**(3): 1091-1093.

Schincaglia, G. P., B. Y. Hong, A. Rosania, J. Barasz, A. Thompson, T. Sobue, F. Panagakos, J. A. Burleson, A. Dongari-Bagtzoglou and P. I. Diaz (2017). "Clinical, Immune, and Microbiome Traits of Gingivitis and Peri-implant Mucositis." J Dent Res **96**(1): 47-55.

Scott, A. E., M. Milward, G. J. Linden, J. B. Matthews, M. J. Carlile, F. T. Lundy, M. A. Naeeni, S. Lorraine Martin, B. Walker, D. Kinane, G. R. Brock and I. L. Chapple (2012). "Mapping biological to clinical phenotypes during the development (21 days) and resolution (21 days) of experimental gingivitis." J Clin Periodontol **39**(2): 123-131.

Segata, N., J. Izard, L. Waldron, D. Gevers, L. Miropolsky, W. S. Garrett and C. Huttenhower (2011). "Metagenomic biomarker discovery and explanation." Genome Biol **12**(6): R60.

Shapira, L., A. Wilensky and D. F. Kinane (2005). "Effect of genetic variability on the inflammatory response to periodontal infection." J Clin Periodontol **32 Suppl 6**: 72-86.

Silness, J. and H. Löe (1964). "Periodontal disease in pregnancy II. Correlation between oral hygiene and periodontal condition." Acta Odontologica Scandinavica **22**(1): 121-135.

Silva, T. A., G. P. Garlet, S. Y. Fukada, J. S. Silva and F. Q. Cunha (2007). "Chemokines in oral inflammatory diseases: apical periodontitis and periodontal disease." Journal of dental research **86**(4): 306-319.

Simpson, E. H. (1949). "Measurement of diversity." Nature **163**(4148): 688.

Socransky, S. S. and A. D. Haffajee (2005). "Periodontal microbial ecology." Periodontol 2000 **38**: 135-187.

Socransky, S. S., A. D. Haffajee, M. A. Cugini, C. Smith and R. L. Kent (1998). "Microbial complexes in subgingival plaque." Journal of clinical periodontology **25**(2): 134-144.

Söder, B., L. J. Jin and S. Wickholm (2002). "Granulocyte elastase, matrix metalloproteinase-8 and prostaglandin E2 in gingival crevicular fluid in matched clinical sites in smokers and non-smokers with persistent periodontitis." Journal of clinical periodontology **29**(5): 384-391.

Stingu, C. S., K. Eschrich, A. C. Rodloff, R. Schaumann and H. Jentsch (2008). "Periodontitis is associated with a loss of colonization by Streptococcus sanguinis." J Med Microbiol **57**(Pt 4): 495-499.

Taba, M., Jr., J. Kinney, A. S. Kim and W. V. Giannobile (2005). "Diagnostic biomarkers for oral and periodontal diseases." Dental clinics of North America **49**(3): 551-571, vi.

Tatakis, D. N. and L. Trombelli (2004). "Modulation of clinical expression of plaque-induced gingivitis. I. Background review and rationale." J Clin Periodontol **31**(4): 229-238.

Team, R. C. (2018). R: A Language and Environment for Statistical Computing. Vienna, Austria, R Foundation for Statistical Computing.

Teles, R., D. Sakellari, F. Teles, A. Konstantinidis, R. Kent, S. Socransky and A. Haffajee (2010). "Relationships among gingival crevicular fluid biomarkers, clinical parameters of periodontal disease, and the subgingival microbiota." Journal of periodontology **81**(1): 89-98.

Teles, R., F. Teles, J. Frias-Lopez, B. Paster and A. Haffajee (2013). "Lessons learned and unlearned in periodontal microbiology." Periodontology 2000 **62**(1): 95-162.

Terricabras, E., C. Benjamim and N. Godessart (2004). "Drug discovery and chemokine receptor antagonists: eppur si muove!" Autoimmunity reviews **3**(7): 550-556.

Theilade, E., W. H. Wright, S. B. Jensen and H. Löe (1966). "Experimental gingivitis in man." Journal of periodontal research **1**(1): 1-13.

Tonetti, M. S. (1997). "Molecular factors associated with compartmentalization of gingival immune responses and transepithelial neutrophil migration." Journal of periodontal research **32**(1): 104-109.

Tonetti, M. S., M. A. Imboden, L. Gerber, N. P. Lang, J. Laissue and C. Mueller (1994). "Localized expression of mRNA for phagocyte-specific chemotactic cytokines in human periodontal infections." Infection and immunity **62**(9): 4005-4014.

Tonetti, M. S., M. A. Imboden and N. P. Lang (1998). "Neutrophil migration into the gingival sulcus is associated with transepithelial gradients of interleukin-8 and ICAM-1*." Journal of periodontology **69**(10): 1139-1147.

Trombelli, L., D. N. Tatakis, C. Scapoli, S. Bottega, E. Orlandini and M. Tosi (2004). "Modulation of clinical expression of plaque-induced gingivitis. II. Identification of "high-responder" and "low-responder" subjects." J Clin Periodontol **31**(4): 239-252.

Trombelli, L., D. N. Tatakis, C. Scapoli, S. Bottega, E. Orlandini and M. Tosi (2004). "Modulation of clinical expression of plaque-induced gingivitis." Journal of clinical periodontology **31**(4): 239-252.

Tsai, C.-C., Y.-P. Ho and C.-C. Chen (1995). "Levels of Interleukin-1β and Interleukin-8 in Gingival Crevicular Fluids in Adult Periodontitis*." Journal of periodontology **66**(10): 852-859.

Tsai, I. S., C. C. Tsai, Y. P. Ho, K. Y. Ho, Y. M. Wu and C. C. Hung (2005). "Interleukin-12 and interleukin-16 in periodontal disease." Cytokine **31**(1): 34-40.

Tsukamoto, Y., M. Usui, G. Yamamoto, Y. Takagi, T. Tachikawa, M. Yamamoto and M. Nakamura (2012). "Role of the junctional epithelium in periodontal innate defense and homeostasis." J Periodontal Res **47**(6): 750-757.

Van der Weijden, G. A., M. F. Timmerman, M. M. Danser, A. Nijboer, C. A. Saxton and U. Van der Velden (1994). "Effect of pre-experimental maintenance care duration on the development of gingivitis in a partial mouth experimental gingivitis model." J Periodontal Res **29**(3): 168-173.

Wade, W. G. (2011). "Has the use of molecular methods for the characterization of the human oral microbiome changed our understanding of the role of bacteria in the pathogenesis of periodontal disease?" J Clin Periodontol **38 Suppl 11**: 7-16.

Wade, W. G. (2013). "The oral microbiome in health and disease." Pharmacol Res **69**(1): 137-143.

Wiedemann, W., J. Lahrsow and R. Naujoks (1979). "[The effect of periodontal resistance on experimental gingivitis]." Dtsch Zahnarztl Z **34**(1): 6-9.

Wolff, L. F., Q. T. Smith, W. K. Snyder, J. A. Bedrick, W. F. Liljemark, D. A. Aeppli and C. L. Bandt (1988). "Relationship between lactate dehydrogenase and myeloperoxidase levels in human gingival crevicular fluid and clinical and microbial measurements." Journal of clinical periodontology **15**(2): 110-115.

Wuyts, A., A. Haelens, P. Proost, J. P. Lenaerts, R. Conings, G. Opdenakker and J. Van Damme (1996). "Identification of mouse granulocyte chemotactic protein-2 from fibroblasts and epithelial cells. Functional comparison with natural KC and macrophage inflammatory protein-2." Journal of immunology (Baltimore, Md.: 1950) **157**(4): 1736-1743.

Xu, J. and J. I. Gordon (2003). "Honor thy symbionts." Proceedings of the National Academy of Sciences of the United States of America **100**(18): 10452-10459.

Yamasaki, A., H. Nikai, K. Niitani and N. Ijuhin (1979). "Ultrastructure of the Junctional Epithelium of Germfree Rat Gingiva*." Journal of periodontology **50**(12): 641-648.

Yoshinari, N., Y. Kameyama, Y. Aoyama, H. Nishiyama and T. Noguchi (1994). "Effect of long-term methotrexate-induced neutropenia on experimental periodontal lesion in rats." Journal of periodontal research **29**(6): 393-400.

Yu, J. J., M. J. Ruddy, G. C. Wong, C. Sfintescu, P. J. Baker, J. B. Smith, R. T. Evans and S. L. Gaffen (2007). "An essential role for IL-17 in preventing pathogen-initiated bone destruction: recruitment of neutrophils to inflamed bone requires IL-17 receptor-dependent signals." Blood **109**(9): 3794-3802.

Zenobia, C., X. L. Luo, A. Hashim, T. Abe, L. Jin, Y. Chang, Z. C. Jin, J. X. Sun, G. Hajishengallis and M. A. Curtis (2013). "Commensal bacteria-dependent select expression of CXCL2 contributes to periodontal tissue homeostasis." Cellular microbiology **15**(8): 1419-1426.

Zhou, Y., K. A. Mihindukulasuriya, H. Gao, P. S. La Rosa, K. M. Wylie, J. C. Martin, K. Kota, W. D. Shannon, M. Mitreva, E. Sodergren and G. M. Weinstock (2014). "Exploration of bacterial community classes in major human habitats." Genome Biol **15**(5): R66.

Zhu, B., L. C. Macleod, E. Newsome, J. Liu and P. Xu (2019). "Aggregatibacter actinomycetemcomitans mediates protection of Porphyromonas gingivalis from Streptococcus sanguinis hydrogen peroxide production in multi-species biofilms." Sci Rep **9**(1): 4944.

Zlotnik, A. and O. Yoshie (2000). "Chemokines: a new classification system and their role in immunity." Immunity **12**(2): 121-127.

Shatha Bamashmous

sbamashmous@gmail.com

Education:

- **Doctor of Philosophy (PhD), Oral Health Sciences (2019)**

School of Dentistry, University of Washington, Seattle, WA, USA
Thesis title: "Investigation of Chemokine and Microbiome Profiles in Gingival Health and Disease in Humans"
Supervised by: Dr. Richard P. Darveau

- **Master of Science in Dentistry (MSD) (2016)**

School of Dentistry, University of Washington, Seattle, WA, USA
Title: "Effect of conditional knockout of the progressive ankylosis (Ank) gene in mice on the development of periodontal tissues"
Supervised by: Dr. Martha Somerman

- **Certificate in Periodontics (2013)**

School of Dentistry, University of Washington Seattle, WA, USA

- **Bachelor Degree in Dental Medicine & Surgery (BDS) (2006)**

Faculty of Dentistry, King Abdul-Aziz University (KAU), Jeddah, Saudi Arabia.

Professional and Work Experience:

- **Supervised dental students in pre-doctoral clinics, PERIO 631/641, (2014-2019)**
  Department of Periodontics, School of Dentistry, University of Washington, Seattle, WA, USA
- **Lectured first year dental students, DENTPC 511 (PERIO 517), Introduction to Periodontics (Autumn 2015-2018)**
  Department of Periodontics, School of Dentistry, University of Washington, Seattle, WA, USA
- **Participated as Mock Board Examiner for Graduate Periodontics Residents (May 2015-2018)**
  Department of Periodontics, School of Dentistry, University of Washington, Seattle, WA, USA
- **Lectured first year dental students, DENTFN 513, Oral Microbiology (Autumn 2017)**
  School of Dentistry, University of Washington, Seattle, WA, USA
- **Lectured third year dental students, PERIO 531, Principles of Periodontics II (Winter 2015)**
  Department of Periodontics, School of Dentistry, University of Washington, Seattle, WA, USA

- **Residency Training in Periodontics (6/2010-6/2013)**
  Department of Periodontics, School of Dentistry, University of Washington Seattle, WA, USA
- **Clinical Instructor (3/2008-5/2009)**
  Division of Periodontics, Faculty of Dentistry, King Abdulaziz University,Jeddah, Saudi Arabia
- **Dental Intern (9/2006-8/2007).**
  Faculty of Dentistry, King Abdulaziz University, Jeddah, Saudi Arabia

Honors and Awards:

- **University of Washington Magnuson Scholar (2016/2017)**
  University of Washington, Seattle, WA, USA
- **Certificate of Appreciation for Affiliate Faculty Member (2014-2016)**
- Department of Periodontics, School of Dentistry, University of Washington Seattle, WA, USA
- **The Richard Kao Basic Science Research Award, 2012 California Society of Periodontists (CSP) Student Award.**
  Title: "Effect of conditional knockout of progressive ankylosis gene in mice"
- **Plaque of Scientific Excellency (2007)**
  Faculty of Dentistry, King Abdulaziz University, Jeddah, Saudi Arabia
- **Certificate of Overall Academic Achievement (2007)**
  King Abdulaziz University, Jeddah, Saudi Arabia
- **Certificate of Scientific Excellency (2002 - 2006)**
  Faculty of Dentistry, King Abdulaziz University, Jeddah, Saudi Arabia
- **Certificate of Scientific Excellency (2000)**
  Ministry of Education, Jeddah, Saudi Arabia

Publications and Poster Presentations:

- **The Progressive Ankylosis Protein Regulates Cementum Apposition and Extracellular Matrix Composition.**
  Foster BL, Nagatomo KJ, Bamashmous SO, Tompkins KA, Fong H, Dunn D, Chu EY, Guenther C, Kingsley DM, Rutherford RB, Somerman MJ. Cells Tissues Organs. 2011;194(5):382-405
- **Short-Term Effects of Photodynamic Therapy on Periodontal Status and Glycemic Control of Patients With Diabetes.**
  Al-Zahrani MS, Bamashmous SO, Alhassani AA, Al-Sherbini MM. J Periodontol. 2009 Oct;80(10):1568-73
- **Gingival Health Diagnostic Model for Neutrophil Migration.**
  School of Dentistry's 2017 Research Day Poster, University of Washington, Seattle, Washington, January 31, 2017. Bamashmous S, Kim AS, McLean JS, Kotsakis GA, Darveau RP
- **ENAM Gene and Enamel Thickness: Adaptive Evolution in Humans**.

- Poster Session, IADR General Session, Seattle, Washington. March 23, 2013. D.M. DAUBERT, Y. UDOD, S. BAMASHMOUS, C. HABOR DESOUZA, C. KLEIST, I. KHOSH, J. KELLEY, W.J. SWANSON, and F.A. ROBERTS
- **The Progressive Ankylosis Protein (ANK) Functions Locally to Regulate Cementogenesis**.
  Research Forum Poster Session at the American Academy of Periodontology's 2012 Annual Meeting, Los Angeles, California, September 29-October 2, 2012. S. BAMASHMOUS, B.L. FOSTER, J. WADE, and M.J. SOMERMAN
- **The Progressive Ankylosis Protein (ANK) Functions Locally to Regulate Cementogenesis**.
  Poster Session, IADR General Session, San Diego, California. March 18, 2011. S. BAMASHMOUS, B.L. FOSTER, K.J. NAGATOMO, J. WADE, and M.J. SOMERMAN.
- **Effect of Adjunctive Use Of Photodynamic Therapy During Supportive Periodontal Therapy In Diabetic Patients.**
  Research Forum Poster Session at 96th Annual Meeting American Academy of Periodontology (AAP), Oct 20- Nov 2, 2010 in Honolulu, Hawaii. S.O. Bamashmous, M.S. Al-Zahrani, N.F. Bissad.
- **Genetics of Tooth Enamel Thickness.**
  Poster session, AADR Annual meeting, Washington, DC. March 6, 2010.I. TIKHONOV, D. DAUBERT, S. BAMASHMOUS, C. HABER DESOUZA, C. KLEIST, I. KHOSH, J. KELLEY, W. SWANSON, and F. ROBERTS,
- **Undiagnosed hypertension in a sample of dental school female patients.**
  Poster Session, IADR General Session. Toronto, Canada. July 4, 2008M. AL-. ZAHRANI, S. BAMASHMOUS, and N. FARSI

Professtional Affiliation

- American Board of Periodontology (ABP)
- American Academy of Periodontology (AAP)
- American Dental Association (ADA)
- Washington State Dental Association (WSDA)
- American Dental Education Association (ADEA)